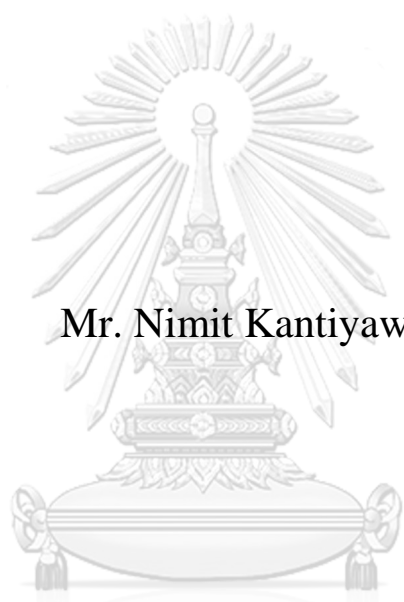


ELECTRODE IMPROVEMENT USING DIAMOND-LIKE
CARBON FOR ELECTROCHEMICAL ADVANCED
OXIDATION IN DIURON DEGRADATION



Mr. Nimit Kantiyawong

จุฬาลงกรณ์มหาวิทยาลัย
CHULALONGKORN UNIVERSITY

A Thesis Submitted in Partial Fulfillment of the Requirements
for the Degree of Master of Engineering in Chemical Engineering
Department of Chemical Engineering
Faculty of Engineering
Chulalongkorn University
Academic Year 2018
Copyright of Chulalongkorn University

การปรับปรุงข้ออิเล็กทรอนิกส์โดยใช้คาร์บอนคล้ายเพชรสำหรับปฏิกิริยาออกซิเดชันเชิงไฟฟ้าเคมีขึ้น
สูงในการย่อยสลายสารไดยูรอน



วิทยานิพนธ์นี้เป็นส่วนหนึ่งของการศึกษาตามหลักสูตรปริญญาวิศวกรรมศาสตรมหาบัณฑิต
สาขาวิชาวิศวกรรมเคมี ภาควิชาวิศวกรรมเคมี
คณะวิศวกรรมศาสตร์ จุฬาลงกรณ์มหาวิทยาลัย
ปีการศึกษา 2561
ลิขสิทธิ์ของจุฬาลงกรณ์มหาวิทยาลัย

Thesis Title	ELECTRODE IMPROVEMENT USING DIAMOND-LIKE CARBON FOR ELECTROCHEMICAL ADVANCED OXIDATION IN DIURON DEGRADATION
By	Mr. Nimit Kantiyawong
Field of Study	Chemical Engineering
Thesis Advisor	Associate Professor Dr. Varong Pavarajarn, Ph.D.
Thesis Co Advisor	Assistant Professor Dr. Boonchoat Paosawatyanong, Ph.D.

Accepted by the Faculty of Engineering, Chulalongkorn University in Partial Fulfillment of the Requirement for the Master of Engineering

..... Dean of the Faculty of Engineering
(Associate Professor Dr. Supot Teachavorasinskun,
D.Eng.)

THESIS COMMITTEE

..... Chairman
(Professor Dr. Sarawut Rimdusit, Ph.D.)

..... Thesis Advisor
(Associate Professor Dr. Varong Pavarajarn, Ph.D.)

..... Thesis Co-Advisor
(Assistant Professor Dr. Boonchoat Paosawatyanong,
Ph.D.)

..... Examiner
(Dr. Rungthiwa Methaapanon, Ph.D.)

..... External Examiner
(Assistant Professor Dr. Nathaporn Promros, Ph.D.)

จุฬาลงกรณ์มหาวิทยาลัย
CHULALONGKORN UNIVERSITY

นิมิตร กันธิยะวงศ์ : การปรับปรุงขั้วอิเล็กโทรดโดยใช้คาร์บอนคล้ายเพชรสำหรับปฏิกิริยาออกซิเดชันเชิงไฟฟ้าเคมีขั้นสูงในการย่อยสลายสารไดูรอน. (**ELECTRODE IMPROVEMENT USING DIAMOND-LIKE CARBON FOR ELECTROCHEMICAL ADVANCED OXIDATION IN DIURON DEGRADATION**) อ.ที่ปรึกษาหลัก : รศ. ดร.วงศ์ ปวราจารย์, อ.ที่ปรึกษาร่วม : ผศ. ดร.บุญโชติ เผ่าสวัสดิ์ชัยทรง

ไดูรอนเป็นสารกำจัดวัชพืชที่มีการใช้ทางการเกษตรในปริมาณที่มากจึงทำให้เกิดการตกค้างนำไปสู่การปนเปื้อนในแหล่งน้ำซึ่งเป็นปัญหาทางสิ่งแวดล้อมและส่งผลกระทบต่อสุขภาพของมนุษย์ โดยกระบวนการที่ใช้ในการกำจัดสารพิษที่ปนเปื้อนในน้ำมีอยู่หลายกระบวนการ ในปัจจุบันกระบวนการทางไฟฟ้าเคมีขั้นสูงและเครื่องปฏิกรณ์ขนาดไมโครเมตรได้ถูกใช้ในการย่อยสลายสารไดูรอนเนื่องจากมีประสิทธิภาพในการย่อยสลายที่สูง ในงานวิจัยนี้ฟิล์มบางคาร์บอนคล้ายเพชรถูกนำมาใช้เป็นขั้วทางไฟฟ้าเคมีเนื่องจากเป็นวัสดุคาร์บอนที่มีความแข็งแรงคงทนและสามารถนำไฟฟ้าได้ วิทยานิพนธ์ฉบับนี้วิทยานิพนธ์ฉบับนี้ประสบความสำเร็จในการสังเคราะห์ฟิล์มบางคาร์บอนคล้ายเพชรจากแกรไฟต์ลงบนพื้นผิวของ 304 สแตนเลสสตีลด้วยกระบวนการดีซีแมกนีตรอนสปีดเดอริง โดยใช้ขั้วไฟฟ้าฟิล์มบางคาร์บอนคล้ายเพชรที่สังเคราะห์ได้นั้นสามารถย่อยสลายสารไดูรอนได้ด้วยปฏิกิริยาเชิงไฟฟ้าเคมีขั้นสูงในเครื่องปฏิกรณ์ขนาดไมโครเมตรจากการทดลองพบว่าขั้วไฟฟ้าฟิล์มบางคาร์บอนคล้ายเพชรสามารถลดการก่อก้อนที่เกิดขึ้นระหว่างการทำปฏิกิริยาเมื่อเปรียบเทียบกับขั้วไฟฟ้าแกรไฟต์ โดยความสามารถในการย่อยสลายสารไดูรอนขึ้นอยู่กับคุณสมบัติของขั้วคาร์บอนคล้ายเพชร อันได้แก่อัตราส่วนระหว่างโครงสร้างพันธะคู่ต่อพันธะเดี่ยวของคาร์บอน อัตราส่วนระหว่างพันธะคาร์บอนกับไฮโดรเจน และอัตราส่วนระหว่างพันธะคาร์บอนกับออกซิเจน โดยขั้วไฟฟ้าฟิล์มบางคาร์บอนคล้ายเพชรที่มีพันธะคาร์บอนกับออกซิเจนจะทำให้เกิดการก่อก้อนของฟิล์มบางคาร์บอนคล้ายเพชรในอัตราที่สูงมากถึง 5.96 ไมโครกรัมต่อชั่วโมง ส่วนขั้วไฟฟ้าคาร์บอนคล้ายเพชรที่มีพันธะคาร์บอนกับไฮโดรเจนสามารถปรับปรุงความสามารถในการนำไฟฟ้าไม่มากขึ้นโดยมีค่าความต้านทานจำเพาะ 0.076 โอห์มต่ออนาโนเมตร ทำให้มีประสิทธิภาพในการย่อยสลายเพิ่มขึ้นมาถึง 70 เปอร์เซ็นต์ ในระยะเวลา 100 วินาทีที่สารอยู่ในเครื่องปฏิกรณ์ขนาดไมโครเมตร นอกจากนี้แล้วทั้งสามคุณสมบัติของขั้วคาร์บอนคล้ายเพชรยังส่งผลต่อการสลายตัวของสาร ไดูรอนทำให้เกิดสารตัวกลางที่แตกต่างกัน

จุฬาลงกรณ์มหาวิทยาลัย
CHULALONGKORN UNIVERSITY

สาขาวิชา วิศวกรรมเคมี

ลายมือชื่อนิติ

ปีการศึกษา 2561

ลายมือชื่อ อ.ที่ปรึกษาหลัก

ลายมือชื่อ อ.ที่ปรึกษาร่วม

5970227921 : MAJOR CHEMICAL ENGINEERING

KEYWORD Degradation of diuron; Advanced oxidation process; Microreactor;
D: Sputtering Diamond-like carbon

Nimit Kantiyawong : ELECTRODE IMPROVEMENT USING DIAMOND-LIKE CARBON FOR ELECTROCHEMICAL ADVANCED OXIDATION IN DIURON DEGRADATION. Advisor: Assoc. Prof. Dr. Varong Pavarajarn, Ph.D. Co-advisor: Asst. Prof. Dr. Boonchoat Paosawatyanong, Ph.D.

Diuron is one of the pesticides. Its residual can contaminate natural water resource resulting in environmental and human health problems. Several processes have been used to remove diuron contamination. Nowadays, an electrochemical advanced oxidation process (EAOP) in a microchannel reactor is used to degrade diuron owing to its high efficiency. In this research, the diamond-like carbon (DLC) thin film was used as an electrochemical electrode because it has superior hardness and electrical conductivity. In this research, we have successfully synthesized the DLC thin films using graphite as target material on the surface of 304 stainless steel substrate by the direct current (dc) magnetron sputtering process. It was found that using the DLC thin film electrode caused less corrosion during the reaction when compared to the graphite electrode. The performance of diuron degradation depends on the properties of the thin film electrode, i.e., the sp^2 -to- sp^3 ratio, the C-H bonds, and the C=O bonds. The DLC thin film electrode with the C=O bond led to the highest corrosion, up to 5.96 $\mu\text{g/h}$. The C-H bond in the DLC thin film improves the electrical conductivity ($R_{\text{specific}} = 0.076 \Omega/\text{nm}$) of electrode leading to high degradation performance, up to 70% within 100 seconds of residence time. Furthermore, each property of the DLC thin film results in different kind of intermediate during diuron decomposition.

จุฬาลงกรณ์มหาวิทยาลัย
CHULALONGKORN UNIVERSITY

Field of Study: Chemical Engineering

Student's Signature

Academic 2018

.....
Advisor's Signature

Year:

.....
Co-advisor's Signature

.....

ACKNOWLEDGEMENTS

Firstly, I would like to specify my gratitude to my advisor and co-advisor, Associate Professor Varong Pavarajarn, and Assistant Professor Boonchoat Paosawatyanong, for their advice. I get experience in practical problem-solving skills. I think that these skills are also very valuable for developing my attitude.

Secondly, I would like to thank to Professor Sarawut Rimdusid as a chairman, Dr. Rungthiwa Methaaphanon and Assistant Professor Nathaporn Promros as the members of the thesis committee, for their recommendations.

Moreover, I would like to extend my thanks to the members of Center of Excellence in Particle Technology (CEPT), Department of Chemical Engineering, Faculty of Engineering, Chulalongkorn University. Mainly, people at 11th floor, for their suggestions and supporting.

Other than, I would like to extend my thanks to Miss Somchintana Puttamat for helping characterization of intermediates at Faculty of Science and Technology, Thammasat University.

Furthermore, I would like to extend my thanks to Assistant Professor Nathaporn Promros for support the instrument for synthesis diamond-like carbon at Faculty of Science, King Mongkut's Institute of Technology Ladkabang.

Finally, I would like to thank my parents for their support and continuous encouragement throughout my year of study.

Nimit Kantiyawong

TABLE OF CONTENTS

	Page
ABSTRACT (THAI)	iii
ABSTRACT (ENGLISH).....	iv
ACKNOWLEDGEMENTS.....	v
TABLE OF CONTENTS.....	vi
LIST OF TABLES.....	viii
LIST OF FIGURES	ix
CHAPTER 1 INTRODUCTION.....	1
CHAPTER 2 FUNDAMENTAL THEORY AND LITERATURE REVIEWS.....	4
2.1 Diuron	4
2.2 Electrochemical Advanced Oxidation Processes (EAOPs) for diuron degradation	5
2.3 Microchannel technology	7
2.4 Diamond-like carbon (DLC) thin films	9
2.5 Deposition techniques for synthesis of DLC thin films.....	10
2.6 DC magnetron sputtering process.....	10
2.7 Improvement of adhesion of The DLC thin films	14
2.8 Characterization of DLC thin films	15
2.9 Possible intermediates generated during diuron degradation	16
CHAPTER 3 EXPERIMENTAL.....	19
3.1 Materials and chemicals	19
3.2 DC magnetron sputtering system apparatus	20
3.3 Microreactor apparatus	21
3.4 Experimental setup and procedures.....	22
3.5 Measurement of Thickness	24
3.6 Electrically Resistive Measurement	25

3.7 Analytical Instruments	25
CHAPTER 4 RESULTS AND DISCUSSION	30
4.1 Synthesis of diamond-like carbon thin films using dc magnetron sputtering process	30
4.2 The behaviors of diuron degradation using the DLC thin films and graphite sheet electrode	38
4.3 Effects of Ti used as an interlayer between the substrate and DLC thin films on the behaviors of diuron degradation	48
4.4 Effects of DLC thin films electrodes properties on behaviors of diuron degradation	55
4.4.1 Effects of carbon structures of DLC thin films electrodes	55
4.4.2 Effects of C-H bond in DLC thin films electrodes	64
4.4.3 Effects of the C=O bond in DLC thin films electrodes	72
4.5 Comparison of properties of DLC thin films electrodes on behaviors of diuron degradation	80
CHAPTER 5 CONCLUSIONS AND RECOMMENDATIONS	87
5.1 Summary of results	87
5.2 Conclusions	88
5.3 Recommendations	89
REFERENCES	90
APPENDIX	94
Appendix A Calibration Data Analysis	95
Appendix B Deconvolution of XPS Data	97
Appendix C Liquid Chromatography-Mass/Mass Spectrum Data	102
Appendix D Additional Data	107
VITA	109

LIST OF TABLES

	Page
Table 2.1 The physical properties of diuron	5
Table 2.2 Structure of diamond, graphite, and diamond-like carbon	9
Table 2.3 Possible intermediates generated during diuron degradation via advanced oxidation processes identified by LC-MS/MS analysis.....	17
Table 2.4 Possible intermediates generated during diuron degradation via advanced oxidation processes identified by LC-MS/MS analysis (Continuous).....	18
Table 4.1 Properties of the carbon electrodes using for degradation of diuron via advanced oxidation process	46
Table 4.2 Properties of the DLC thin films electrodes with different carbon structure	55
Table 4.3 Intermediates produced during diuron degradation using DLC thin films electrodes with various ratio of sp^2 -to- sp^3 via EAOP within the microchannel reactor.	63
Table 4.4 Properties of DLC thin films electrodes with different amount of C-H bond	64
Table 4.5 Properties of DLC thin films electrodes before and after using via EAOP of high C-H bond.....	70
Table 4.6 Intermediates produced during diuron degradation using DLC thin films electrodes with various C-H contents via EAOP within the microchannel reactor.	71
Table 4.7 Properties of DLC thin films electrodes with different amount of C=O bond	72
Table 4.8 Properties of DLC thin films electrodes before and after using via EAOP of high C=O bond.....	77
Table 4.9 Intermediates produced during diuron degradation using DLC thin films electrodes with various C=O contents via EAOP within a microchannel reactor.	79
Table 4.10 Intermediates produced during diuron degradation using DLC thin films electrodes different properties via EAOP within a microchannel reactor.	86

LIST OF FIGURES

	Page
Figure 2.1 The mechanism of diuron degradation via EAOP.....	7
Figure 2.2 The mechanism of the sputtering process	11
Figure 2.3 The mechanism dc magnetron sputtering process.....	12
Figure 2.4 Example of C 1s deconvolution of DLC thin films.....	16
Figure 3.1 The dc magnetron sputtering system.....	20
Figure 3.2 Scheme of the microchannel reactor	21
Figure 3.3 Diagram of the experimental setup of the EAOP of degradation procedure in a microreactor	24
Figure 3.4 The photograph of X-ray photoelectron spectroscopy	26
Figure 3.5 UV-Visible spectrophotometer.....	27
Figure 3.6 High performance liquid chromatography (HPLC)	28
Figure 3.7 The photograph of TOC analyzer.....	29
Figure 4.1 The deposition rate of DLC thin films under various operating pressure in the range of 5 mtorr to 25 mtorr.....	31
Figure 4.2 The survey spectra of XPS on the surface substrate coated with DLC thin films by dc magnetron sputtering process at operating pressure 5 mtorr	32
Figure 4.3 Deconvolution of the C1s peak of diamond-like carbon synthesized by dc magnetron sputtering process at operating pressure of 5 mtorr	33
Figure 4.4 Ratio of sp^2 -to- sp^3 of the DLC thin films electrodes deposited under various the base pressure	35
Figure 4.5 Fraction of C-H bond of DLC thin films electrodes deposited under various the base pressure	36
Figure 4.6 Properties of the DLC thin films electrodes deposited under various the operating pressure	37
Figure 4.7 The correlation between the concentrations of hydrogen peroxide generated in deionized water and time on stream various the electrodes	39
Figure 4.8 The correlation between the percentage of diuron degradation and time on stream various the electrodes	40

Figure 4.9 The corrosion rate of carbon materials electrodes occurred during EAOP within a microchannel reactor.....	42
Figure 4.10 The correlation between the percentage of diuron degradation and time on stream of using the DLC thin films electrode.....	43
Figure 4.11 The absorbance at wavelength 350 nm of deionized water and outlet solution from a microchannel reactor.....	44
Figure 4.12 The correlation between the concentrations of hydrogen peroxide generated in deionized water and time on stream.....	45
Figure 4.13 The concentration of hydrogen peroxide generated via EAOP using different electrodes within a microchannel reactor.....	49
Figure 4.14 The effect of using Ti interlayer on the corrosion rate of the DLC thin films electrodes occurred during the EAOP within the microchannel reactor.....	50
Figure 4.15 The survey spectra of XPS at the surface of the electrode before and after using in EAOP within the microchannel reactor.....	51
Figure 4.16 The concentration of contaminated elements detected in the outlet solution via the EAOP within a microchannel reactor.....	52
Figure 4.17 Correlation of electrical resistance and ratio of sp^2 -to- sp^3 structure in DLC thin films electrodes.....	57
Figure 4.18 Correlation of concentration of hydrogen peroxide generated and time on stream at various the ratio of sp^2 -to- sp^3 of the DLC thin films electrode.....	58
Figure 4.19 Correlation between performance of diuron degradation and time on stream various the ratio of sp^2 -to- sp^3 of DLC thin films.....	59
Figure 4.20 The ratio of sp^2 -to- sp^3 of DLC thin films electrodes after using for EAOP within the microchannel reactor.....	60
Figure 4.21 The correlation between corrosion rate and time on stream of DLC thin films electrode various ratio of sp^2 -to- sp^3	61
Figure 4.22 Correlation between electrical resistance and the fraction of C-H bond in DLC thin film electrode.....	65
Figure 4.23 Correlation of hydrogen peroxide generated and time on stream various fraction of C-H bond in the DLC thin films electrode.....	66
Figure 4.24 Correlation between performance of diuron degradation and time on stream at various fraction of C-H bond in the DLC thin films electrode.....	67
Figure 4.25 Correlation between corrosion rate and time on stream at various fraction of C-H bond in the DLC thin films electrode.....	68

Figure 4.26 Correlation between electrical resistance and fraction of C=O bond.....	73
Figure 4.27 Correlation between concentration of hydrogen peroxide generated and time on stream at various fraction of C=O bond in the DLC thin films electrode	74
Figure 4.28 Correlation between performance of diuron degradation and time on stream at various fraction of C=O bond in the DLC thin films electrode.....	75
Figure 4.29 Correlation between corrosion rate and time on stream with various fraction of C=O bond in DLC thin films electrode.....	76
Figure 4.30 Correlation between electrical resistances and the highest of each property of DLC thin films electrodes.....	81
Figure 4.31 Correlation between concentrations of hydrogen peroxide generated and time on stream with various properties of the DLC thin films electrode.....	82
Figure 4.32 Correlation between performance of diuron degradation and time on stream with various properties of the DLC thin films electrode.....	83
Figure 4.33 The correlation between the corrosion rate and time on stream various the properties of the DLC thin films electrode	84

CHAPTER 1 INTRODUCTION

Among pesticides used in agriculture, herbicides have been used in the highest amount. Thailand is an agricultural country. Thus, the use of herbicides is common. In 2016, diuron is one of the herbicides imported into Thailand in the greatest amount. It is used in agricultural activities for controlling and eliminating weeds. It is a toxic substance with the oral LD₅₀ in rats of 1017-3400 mg/kg [1]. Since diuron has excellent chemical stability, it can remain in soil and can also be dissolved in natural water leading to the problems related to water contamination. Because diuron is persistence, i.e., half-life over a year in nature [2], diuron contamination could spread widely becoming severe pollution. Diuron is a priority toxic compound in The European Union Waste Framework Directive [3]. The treatment of diuron contaminated in water has been proposed in many techniques such as biodegradation processes [4], adsorption processes [5], and advanced oxidation processes (AOPs) such as photocatalytic processes [2], Fenton's processes [3], and electrochemical advanced oxidation processes (EAOPs) [6]. Novel AOPs, especially the EAOP have been recently developed for the removal of many types of organic compounds contaminated in water because of its high degradation efficiency [6-8]. In the EAOP, highly active hydroxyl radicals (OH[•]) are generated from dissociation of water at the surface of the anode [9]. When the electrical current is applied to the electrodes, the hydroxyl radicals can be generated and decompose organic compounds. However, the efficiency of the degradation via EAOP is commonly limited by issues such diffusion of the organic compound to the surface of the electrode. The electrochemical

advanced oxidation is effectively utilized in a microchannel reactor [10]. Because of the short distance between electrodes in micro scale, the diffusion distance of the organic compound is reduced, resulting in increased degradation efficiency.

Usually, the electrode for EAOPs is boron-doped diamond or BDD [6, 11, 12]. However, the process of producing BDD is complicated and expensive. Therefore, graphite sheets have been used in EAOP to generate hydroxyl radicals using electric current. This electrode can be used to degrade diuron up to 90% within 100 s of residence time in a microchannel reactor [10], but the graphite electrodes are usually associated with corrosion problem.

Diamond-like carbon (DLC) thin film is amorphous carbon having combination of sp^2 (graphite-like) and sp^3 (diamond-like) structures. The DLC thin films have been widely studied for many applications [13], such as corrosion protection [14], optical transparency [15], and electronic sensors [16]. It has excellent properties for being the electrochemical electrode; for example, high hardness, high chemical inertness, corrosion resistance, and being electrical conductive [17]. The DC magnetron sputtering process is one of the methods for DLC coating. Its advantages include simplicity, high deposition rate, high purity of the film, and low construction and operation cost [18].

This work aims to study the coating of the electrodes, which are stainless steel with diamond-like carbon via DC magnetron sputtering process under different conditions. The electrodes are subsequently used for the decomposition of diuron contaminated in water via EAOP within a microchannel reactor.

The thesis is consisted of five main chapters as followed:

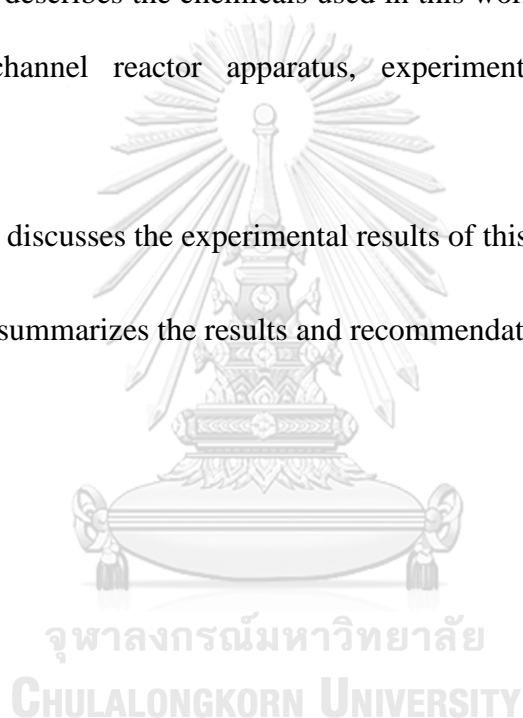
Chapter I presents the motivation and introduction of this work.

Chapter II explains the fundamental theory and reviews literature related to properties of diuron, electrochemical advanced oxidation process, diamond-like carbon properties, and the diamond-like carbon coating process.

Chapter III describes the chemicals used in this work, dc magnetron sputtering apparatus, microchannel reactor apparatus, experimental setup, and analytical methods.

Chapter IV discusses the experimental results of this work.

Chapter V summarizes the results and recommendations.



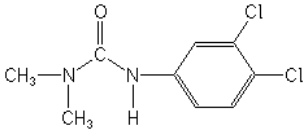
CHAPTER 2 FUNDAMENTAL THEORY AND LITERATURE REVIEWS

This chapter explains the fundamental theory and literature reviews related to properties of diuron, an electrochemical advanced oxidation process, diamond-like carbon properties, and the diamond-like carbon coating process.

2.1 Diuron

Diuron or 3-(3,4-dichlorophenyl)-1,1-dimethylurea is an herbicide which is considered in phenylurea class, it inhibits photosynthesis of weeds. Diuron is commonly and widely used in an agricultural activity for eliminating and controlling weeds. Diuron is a toxic substance with the oral LD₅₀ in rats is 1017-3400 mg/kg. Since the properties of diuron are bio-recalcitrant, and high chemical stability, so it has half-life over a year in nature. Diuron can remain in the soil leading to contamination in natural water. Especially, underground and surface water near the agriculture area. Recently, diuron contamination in the environment become a severe problem [1, 2]. The physical properties of diuron are shown in **Table 2.1**

Table 2.1 The physical properties of diuron

Properties	Data
Synonyms	3-(3,4-dichlorophenyl)-1,1-dimethylurea, Cekiuron
Chemical structure	
Molecular formula	C ₉ H ₁₀ Cl ₂ N ₂ O
Density	1.48 g/cm ³
solubility	42 mg/l in water at 20°C
Half-life	Over 370 days

2.2 Electrochemical Advanced Oxidation Processes (EAOPs) for diuron degradation

Nowadays, many techniques have used for removal of diuron contaminated in aqueous solution, for example, adsorption process [5], biological treatment process [4], and advanced oxidation processes (AOPs) [2, 3, 11]. Due to the high degradation efficiency of AOPs, these processes are widely used in the degradation of organic compounds. All of the advanced oxidation processes are the creation of hydroxyl radicals processes. This process includes ultraviolet photolysis, Ozone oxidation, Fenton reaction, Photocatalysis, and electrochemical advanced oxidation process. Nowadays the AOPs, especially as the EAOPs have been studied for the degradation of many organic compounds. The photocatalytic and EAOPs are the main processes for treatment the pollutant water because these processes have the high performance. The difference between photocatalytic reaction and electrochemical advanced

oxidation is the mechanism of the creation of hydroxyl radicals. In the photocatalytic process, the hydroxyl radical was generated by light at the surface of the catalyst. In the EAOP, the hydroxyl radical was generated by electricity under electrochemical oxidation at the surface of anode [19].

Electrochemical advanced oxidation has been suggested used for degradation of organic compounds such as diuron. In this process, the hydroxyl radicals are generally generated from dissociation of water molecules at the surface of an anode when applied the electric current, in the equation: $\text{H}_2\text{O} \rightarrow \text{OH}^\bullet + \text{H}^+ + \text{e}^-$. This reaction has standard redox potential ($E^0 (\text{OH}^\bullet/\text{H}_2\text{O}) = +2.8 \text{ V/SHE}$). The hydroxyl radical is highly active and influential. Therefore, this radical is rapidly react and decompose the diuron compounds. Also, the diuron degradation produces the intermediates during the EAOP. Moreover, hydroxyl radical interaction with itself can generate the hydrogen peroxide (H_2O_2) near the surface of the electrode, in the equation: $\text{OH}^\bullet + \text{OH}^\bullet \rightarrow \text{H}_2\text{O}_2$ [9]. Consequently, the hydrogen peroxide represents the number of hydroxyl radicals. The mechanism of diuron degradation with the electrochemical advanced oxidation process is shown in **Figure 2.1**.

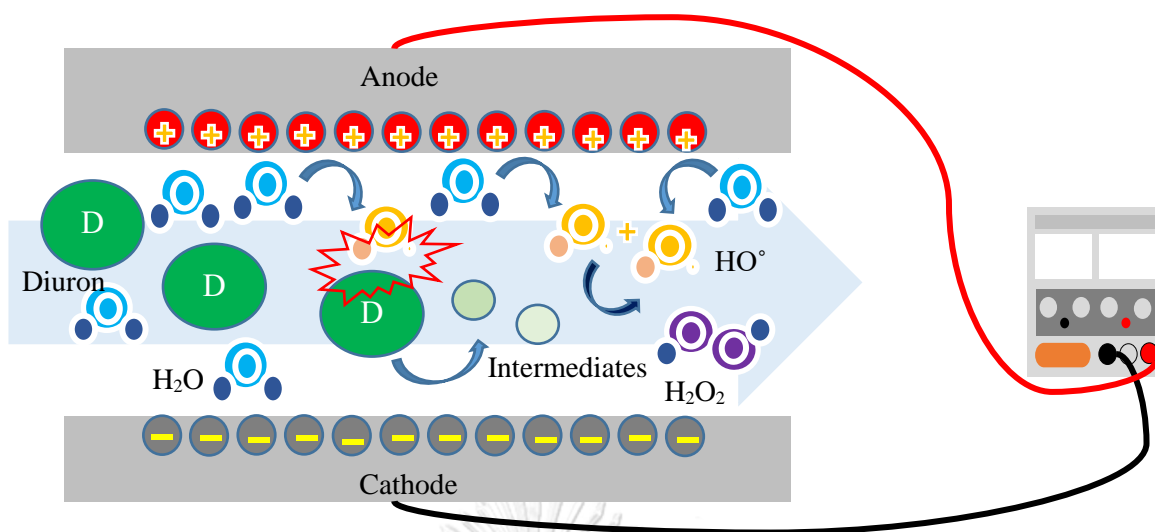


Figure 2.1 The mechanism of diuron degradation via EAOP

2.3 Microchannel technology

At present, the microchannel is used to study in several fields of micro process engineering, for example, micro heat exchanger, and microchannel reactor. The microchannel reactor is a device used for chemical reactions occurred in a microscale channel. This device has the dimension less than 1000 μm . Thus, the microchannel reactor is generally used for the continuous flow reactor. The microchannel reactors have many advantages more than conventional reactors, such as high efficiency, safety, and easy to control process [20, 21]. The advantages of microreactor technology are the reduced size of the reactor and increased mass diffusion of reactants. Due to the dimension of this device less than 1000 μm , the volume of the microreactor is significantly reduced compared to the conventional reactors. The size reduction also decreases the cost of construction. Furthermore, the microreactor has the high performance because of the small distance of mass diffusion. Therefore, this

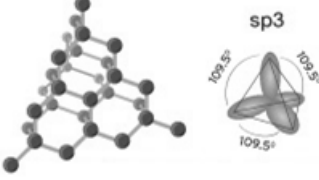
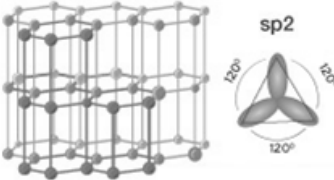
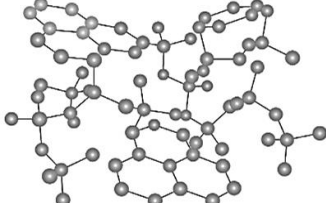
property can improve production efficiency. The performance can be significantly increased in the microchannel reactor. Therefore, the microchannel reactor is interested in diuron degradation using EAOP.

The diuron degradation in an aqueous solution via EAOP within the microreactor was studied by Worachate Khongthon et al. (2016). This process used a graphite sheet as an anode. The degradation of diuron at approximately 90% , the decomposition can be achieved within 100 seconds of residence time in the microreactor, thickness of 250 μm , applied with 1 mA of direct current. The percent of diuron decomposition increases with decreasing the thickness of the microchannel reactor. Diuron degradation mainly occurs from the interaction between diuron and hydroxyl radical near the surface of the graphite sheet (anode). The pathway is very complicated for degradation, involving many reaction intermediates. When applied the electric current, the surface of the graphite electrode occurs the corrosion because this electrode has only the sp^2 carbon structure [10].

2.4 Diamond-like carbon (DLC) thin films

Diamond-like carbon (DLC) thin film is amorphous carbon thin films with combination between graphite-like structure and diamond-like structure, hybridization of sp^2 and sp^3 respectively. The DLC thin films are utilized in many applications such as protective corrosion of the biomedical and micro-electrochemical system [22]. The structure of diamond, graphite, and the DLC thin films have the difference of structure as shown in **Table 2.2**.

Table 2.2 Structure of diamond, graphite, and diamond-like carbon

Diamond	Graphite	Diamond-like carbon
		

The ratio of graphite-like structure to diamond-like structure (sp^2 -to- sp^3) affects the mechanical hardness and electrical conductivity of the DLC thin films. For example, the high sp^2 -to- sp^3 ratio is good conductivity. Since this thin film has high hardness, chemical inertness, and corrosion resistance. Therefore, the DLC thin films have good potential for using electrode in the electrochemical advanced oxidation process.

2.5 Deposition techniques for synthesis of DLC thin films

Many methods have been used for the synthesis of the DLC thin films on the metal substrate. The synthesized methods can be divided into two main methods. The chemical vapor deposition (CVD) methods synthesize the DLC thin films via a chemical interaction occurred between the methane and active sites at the substrate surface under high temperature and vacuum condition. On the other hand, The physical vapor deposition (PVD) methods use the solid graphite as the carbon source. These processes synthesize the DLC thin films under vacuum condition by applying a DC voltage to the target and substrate. The PVD methods include the arc, laser vapor deposition, and sputtering methods [23].

Typically, the sputtering process is one of the PVD methods for synthesis of the DLC thin films. The advantages of this process are control simplicity, high deposition rate, high purity thin films, and easy to operation [18].

2.6 DC magnetron sputtering process

The sputtering processes are used for the synthesis of several materials onto a surface of the substrate such as silver, copper, and diamond-like carbon. This process generates the plasma which is usually used as an argon (Ar) because of inertness. The plasma is consisting of ions and electrons. The collision of argon ions with the surface of solid target emits the sputtered target atoms under the vacuum in the chamber. The sputtering mechanism is shown in **Figure 2.2**. The mechanisms occur when the argon atoms introduced into the vacuum chamber with the operating pressure approximately 1 - 10 mtorr. The high voltage is applied to the target (cathode) and the substrate

holder (anode). The glow discharge of the argon plasma emits the purple light. The argon ion is accelerated to the target surface, and the electron is accelerated to the substrate depending on electrical field [18, 23].

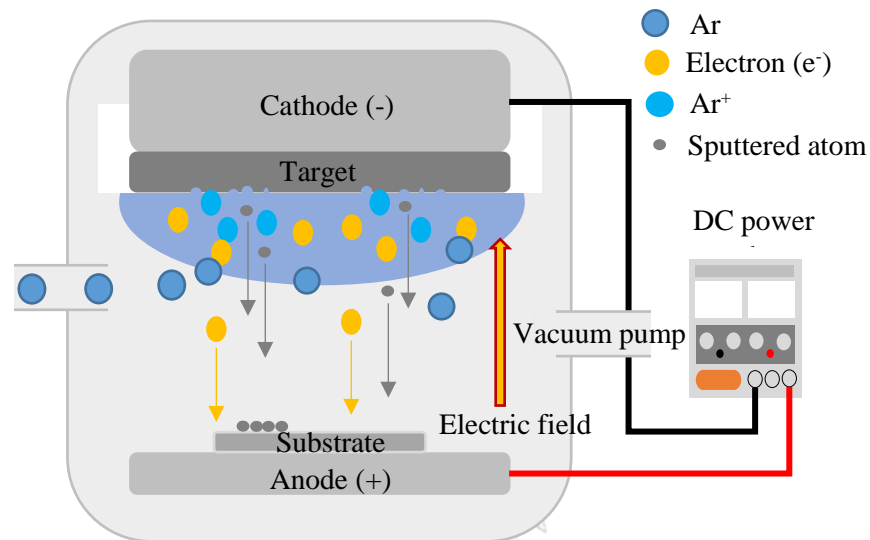


Figure 2.2 The mechanism of the sputtering process

The main difference compared to between the dc sputtering process and the dc magnetron sputtering process is the addition of a magnetic field above the target. In this process, the magnetic field increases the number of argon ions because the electrons are moving helical around the surface of the target with the magnetic field. This mechanism increases the collisions between the electrons and argon near the surface of the target [24]. The dc magnetron sputtering mechanism is shown in **Figure 2.3**. The advantage of dc magnetron sputtering is the plasma contributed around the surface of the target increasing the ionizing of argon atoms. Consequently, the dc magnetron sputtering has a high deposition rate, high uniformity, deposition cover all of the surface areas of the substrate, and high purity of the thin films.

Therefore, the dc magnetron sputtering process is the best methods for synthesis of the DLC thin films [18, 24].

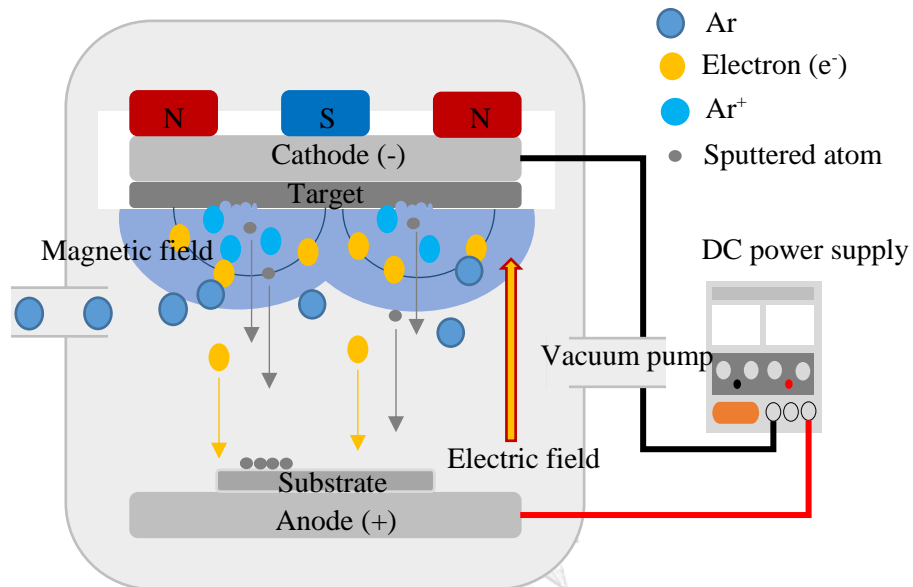


Figure 2.3 The mechanism dc magnetron sputtering process

The dc magnetron sputtering has many parameters effect on the properties of the DLC thin film including base pressure, operating gas pressure, and sputtering power. All of the factors are important as following.

The base pressure of the sputtering process affects the number of residual gases in the chamber. These residual gases can bond with the sputtered carbon atoms making impurity of the DLC thin films.

The operating pressure of the sputtering process affects the mean free path. Although the mean free path is large at low operating pressure, the efficiency of ionization of neutrals argon is low. On the other hand, the operating pressure is

decreased at a fixed voltage, the mean free path is increased. The mean free path is large that means the sputtered atoms are decreased collision leading to small scattering of ejected atoms moving to the surface of the substrate [15].

The effects of operating pressure on DLC properties was studied by Özlem Duyar Coşkun and Taner Zerrin (2015). The DLC was deposited on the glass substrate via dc magnetron sputtering technique at room temperature. The pure graphite was used as a target. The base pressure was controlled at 2×10^{-6} Torr. The working pressure was varied in the range of 2 mtorr to 50 mtorr using Ar gas. The sputtering power was fixed at 60 W. The ratio of sp^3 -to- sp^2 is increased from 0.51 to 2.81 when increasing the operating pressure [15].

The sputtering power relates to the discharge current and the voltage of sputtering. This factor affects the deposition rate of the thin film. When increasing the sputter power, the deposition rate is increasing, the film thickness and ratio of sp^3 -to- sp^2 is increases. The hydrogen-free amorphous carbon deposition on a 440C steel substrate by dc magnetron sputtering was studied by Sam Zhang et al. (2003). The 440C substrate has surface roughness R_a of around 60 nm. The graphite (purity 99.999%) was used as a target. The distance between the target and the substrate holder was fixed at 10 cm. Moreover, the base pressure was fixed at 10^{-7} Torr, and the operating pressure was kept at 3 mtorr with argon flow rate at 50 sccm. The power density is 10.5 W/cm^2 . The synthesized hydrogen-free a-C have high hardness and high toughness, the hardness is the range of 18 to 28 GPa, depending on sp^3 fraction. The adhesion strength of the coating depends on the power density. The sp^3 fraction is increased when increasing the power density [25].

The DLC films with different structure were studied by A. Zeng et al. (2002). In this research, the base pressure has been utilized at 10^{-7} Torr, and the operating pressure was fixed at 10 mtorr using Ar gas. The distance from target to the substrate was kept at 14 cm, and the sputtering power was varied in the range of 500 to 900 W. The results, increasing of the sputtering power is not significant changes of D peak and G peak positions. On the other hand, the sputtering increases in the range of 750-900W, the I_D/I_G ratio was decreased. The results from the electrochemical analysis, the DLC films have excellent properties using as an electrode material [26].

2.7 Improvement of adhesion of The DLC thin films

Normally, the titanium (Ti) was used as an interlayer to enhance the adhesion of DLC thin films and the substrate surface because the Ti can form titanium carbide. Moreover, the Ti has the high adhesion with the surface of metals substrate. Many research has studied the enhancement of the adhesion of DLC thin films using Ti interlayer as following.

The surface modification of stainless steel (SUS304) was studied by Tsutomu Sonoda et al. (2011). The surface was coated with DLC/Ti bi-layered thin films using the sputtering process to increase the adhesion of the synthesized DLC thin films and surface of stainless steel. The DLC sputtering monolithic films were performed under the same condition of sputtering DLC/Ti bi-layer. The DLC monolithic films were less adhesive than the DLC/Ti bi-layered films. Therefore, the corrosive resistance of stainless steel able to improve by using Ti interlayer [27].

The using of Ti interlayer on the performance of DLC thin films bioelectrodes was studied by Tomi Laurila et al. (2014). The Ti/DLC interface was detected oxygen-containing, it has the formation of Ti[O,C] layers. In the result of the experimental, the DLC films had stable in the sulphuric acid, and phosphate buffered solutions when using the Ti interlayer between the Pt(Ir) microwire surface and DLC thin films. Therefore, The Ti interlayer can improve the adhesion of the DLC thin films of electrode [28].

2.8 Characterization of DLC thin films

Normally, the methods using for characterization of DLC thin films properties are Raman spectroscopy and X-ray photoelectron spectroscopy (XPS). However, the Raman spectroscopy is the method that required the thickness of the sample more than 1 μm . In this work, the thickness of DLC thin films is approximately 500 nm so the Raman spectroscopy is unsuitable for this work.

Therefore, X-ray Photoelectron Spectroscopy (XPS) can characterize the properties at the surface of DLC thin films, such as type of elements, chemical structure, and chemical bonding. This instrument is used Al K_{α} X-ray with energy 1486.6 eV for characterization. The C1s peak of XPS spectrum is used in deconvolving for determination of the carbon structures and chemical bonds at the surface of the DLC thin films. In several research, the C1s peak of DLC thin films contains the sp^2 hybridized carbon structure (C=C) peak and the sp^3 hybridized carbon structure (C-C) peak at binding energy 284.4 eV and 285.2 eV respectively. Not only the C1s peak contains sp^2 and sp^3 carbon structure, but also it has the contain

hydrogen bond (C-H) at 283.5 eV and carbon to oxygen bonds (C-O, C=O, and O-C=O) at 286.5 eV, 287.8 eV, and 289.4 eV respectively as shown in **Figure 2.4** [29-31]. Consequently, the XPS is a suitable instrument for characterization of DLC thin films.

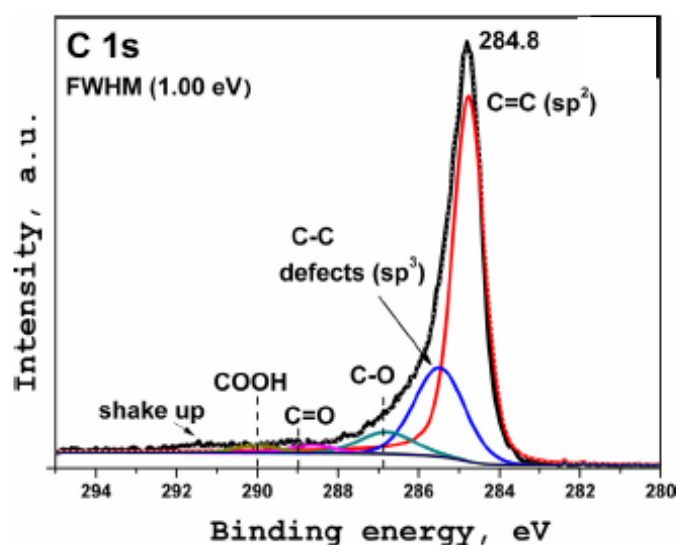


Figure 2.4 Example of C 1s deconvolution of DLC thin films

จุฬาลงกรณ์มหาวิทยาลัย
CHULALONGKORN UNIVERSITY

2.9 Possible intermediates generated during diuron degradation

The possible intermediates of diuron degradation via advanced oxidation processes were reported by many researchers. The intermediates products are mainly generated by hydroxyl radicals. The intermediate was investigated by liquid chromatography-mass/mass spectrometer (LC-MS/MS). The possible intermediates of diuron degradation via advanced oxidation processes are shown in **Table 2.3**.

Table 2.3 Possible intermediates generated during diuron degradation via advanced oxidation processes identified by LC-MS/MS analysis

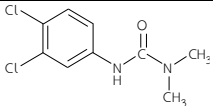
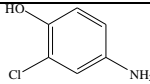
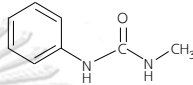
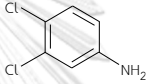
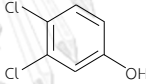
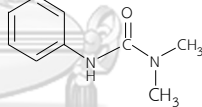
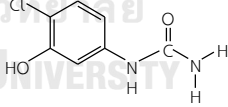
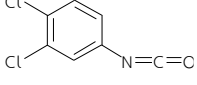
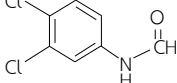
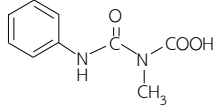
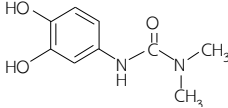
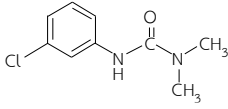
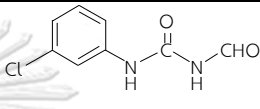
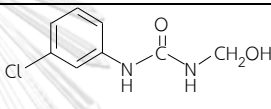
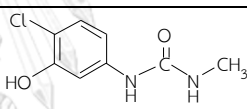
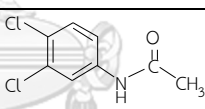
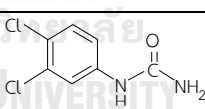
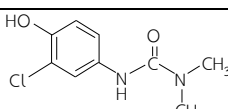
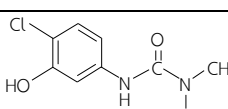
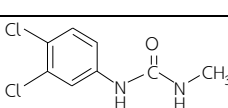
Compound	m/z	Molecular mass (avg.)	Structure
1. Diuron	231/232	233.09 Mono. Mass=232.02	 <chem>CN(C)C(=O)Nc1ccc(Cl)c(Cl)c1</chem> $C_9H_{10}ON_2Cl_2$
2. [32]	142/144	143.57 Mono. Mass=143	 <chem>Nc1ccc(Cl)c(Cl)c1</chem> C_6H_6OCIN
3. [33]	149/151	150.07 Mono. Mass=150.18	 <chem>CN(C)C(=O)Nc1ccccc1</chem> $C_8H_{10}N_2O$
4. Standard [32, 34-38]	160/162	162 Mono. Mass=160.98	 <chem>Nc1ccc(Cl)c(Cl)c1</chem> $C_6H_5NOCl_2$ 3,4-dichloroaniline
5.	161/163	163 Mono. Mass=161.96	 <chem>Oc1ccc(Cl)c(Cl)c1</chem> $C_6H_4OCl_2$ 3,4-dichlorophenol
6.	163/165	164.2 Mono. Mass=164.09	 <chem>CN(C)C(=O)Nc1ccccc1</chem> $C_9H_{12}ON_2$
7.	185/187	186.6 Mono. Mass=186.02	 <chem>NC(=O)Nc1ccc(Cl)c(Cl)c1</chem> $C_7H_7N_2O_2Cl$
8. Standard [37, 39]	186/188	188.01 Mono. Mass=186.96	 <chem>N=C=Oc1ccc(Cl)c(Cl)c1</chem> $C_7H_7N_2O_2Cl$, 3, 4-dichlorophenyl isocyanate
9. [38]	188/190	190.03 Mono. Mass=188.97	 <chem>NC(=O)Nc1ccc(Cl)c(Cl)c1</chem> $C_7H_5NOCl_2$, N-(3, 4-dichlorophenyl) formamide
10.	193/195	194.19 Mono. Mass=194.07	 <chem>CN(C)C(=O)Nc1ccc(Cl)c(Cl)c1</chem> $C_9H_{10}O_3N_2$

Table 2.4 Possible intermediates generated during diuron degradation via advanced oxidation processes identified by LC-MS/MS analysis (Continuous)

Compound	m/z	Molecular mass (avg.)	Structure
11.	195/197	196.2 Mono. Mass=196.08	 <chem>CN(C)C(=O)Nc1ccc(O)c(O)c1</chem> $C_9H_{12}O_3N_2$
12. Standard	197/199	198.65 Mono. Mass=198.056	 <chem>CN(C)C(=O)Nc1ccc(Cl)cc1</chem> $C_9H_{11}ON_2Cl$
13. Standard	197/199	198.65 Mono. Mass=198.056	 <chem>NC(=O)Nc1ccc(Cl)cc1</chem> $C_8H_7O_2N_2Cl$
14. [33, 40-42]	199/201	200.62 Mono. Mass=200.04	 <chem>NC(=O)NCOc1ccc(Cl)cc1</chem> $C_8H_9O_2N_2Cl$
15. [33, 40-42]	199/201	200.62 Mono. Mass=200.04	 <chem>CN(C)C(=O)Nc1cc(O)c(Cl)cc1</chem> $C_8H_9O_2N_2Cl$
16. [38]	202/204	204.05 Mono. Mass=202.99	 <chem>CC(=O)Nc1cc(Cl)c(Cl)cc1</chem> $C_8H_7ONCl_2$
17. [38, 40, 43, 44]	203/205/ 207	205.04 Mono. Mass=203.98	 <chem>NC(=O)Nc1cc(Cl)c(Cl)cc1</chem> $C_6H_6ON_2Cl_2$, 1-(3,4-dichlorophenyl) urea
18. [32, 36, 40, 41, 45]	215/217	216.65 Mono. Mass=216.03	 <chem>CN(C)C(=O)Nc1cc(O)c(Cl)cc1</chem> $C_9H_{11}O_2N_2Cl$
19. [33, 40, 41]	215/217	216.65 Mono. Mass=216.03	 <chem>CN(C)C(=O)Nc1cc(O)c(Cl)cc1</chem> $C_9H_{11}O_2N_2Cl$
20. Standard [32, 35, 40-42, 44-46]	217/219/ 221	219.07 Mono. Mass=218	 <chem>CN(C)C(=O)Nc1cc(Cl)c(Cl)cc1</chem> $C_8H_8ON_2Cl_2$, 1-(3,4-dichloro-phenyl)-3-methylurea

CHAPTER 3 EXPERIMENTAL

Chapter three describes the experimental procedure in the deposition of DLC by dc magnetron sputtering process and the degradation of diuron via EAOP within a microchannel reactor. This chapter is divided into five main parts including materials and chemicals, the dc magnetron sputtering system, microchannel reactor, experimental setup and procedures, and analytical instrument.

3.1 Materials and chemicals

Diuron or 3-(3,4-dichlorophenyl)-1,1-dimethyl urea (99.5% purity) was purchased from Sigma Aldrich. Hydrogen peroxide (H₂O₂) 30% w/w in water was purchased from Carlo Erba. They were used as reference standard compounds. The reagents used as detection of hydrogen peroxide include Potassium iodide (KI) was purchased from Kanto Chemical, Potassium hydrogen phthalate (C₈H₅KO₄), Ammonium molybdate (NH₄)₆Mo₇O₂₄, Sodium hydroxide (NaOH), these chemicals were purchased from Ajax Finechem. All of the chemicals were used in analytical grade. In the sputtering process, the carbon target (99.999% purity) was purchased from Kurt J. Lesker, and Argon gas (99.999% purity) was purchased from Praxair. Finally, the stainless steel 304 grade was used for the substrate.

3.2 DC magnetron sputtering system apparatus

The dc magnetron sputtering system in this work consists of the chamber, dc power supply, rotary pump, diffusion pump, isolated valve, and cooler. The sputtering system is shown in **Figure 3.1**. There are two main parts inside a chamber; magnetron sputtering head with a target at the top of the chamber (diameter of 52 mm) and substrate holder. The magnetron sputtering head was connected with the cathode, and the substrate holder was connected with anode from a dc power supply. The cooler used for removing heat generated from magnetron sputtering head and diffusion pump during operation. The isolated valve between the chamber and the diffusion pump used for controlling the pressure during operation.

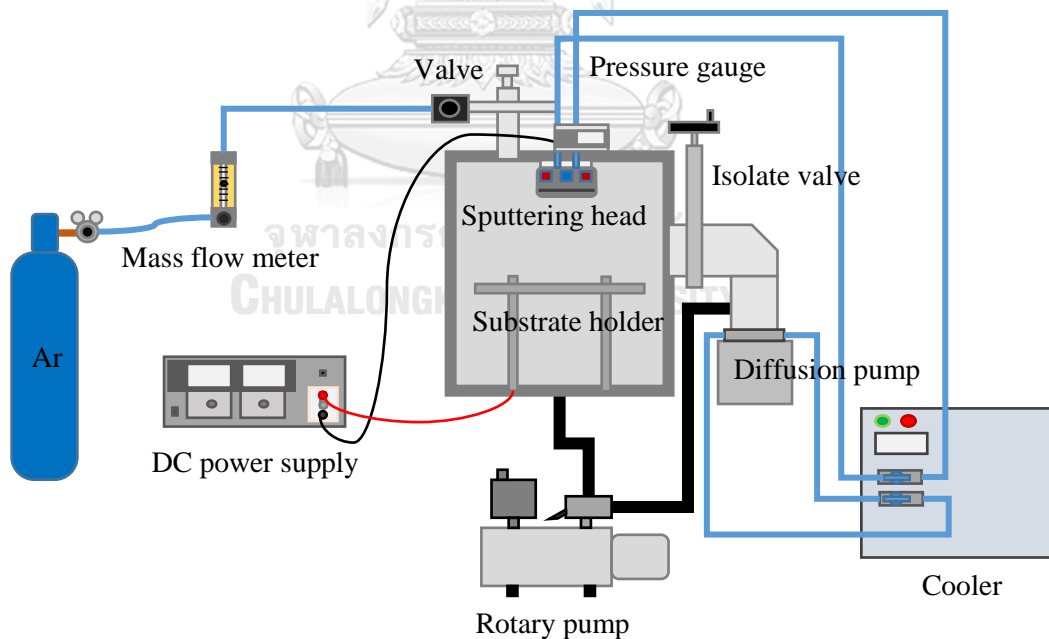


Figure 3.1 The dc magnetron sputtering system

3.3 Microreactor apparatus

Microreactor or microchannel reactor in this work was made from stainless steel. The size of the reactor is 50 mm and 70 mm, in wide and length respectively. The microchannel reactor was used Teflon sheet, the thickness of 250 μm , as the middle of Teflon sheet was cut a hexagonal area (30 mm length, 10 mm width) making placed between two conductive electrodes. The cathode is a stainless steel plate, whereas the anode is a stainless steel modified surface with DLC by dc magnetron sputtering process. The scheme of the microchannel reactor is shown in

Figure 3.2.

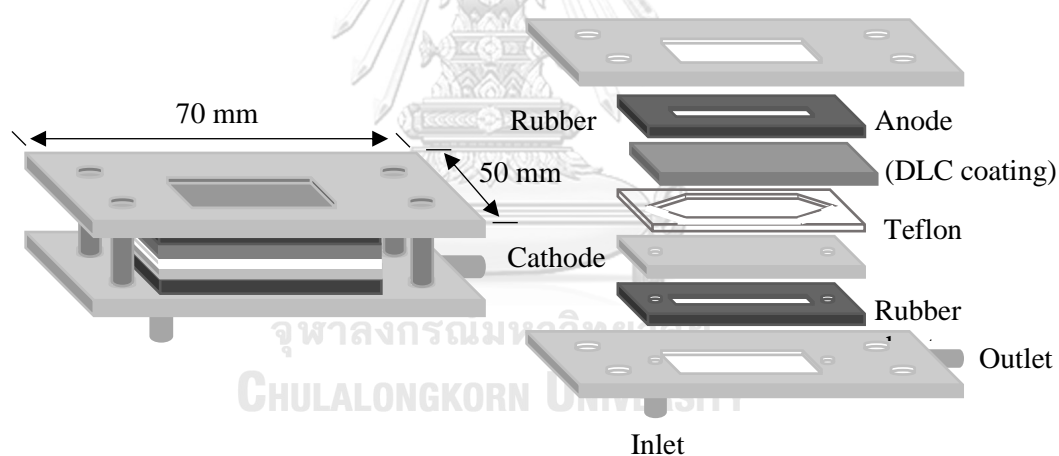


Figure 3.2 Scheme of the microchannel reactor

3.4 Experimental setup and procedures

3.4.1 Titanium coating via dc magnetron sputtering process

The experimental setup of the Ti coating process is shown in Figure 3.1. The rotary pump was evacuated to the base pressure at 1×10^{-2} torr. After that, the diffusion pump with a rotary pump was evacuated to a base pressure at 4×10^{-5} mbar. Then, argon gas from storage tank was entered the sputtering chamber at the flow rate 4 ml/min by mass flow controller. The sputtering target was using titanium target 99.999%. Moreover, the distance of the target and the substrate holder was set at 10 cm. The Ti thin films were synthesized on the surface of stainless steel substrates at room temperature. The sputtering process was performed at operating pressure 10 mtorr and sputtering power 60 W. When the conditions of sputtering controlled as stable, the sputtering would be started coating of Ti on the surface of stainless steel for 30 minutes.

3.4.2 DLC thin films synthesized via dc magnetron sputtering process

The synthesized process, the rotary pump was evacuated to base pressure at 1×10^{-2} torr. After that, the diffusion pump with a rotary pump was evacuated to base pressure. The argon gas from storage tank enters the sputtering chamber at a flow rate of 2 ml/min by the mass flow controller. The sputtering target was using carbon target 99.999%. Moreover, the distance of the target and the substrate holder was set at 5 cm. The DLC thin films were synthesized on the surface of Ti/SS and stainless steel substrates at room temperature. The sputtering process was performed at various operating pressure, in range the of 5 mtorr to 25 mtorr. Moreover, the base pressure is varied in the range of 4×10^{-5} mbar to 7×10^{-5} mbar. The sputtering power was fixed

at the 30 W. When the conditions of sputtering controlled as stable, the sputtering would start the coating of DLC on the surface of the substrate for the time required, in the range of 10 to 30 minutes.

3.4.3 Electrochemical advanced oxidation process (EAOP) of degradation procedure in a microreactor

In the experiment, diuron solution was prepared the concentration of 10 ppm in deionized water. The diuron solution flowed through the microreactor by a syringe pump. The syringe pump was set the total flow rate at 1.5 ml/h to fixed mean residence time at 100 s. Before starting to apply electric current to the electrodes, the diuron solution was flowed through the electrodes for 1 hour making the adsorption of diuron took place all of the surfaces of the DLC thin film electrodes. Subsequently, the dc power supply was used for supplying current across the gap of the electrodes. The electric current was fixed at 1 mA. The outlet solution from the microreactor was sampling and analyzed in reaction time. Diagram of the EAOP experiment is shown in **Figure 3.3**.

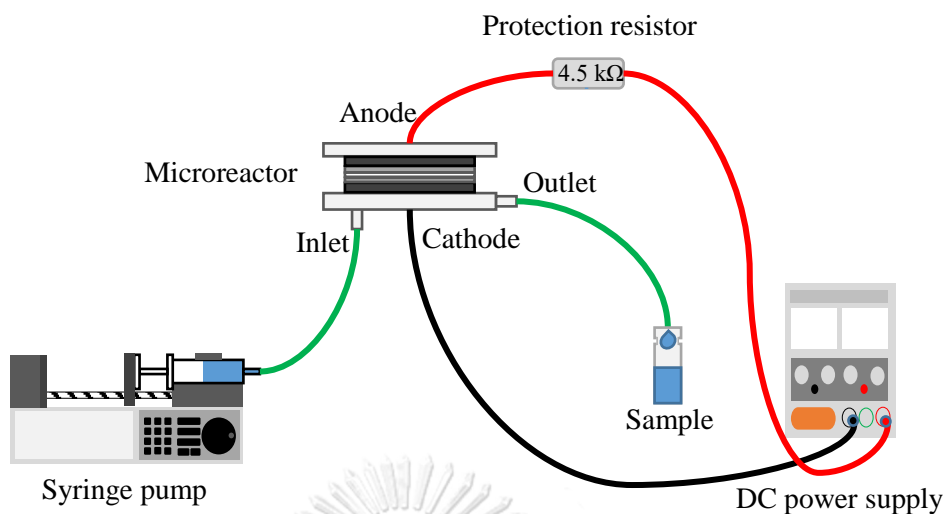


Figure 3.3 Diagram of the experimental setup of the EAOP of degradation procedure in a microreactor

3.5 Measurement of Thickness

The thickness of DLC thin films was measured by ZeGage™ 3D Optical Surface Profiler. This instrument can measure 2D and 3D of the surface. The 2D and 3D photography can be measured in micrometer scale. The half of the stainless steel substrate was coated with DLC thin films. The height between the surface of stainless steel and the surface of DLC is the thickness of DLC thin films.

3.6 Electrically Resistive Measurement

In the experiment, the resistance of DLC thin films was measured by two-wire resistive measurement method. This method is conventional and accurate for measurement of electrical resistance. The two-wire probe was drop at the surface of DLC thin film. The very small direct current from hp DC voltage source was applied to the unknown resistive thin film, in the range of -0.2 to 0.2 A. The Voltage drop across two probe was detected by the resistive measurement program in step-side of 0.01 A. The program displayed the relationship between measured voltage and applied current. This relation could calculate the resistance of DLC thin film from the slope of graph followed Ohm's law.

3.7 Analytical Instruments

3.5.1 X-ray Photoelectron spectroscopy

X-ray Photoelectron Spectroscopy (XPS) is a qualitative and quantitative method. This instrument can characterize the chemical properties at the surface, such as type of elements, chemical structure, chemical bonding, and the oxidation state of the atoms. In this work, this instrument is used for detecting the structures of carbon and bonding types of the synthesized DLC thin films. The Al K_{α} X-ray with energy 1486.6 eV was used for characterization. The photograph of X-ray photoelectron spectroscopy is shown in **Figure 3.4**.



Figure 3.4 The photograph of X-ray photoelectron spectroscopy

3.5.2 UV-Visible spectrophotometer

UV-Visible (ultraviolet and visible) spectrophotometry is a technique that used for the light absorbance analyzed at a specific wavelength to determine the concentration. In this work, this instrument is used for measuring the concentration of hydrogen peroxide (H_2O_2) by the colorimetric method at wavelength 350 nm. The colorimetric method uses the two reagents to detecting the hydrogen peroxide. The reagent A is the mixture of 0.01 g of ammonium molybdate, 0.1 g of sodium hydroxide, and 3.3 g of potassium iodide in 50 ml of DI water. Furthermore, the reagent B is the purity 1 g of potassium hydrogen phthalate in 50 ml of DI water. The mixing of 1 ml of sample, 1 ml of reagent A, and 1 ml of reagent B are used to determining the concentration of hydrogen peroxide. The photograph of UV-Visible spectrophotometer is shown in **Figure 3.5**.



Figure 3.5 UV-Visible spectrophotometer

3.5.3 High performance liquid chromatography (HPLC)

High-performance liquid chromatography (HPLC) is a specific form of column chromatography. In this work, this instrument is used to measure the concentration of diuron at retention time around 3.12 minutes at 254 nm with C18 column (phenomenex, Luna 5 μ , 250 x 4.6 mm). The mobile phases were used acetonitrile (70% v/v) and deionized water (30% v/v). The total flow rate is 1.5 ml/min, and the column temperature is 30 °C. The injection volume of sample is 20 μ L. The photograph of HPLC is shown in **Figure 3.6**.



Figure 3.6 High performance liquid chromatography (HPLC)

3.5.4 TOC analyzer

Total Organic Carbon (TOC) analyzer is commonly used for the determination of organic concentration in water. TOC is a measurement of organic carbon molecules contaminated in water. In this work, this instrument is used detection the solution outlet from microchannel reactor, measured as carbon concentration. The sample solution was used for analysis approximately 12 ml. The temperature used to analysis of the TOC is 680 °C. The photograph of TOC analyzer is shown in **Figure 3.7**.



Figure 3.7 The photograph of TOC analyzer

3.5.5 Liquid chromatography-mass/mass spectrometer (LC-MS/MS)

In this work, this instrument is used detection the intermediates of diuron from EAOP within a microchannel reactor. MS spectra are acquired in ultra-scan mode between m/z 50 – 250 in positive ionization. The mobile phases were used acetonitrile (70% v/v) and deionized water (30% v/v). The total flow rate is 1 ml/min, and the column temperature is 30 °C. The injection volume is 100 μ L. The column for separation of intermediates was used the C18 column (phenomenex, Luna 5 μ , 250 x 4.6 mm).

CHAPTER 4

RESULTS AND DISCUSSION

This chapter discusses all results of diamond-like carbon (DLC) thin films synthesis used as an electrode for electrochemical advanced oxidation process (EAOP) in diuron degradation. The chapter consists of five main parts; (1) synthesis of DLC thin films using dc magnetron sputtering process, (2) diuron degradation behaviors using the DLC thin films and graphite sheet electrode, (3) influence of titanium as an interlayer between DLC thin films and substrate on the corrosion, (4) influence of the DLC thin film properties on diuron degradation behaviors, and (5) comparison between the properties of DLC thin film electrodes in behaviors of diuron degradation.

4.1 Synthesis of diamond-like carbon thin films using dc magnetron sputtering process

The diamond-like carbon DLC thin films were successfully synthesized via dc magnetron sputtering process. The synthesized DLC thin films were measured the thickness by ZeGage™ 3D Optical Surface Profiler for measuring the deposition rate. The variation of the operating pressure (in the range of 5 mtorr to 25 mtorr) affects the deposition rate of DLC thin films as shown in **Figure 4.1**. The increased operating pressure increases the number of argon atoms in the chamber which increase the collision of sputtered carbon atoms with the argon atoms leading to scattering of sputtered carbon atoms. Therefore, the mean free path has small distance at high operating pressure. Hence, the sputtered carbon atoms cannot easily travel to the

surface of the substrate. Nevertheless, variation of base pressure in the range of 4×10^{-5} to 7×10^{-5} mbar in the synthesis does not significantly affect the deposition rate. The operating pressure was fixed during the variation of the base pressure. Consequently, the number of residual gases was changed but the number of argon atoms is the same for each base pressure. Therefore, the mean free path in the chamber is invariable because the size of argon atoms gas is bigger than the other residual gases. Accordingly, the sputtered carbon atoms can travel to the surface of the substrate at nearly same rate at 15 nm/min for each base pressure.

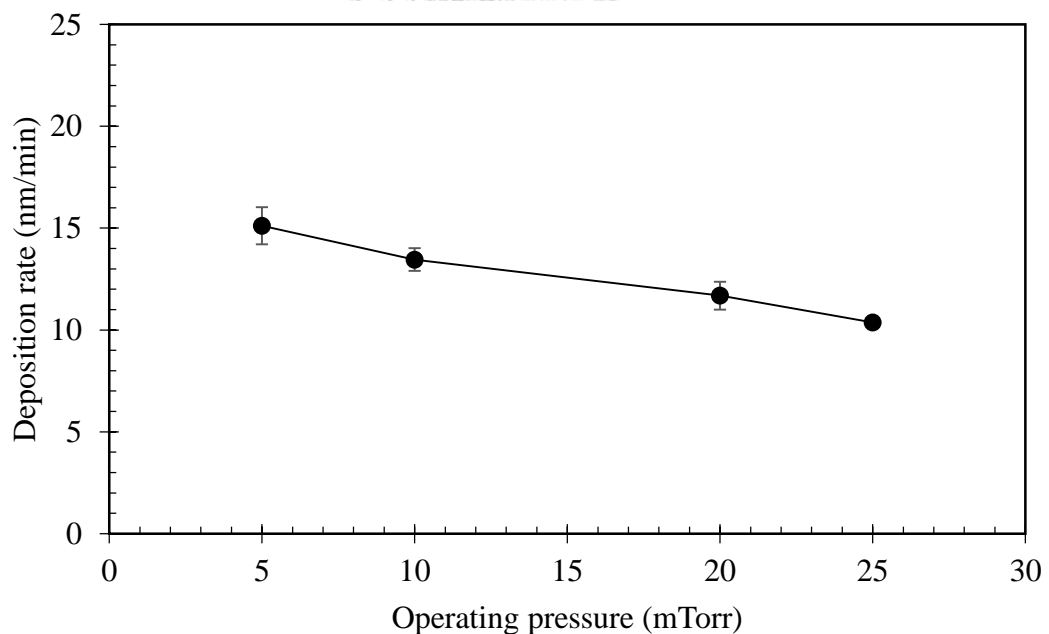


Figure 4.1 The deposition rate of DLC thin films under various operating pressure in the range of 5 mtorr to 25 mtorr

All of the DLC thin films coated from various conditions were characterized using X-ray Photoelectron Spectroscopy (XPS) before using an electrode. The results

show that the survey spectra of XPS show the peaks of C1s, O1s, and N1s at the binding energy 284.3 eV, 531.3 eV, and 399.3 eV respectively [29]. The survey spectra of XPS at the surface of the substrate coated with DLC thin film using operating pressure 10 mtorr is shown in **Figure 4.2**. The synthesized DLC thin films have the highest intensity of carbon (C 1s). The peaks of nitrogen and oxygen molecules indicate that there was some residual air (O₂ 21% and N₂ 79%) inside the chamber during a deposition process. Moreover, there was no iron (Fe) peak which indicates that the DLC thin films cover all surface of the stainless steel substrate. The thickness measured by ZeGage™ 3D Optical Surface Profiler of DLC thin films is in the range of 350 – 500 nm. Therefore, the DLC thin film coated on the surface of the stainless steel substrate has the potential for using as the electrochemical electrode.

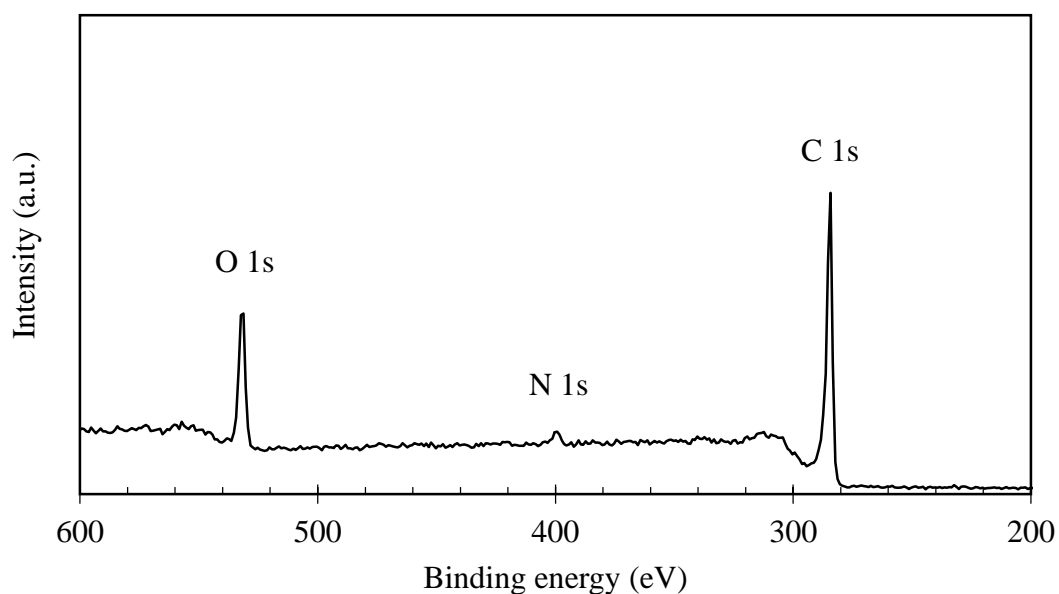


Figure 4.2 The survey spectra of XPS on the surface substrate coated with DLC thin films by dc magnetron sputtering process at operating pressure 5 mtorr

The C1s peak is used in deconvolving for determination of the carbon structures and chemical bonds on the surface of the DLC thin films electrodes. The results from the characterization of the carbon structures are shown in **Figure 4.3**. The C1s peak of DLC thin films contains the sp^2 hybridized carbon structure (C=C) peak and the sp^3 hybridized carbon structure (C-C) peak at binding energy 284.4 eV and 285.2 eV respectively. Not only the C1s peak contains sp^2 and sp^3 carbon structure, but also it has the deconvolution peaks at binding energy at 283.5 eV, 286.5 eV, 287.8 eV, and 289.4 eV corresponding to carbon to hydrogen bond (C-H) at 283.5 eV and carbon to oxygen bonds (C-O, C=O, and O-C=O) at 286.5 eV, 287.8 eV, and 289.4 eV respectively [29-31]. These chemical bonds indicate that there were residual hydrogen and oxygen during the deposition process. These molecules represent H₂O molecules from moisture in the ambient surrounding.

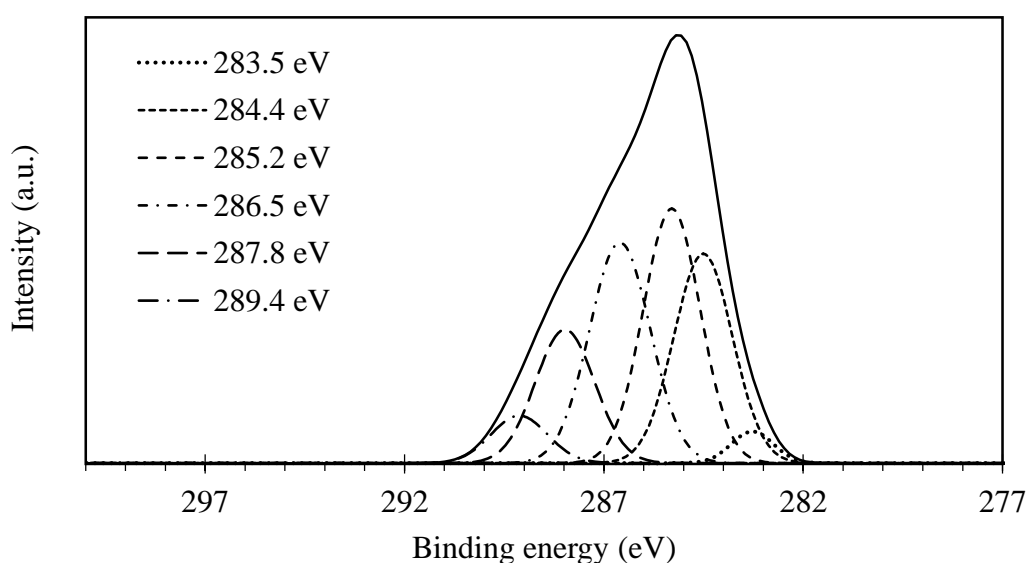


Figure 4.3 Deconvolution of the C1s peak of diamond-like carbon synthesized by dc magnetron sputtering process at operating pressure of 5 mtorr

From the results of deconvolution of the C1s peak, varying operating pressure and base pressure can affect to three properties of the DLC thin films electrode as follows; the sp^2 -to- sp^3 ratio, the hydrogen contents (C-H), and the oxygen contents (C=O). Although the operating pressure effect on the deposition rate, the operating pressure is not significantly affect the sp^2 -to- sp^3 ratio. However, the decrease of the sp^2 -to- sp^3 ratio was observed when the base pressure increased. The synthesized thin film is called DLC because it has the highest fraction of carbon. Moreover, the ratio of sp^2 -to- sp^3 is less than 1 (in the range of 0.87 to 0.52), so this thin film has the diamond-like more than graphite structures. The DLC thin films synthesized under various base pressure were different sp^2 -to- sp^3 ratio as shown in **Figure 4.4**. From the figure, increasing of base pressure results in lower of the sp^2 -to- sp^3 ratio due to the carbon atom bonding with other residual molecules. The variation of this factor affects the number of residual gases in the chamber. These residual molecules decrease when decreasing the base pressure. Therefore, the amount of sp^2 structure depends on the base pressure.

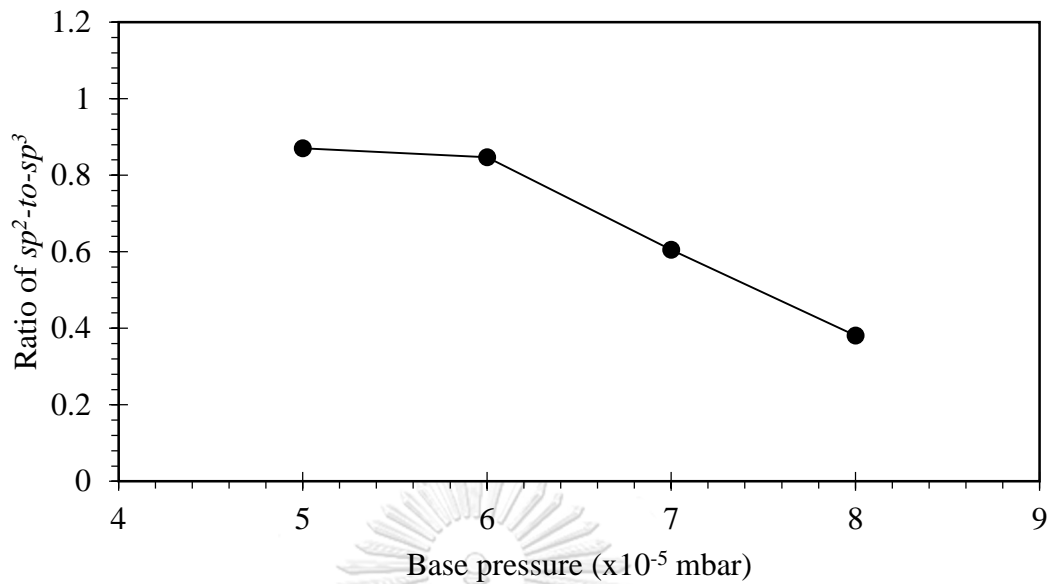


Figure 4.4 Ratio of sp^2 -to- sp^3 of the DLC thin films electrodes deposited under various the base pressure

The rise of C-H bond of the DLC thin film was clearly observed the base pressure increase, as shown in **Figure 4.5**. The moisture from water molecules is the source of hydrogen that can bond with the sputtered carbon atoms (formed C-H bond) during the sputtering process. Therefore, the increasing of base pressure at room temperature increases the residual moisture in the chamber, resulting in increase the amount of hydrogen atom.

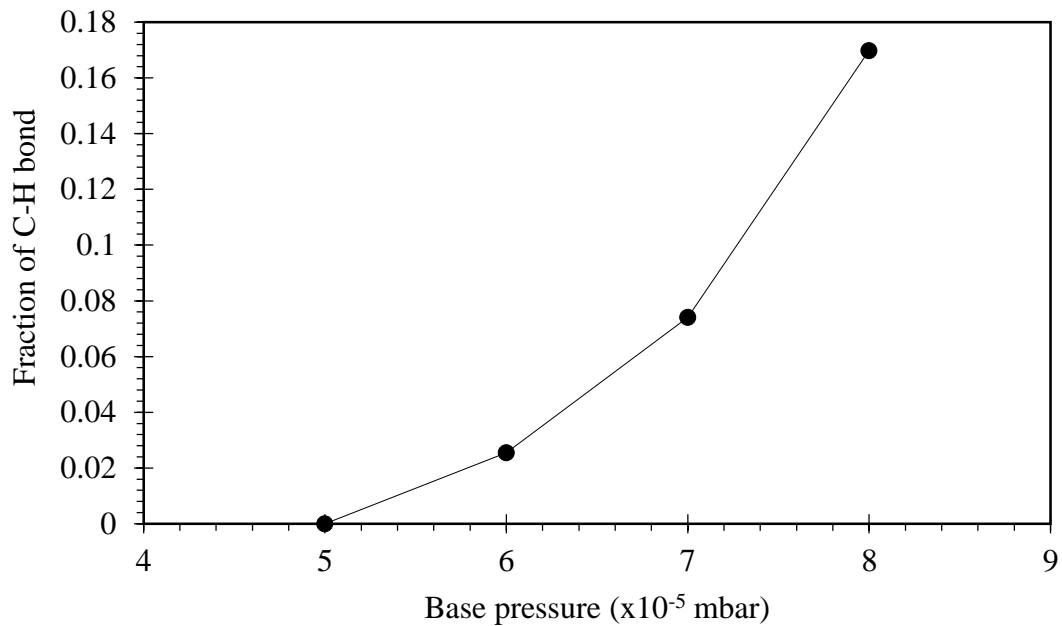


Figure 4.5 Fraction of C-H bond of DLC thin films electrodes deposited under various the base pressure

The increasing of the operating pressure results in higher C=O bond because the oxygen molecules can bond with the sputtered carbon atoms (C=O, C-O). As shown in **Figure 4.6**. For the synthesis of DLC thin films, when the operating pressure was varied, the base pressure was fixed. Hence, the number of residual molecules is the same for each condition. Therefore, the operating pressure affects the fraction of oxygen molecules in the chamber. The air which contains oxygen and nitrogen is the source of oxygen molecules. Consequently, the C=O bond increases with increasing the operating pressure. However, insignificantly different of fraction of C-O in the DLC thin films are noticed after increasing the operating pressure.

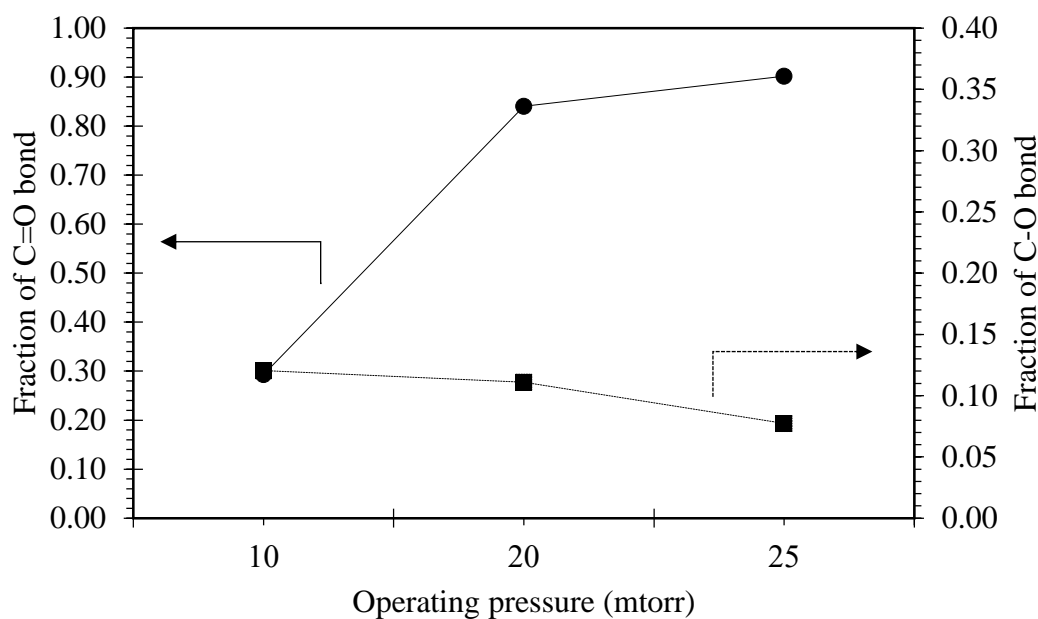


Figure 4.6 Properties of the DLC thin films electrodes deposited under various the operating pressure

To summarize, varying the operation condition, i.e., operating pressure, and base pressure has considerable influence on the properties of synthesized DLC thin films. The synthesized DLC thin films electrodes can be divided into three properties from the results of XPS such as structures of carbon (sp^2 -to- sp^3), carbon to hydrogen bond (C-H), and carbon to oxygen bond (C=O). Consequently, these synthesized thin films have the potential to be used as the electrochemical electrode for the study of the DLC properties effect on diuron degradation.

4.2 The behaviors of diuron degradation using the DLC thin films and graphite sheet electrode

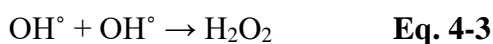
The synthesized DLC thin films electrodes were used as an electrode for electrochemical advanced oxidation process (EAOP) in a microchannel reactor. The behaviors of diuron degradation of DLC thin films were compared to commercial graphite electrode. The ability of diuron degradation of the DLC thin films and graphite electrodes depends on the number of generated hydroxyl radicals (OH°) at the surface of an anode. The hydroxyl radicals are generally generated from dissociation of water molecules when the electric current was applied to the electrode according to the **Eq. 4-1** [9].



These hydroxyl radicals rapidly react and decompose diuron compounds near the surface of the electrode because these radicals are the highly active oxidizer according to the **Eq. 4-2**.



Moreover, the hydroxyl radical can also interact with another hydroxyl radicals resulting in the formation of hydrogen peroxide (H_2O_2) near the electrode surface according to **Eq. 4-3** [9]. Hence, the H_2O_2 molecules are considered to be one of the represent the hydroxyl radicals. Therefore, the electrochemical performance of the DLC thin films electrodes was investigated by measuring the concentration of H_2O_2 generated during EAOP within a microchannel.



The DLC thin films electrode can generate the steady hydrogen peroxide concentration with the small difference compared to the graphite electrode. Both electrodes can produce the hydrogen peroxide more than the stainless steel electrode as shown in **Figure 4.7**. This result demonstrates that the DLC thin films electrode has the potential for using as an anode in the degradation of diuron within a microchannel reactor.

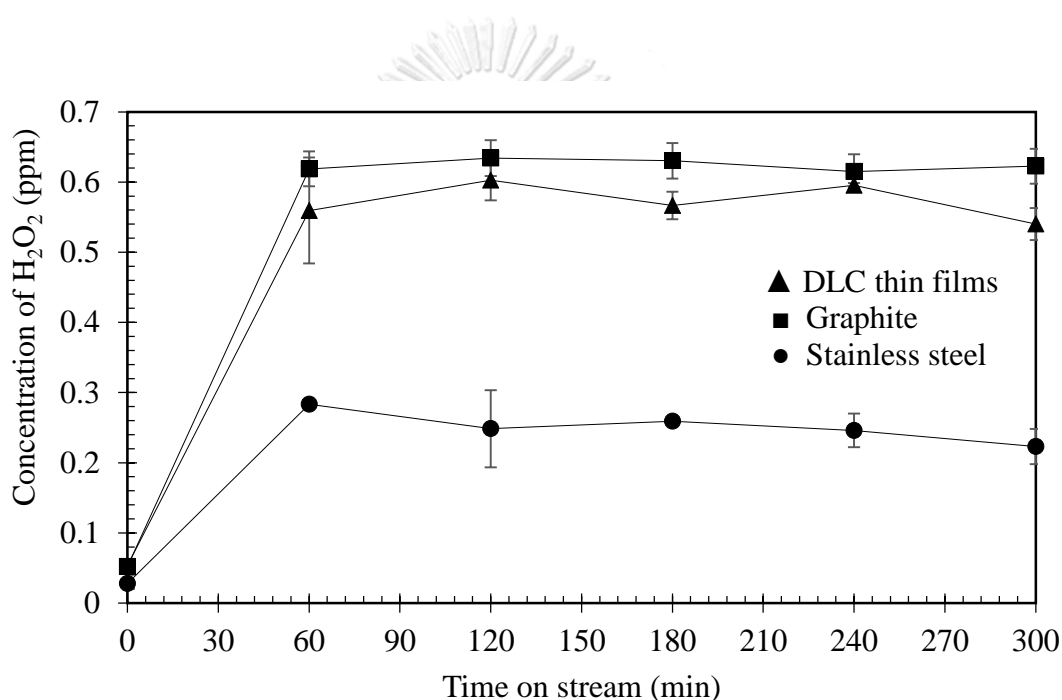


Figure 4.7 The correlation between the concentrations of hydrogen peroxide generated in deionized water and time on stream various the electrodes

As illustrated in **Figure 4.8**, the ability of diuron degradation of graphite and stainless steel electrodes are 93% and 19% respectively. These electrodes are able to degrade diuron contaminated steadily because graphite electrode has a high thickness (1 mm). The corrosion does not effect on the ability of diuron degradation of the graphite electrode. For the DLC thin films electrode, unsteady of diuron degradation

can be observed. The highest performance of the DLC thin films electrode is up to 70% with 100 seconds of residence time within a microchannel reactor. Although the DLC thin films electrode can generate the steady hydrogen peroxide concentration with small difference compared to the graphite electrode, it can degrade less diuron than the graphite electrode. The decreased performance of diuron degradation occurs from the amount of carbon at the surface of the DLC thin films that change during the degradation process because of the corrosion.

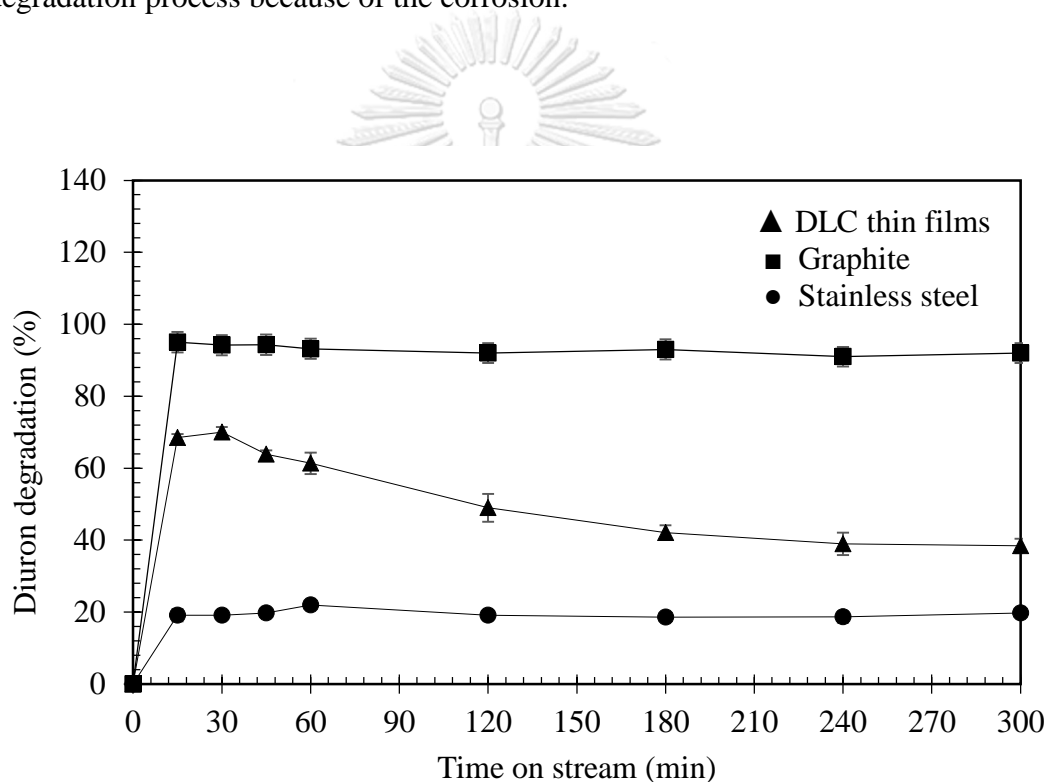


Figure 4.8 The correlation between the percentage of diuron degradation and time on stream various the electrodes

The performance of DLC thin film electrode is stable after the shoot up because the DLC thin film has stable properties. The DLC thin film electrode is corroded the graphite-like structure during EAOP. This increase the fraction of

diamond-like structure. Therefore, the corrosion is decreased this leading to the stable properties of the electrode, so the performance of diuron degradation is stable. The performance of DLC thin films electrodes does not approach to the performance of stainless steel electrode because the DLC thin films electrodes still have the remaining carbon at the surface.

The graphite electrode has stable the performance of diuron degradation because it has a thickness of 1 mm. Consequently, the corrosion does not effect on the performance while the graphite electrode has a high corrosion rate. This corrosion was investigated by the total organic carbon in solution using TOC analyzer. The corrosion rate during EAOP is shown in **Figure 4.9**. However, the corrosion rate and degradation performance of the DLC thin films electrode are unsteady because this electrode has a thin thickness in the range of 450 to 550 nm. So, the amount of carbon at the surface of electrode is significantly affected by the corrosion leading to the unsteady of diuron degradation.

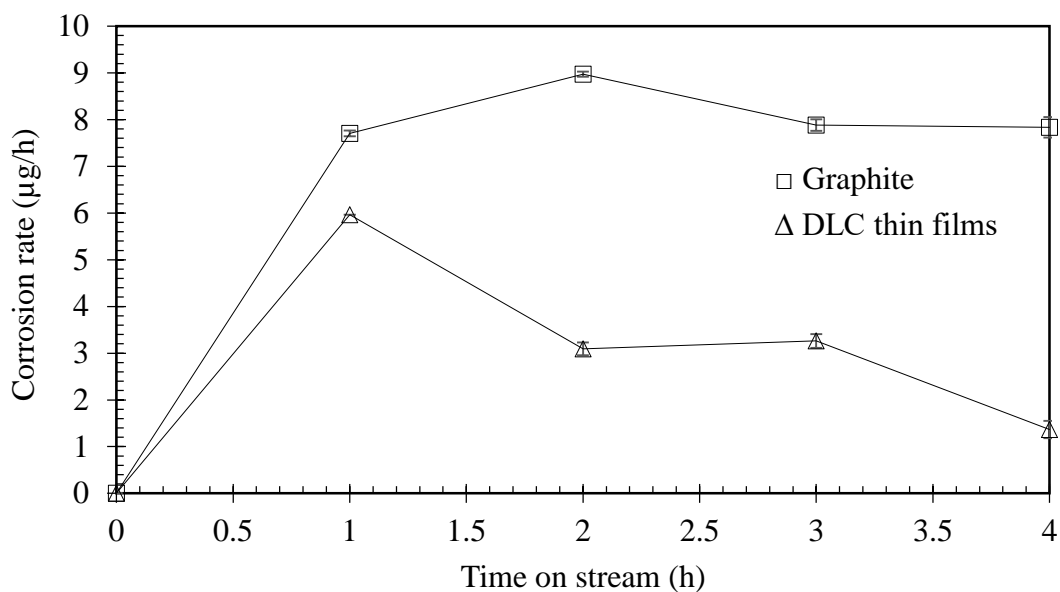


Figure 4.9 The corrosion rate of carbon materials electrodes occurred during EAOP within a microchannel reactor

The rise of the degradation performance at the initial time of the DLC thin films electrode does not occur from the dynamic of the microchannel reactor. This behavior is improved by reusing the electrode as shown in **Figure 4.10**. The performance at the initial time of reused electrode is not rising over than previous using. Consequently, this behavior depends on the surface property of the electrodes.

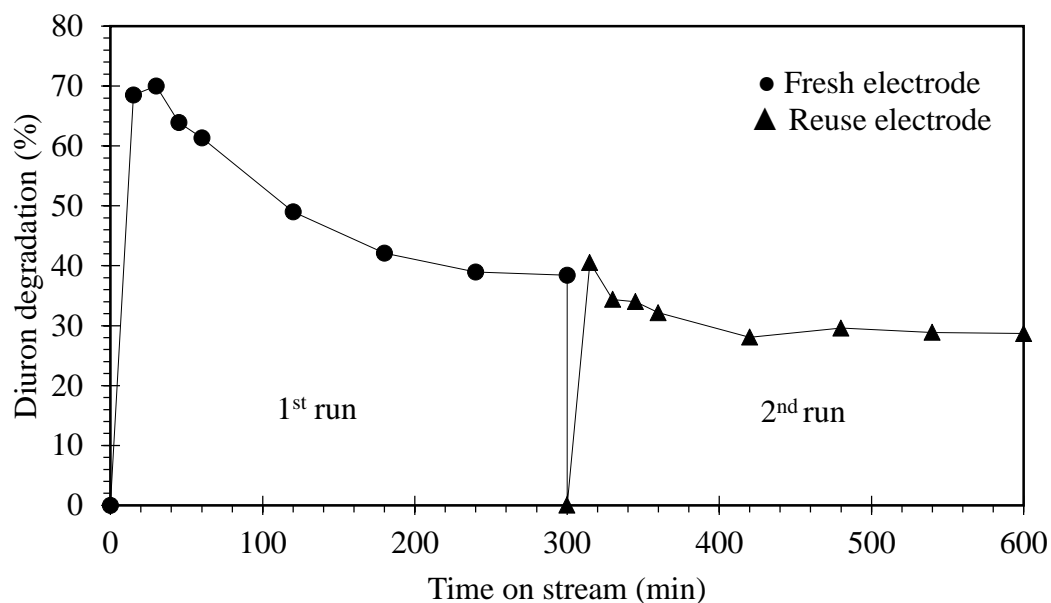


Figure 4.10 The correlation between the percentage of diuron degradation and time on stream of using the DLC thin films electrode

The concentration of hydrogen peroxide generated from the DLC thin films electrodes is stable with slightly lower than of graphite electrode, its degradation performance is unstable and lower than the graphite electrode. Therefore, the hydrogen peroxide generated from the DLC electrode does not only represent the hydroxyl radicals from according to **Eq. 4-2**. This behavior may be affected by either the carbon atoms contaminated in DI water or the dissolved oxygen in DI water. Because the colorimetric method for detecting the hydrogen peroxide interferes with the signal of corroded carbon atoms, the effect of carbon atoms contaminated was investigated by removing the hydrogen peroxide using the scavenger (NaCO_3) [47]. The results of removed hydrogen peroxide are shown in **Figure 4.11**. The absorbance of DI water before and after removing the hydrogen peroxide is a negligible difference. However, the outlet solution from EAOP within a microchannel reactor

before and after removing hydrogen peroxide is greatly different due to hydrogen peroxide generated in the solution. Because of carbon atoms from the corrosion, the absorbance after removing hydrogen peroxide of the outlet solution is difference with the concentration of hydrogen peroxide in inlet solution (DI water). Therefore, the carbon atoms from the corrosion affect the signal of the concentration of the hydrogen peroxide. However, the corroded carbon atom is insignificantly affected the amount of hydrogen peroxide generated via EAOP.

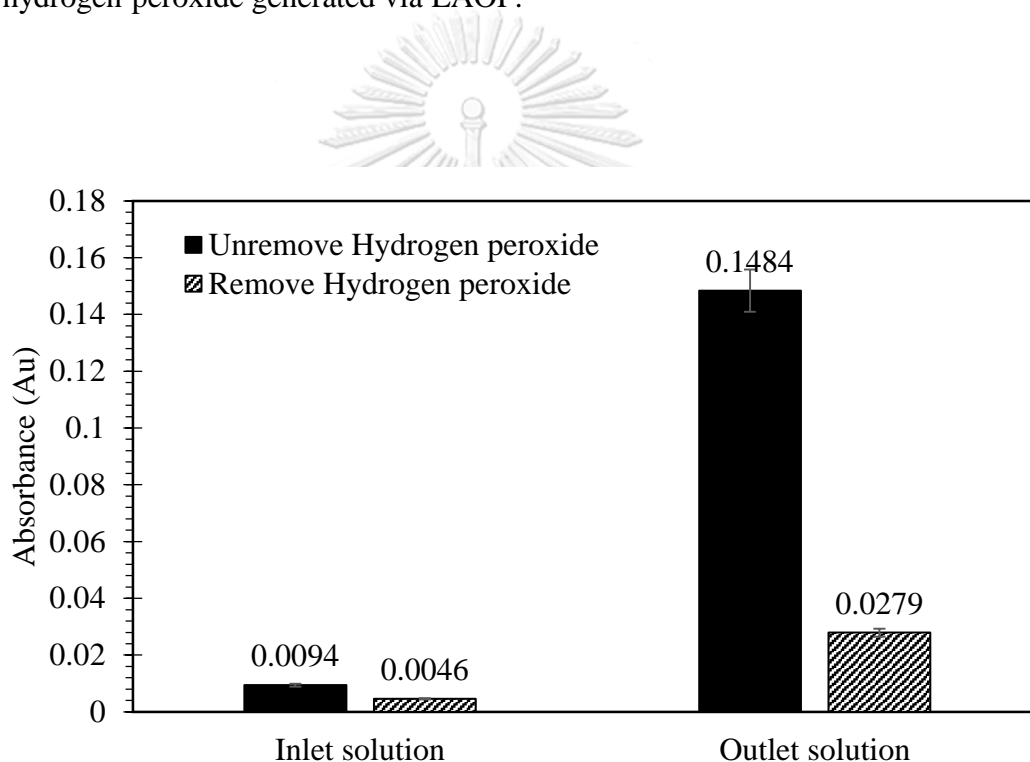


Figure 4.11 The absorbance at wavelength 350 nm of deionized water and outlet solution from a microchannel reactor

The effect of dissolved oxygen in DI water on hydrogen peroxide generated was investigated by removing dissolved oxygen using nitrogen gas purging about 45 minutes. This method can remove oxygen dissolved in DI water up to 97% [48]. As

shown in **Figure 4.12**, removing oxygen in the inlet solution has no effect on the hydrogen peroxide generation of graphite electrode, but this removed oxygen solution significantly affects the generation of hydrogen peroxide of DLC thin films electrode. The hydroxyl radicals are generally generated from dissociation of water molecules at the surface of an anode. Therefore, the generation of hydroxyl radicals depends on the surface area of the electrode. The graphite electrode can generate lots of hydroxyl radicals because it has good electrical conductivity, so the dissolved oxygen is not a significant effect on the concentration of hydrogen peroxide. However, the DLC thin films electrode has the electrical conductivity lower than the graphite electrode, so the dissolved oxygen is a significant effect on the hydrogen peroxide concentration.

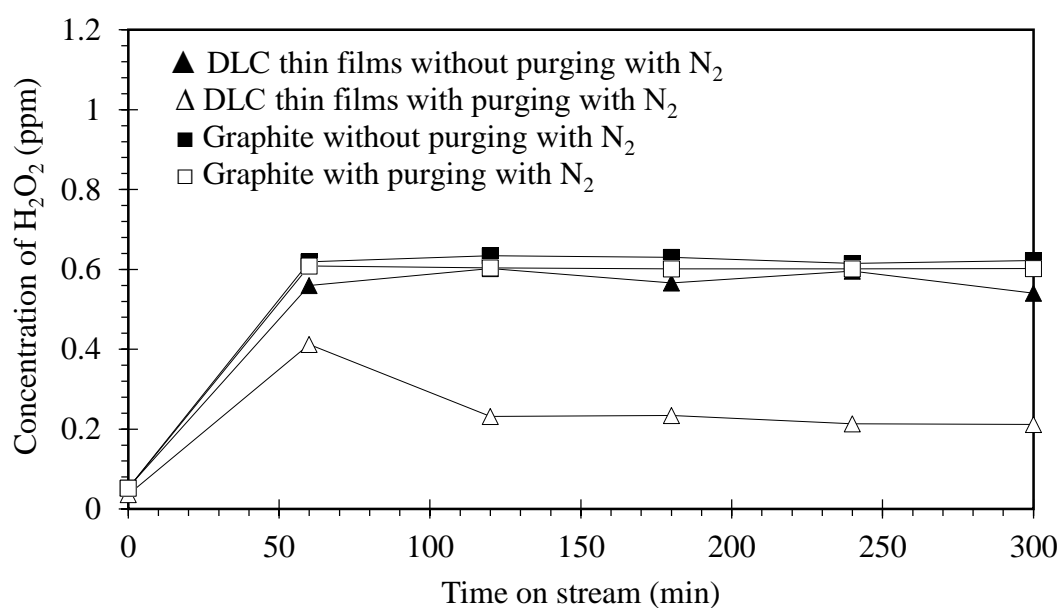
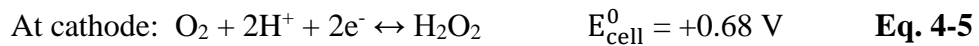
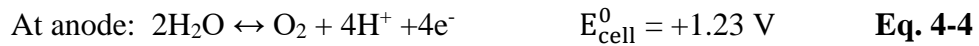


Figure 4.12 The correlation between the concentrations of hydrogen peroxide generated in deionized water and time on stream

This behavior indicates that the dissolved oxygen in DI water significantly affect the concentration of hydrogen peroxide because the hydrogen peroxide can be formed by dissolved oxygen according to **Eq. 4-4 to 4-5** [49, 50].



However, the DLC thin films should have a thickness of 1 μm because the working time of DLC thin films is increased. However, the thick DLC films increase the electrical resistance. Due to the heat generated during the synthesis process, it makes high temperature when over one hour of sputtering time. The high-temperature DLC thin films are oxidized with remaining oxygen molecules in the chamber. This causes damage to the DLC thin films. Properties of the carbon electrodes using for degradation of diuron via advanced oxidation process are shown in **Table 4.1**.

Table 4.1 Properties of the carbon electrodes using for degradation of diuron via advanced oxidation process

Electrodes	Thickness	R_{specific} ($\text{k}\Omega/\text{nm}$)	Removal of diuron	Residence time (s)	Type of reactor
BDD [6, 51]	$\sim 1\mu\text{m}$	2.31×10^{-7}	95.6%	8000	Batch
Graphite [52]	1mm	4	95.6%	14400	Batch
Graphite [10]	1mm	4	90%	100	Microchannel
DLC	$\sim 500 \text{ nm}$	76-192	70%	100	Microchannel

The boron-doped diamond (BDD) is the best electrical conductivity, but the process for synthesis of BDD is complicated. Although graphite electrode is better performance of diuron degradation than DLC thin films, the DLC thin films can improve the corrosion because the DLC thin films electrode occurs the corrosion less than the graphite electrode during the EAOP within a microchannel. The DLC thin film has potential to be used as electrochemical electrode because it can generate hydroxyl radicals and decompose the diuron contaminated.



4.3 Effects of Ti used as an interlayer between the substrate and DLC thin films on the behaviors of diuron degradation

The synthesized DLC thin film is corroded during EAOP. Therefore, the Titanium was used for improving the corrosion. Titanium is the most inert material for mechanical and biomedical uses because it has excellent properties, i.e., high strength, high conductivity, and high corrosion resistance. Moreover, the Ti layer can form the titanium carbide (TiC) with the sputtered carbon atoms. Furthermore, this interlayer has high adhesion with the surface of the stainless steel substrate. In this work, the Ti thin film was used as an interlayer to enhance the adhesion between DLC thin films and the surface of substrate. In this work, the effects of using Ti as an interlayer between DLC thin films and substrate were investigated by behaviors of corrosion and diuron degradation.

The effect of Ti as an interlayer on the generation of hydrogen peroxide is shown in **Figure 4.13**. These results indicated that the hydrogen peroxide could be generated on the surface of SS, SS/Ti, SS/DLC, and SS/Ti/DLC electrodes via the EAOP within a microchannel reactor. The SS/Ti/DLC and SS/DLC electrodes can generate the hydrogen peroxide higher than the metal electrodes because the metal electrodes are not inert. The SS electrode generates equal the hydrogen peroxide to the SS/Ti electrode indicating that the Ti layer does not affect the performance of the electrode. Moreover, both SS and SS/Ti electrodes generate the amount of hydrogen peroxide less than the carbon electrodes because the electrode for electrochemical must be inert. Consequently, the SS and SS/Ti electrodes are unsuitable for using in EAOP because both electrodes are reactive surface. From XPS results, the coated

DLC thin films cover all of the substrate surfaces because the Ti thin film has a thickness of 400-500 nm. Moreover, the Ti thin film is coated via a dc magnetron sputtering process, so the Ti is coated all over the substrate surface. The Ti interlayer has no effect on the ability of diuron degradation. Hence, there is no significant difference in hydrogen peroxide concentration generated by the SS/DLC and SS/Ti/DLC electrodes. Therefore, the properties of Ti coated on stainless steel substrate does not impact on the performance of the electrode. To sum up, the ability of diuron removal depends on the properties of the DLC thin films electrodes.

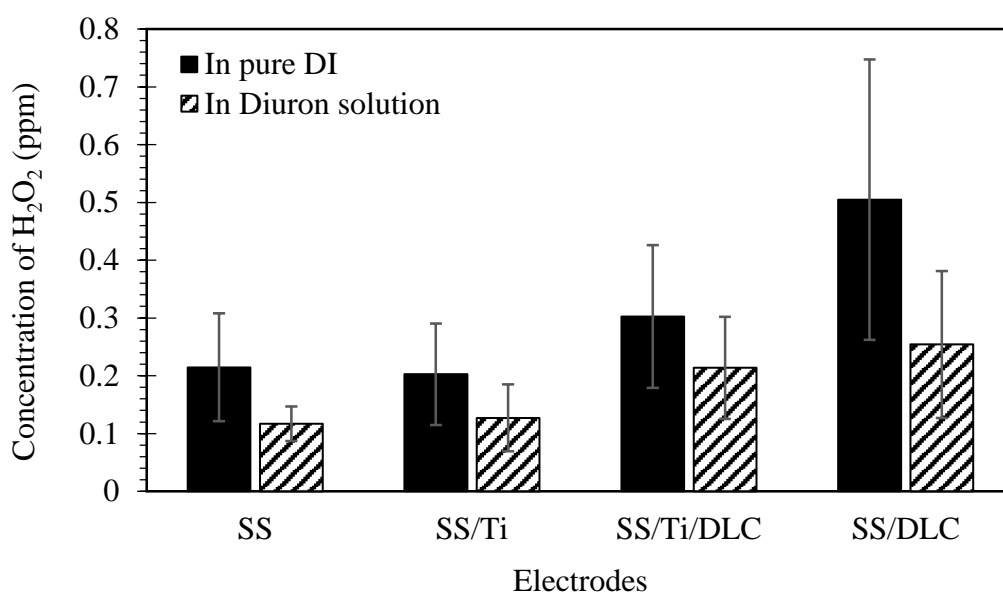


Figure 4.13 The concentration of hydrogen peroxide generated via EAOP using different electrodes within a microchannel reactor

The corrosion of DLC was investigated using TOC analyzer. The corrosion of the SS/DLC and SS/Ti/DLC electrodes has insignificant effect on the performance of

diuron degradation. However, the Ti interlayer between the surface of the stainless steel substrate and DLC thin films have small decrease the corrosion of the electrode as shown in **Figure 4.14**. The corrosion rate of SS/Ti/DLC electrode small reduces because the Ti layer can form the titanium carbide (TiC) with the sputtered carbon atoms. Furthermore, this interlayer has high adhesion with the surface of the stainless steel. Therefore, using Ti as an interlayer can enhance the adhesion of the DLC thin film and surface of the electrode. However, the corrosion is not depending on the adhesion because the corroded carbon occurred from the oxidation reaction at the surface of the electrode. Therefore, the corrosion of SS/DLC and SS/Ti/DLC electrodes are not different because it depends on the properties of DLC.

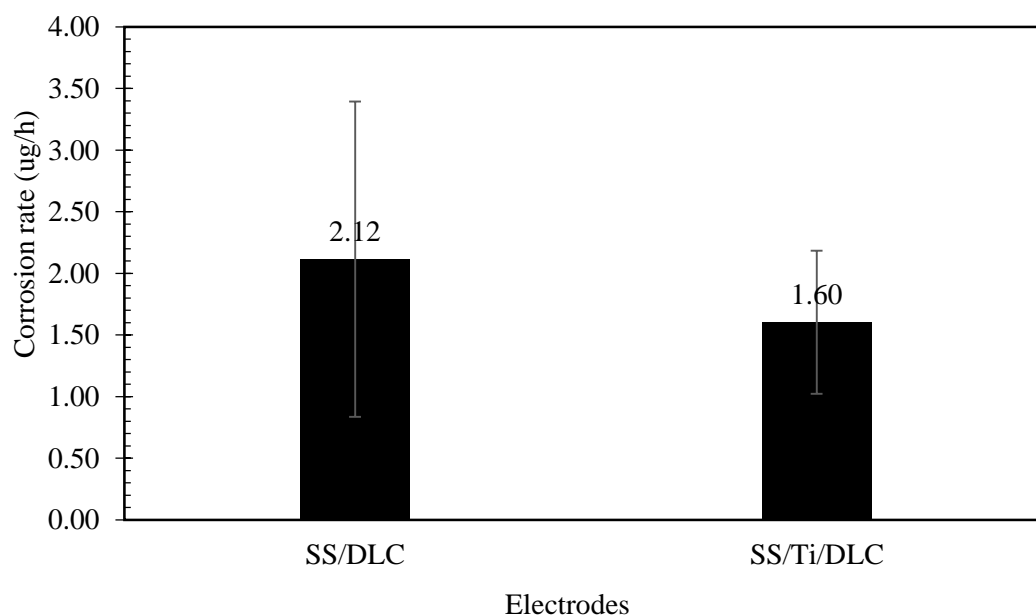


Figure 4.14 The effect of using Ti interlayer on the corrosion rate of the DLC thin films electrodes occurred during the EAOP within the microchannel reactor

The surface properties of the SS/Ti/DLC electrode before and after used in EAOP investigated by XPS as shown in **Figure 4.15**. The electrode after used in EAOP contains the peaks of Ti 2p and Fe 2p at binding energy 457.9 eV and 710.9 eV respectively. It is found that after used in EAOP, the amount of Ti element is detected from electrode surface. This indicates that the DLC layer is corroded. The XPS Penetration depth is about 10 nm from the surface of the sample. From the results, the SS/Ti/DLC electrode before using in EAOP does not have the signal of titanium and iron. However, this electrode after using EAOP has the signal of carbon vary less than the signal of titanium. Moreover, it has the signal of iron this indicate that the carbon is corroded to the surface of titanium. Not only the DLC thin films have the corrosion but also the Ti layer is corroded during the EAOP because the amount of Ti element is detected in outlet solution.

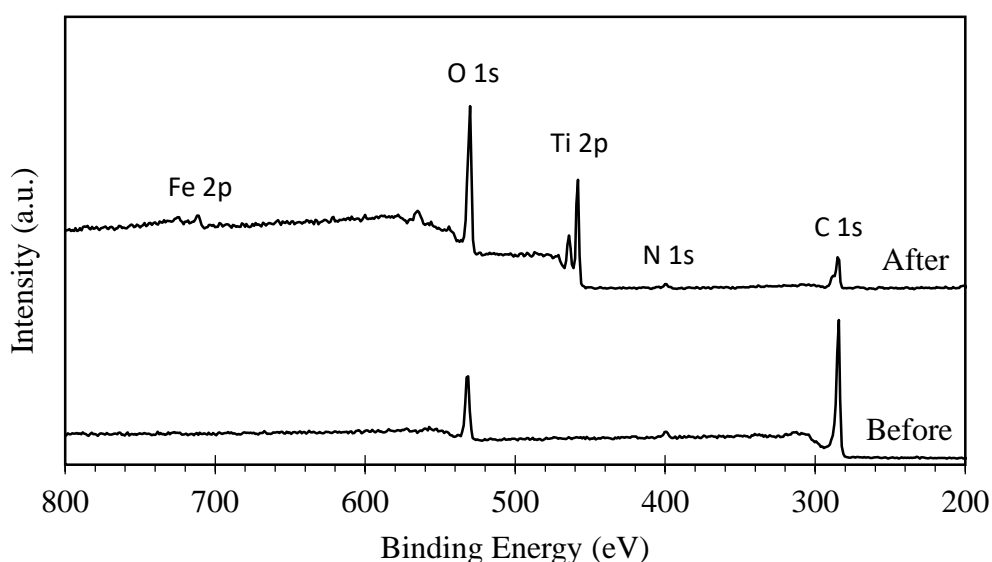


Figure 4.15 The survey spectra of XPS at the surface of the electrode before and after using in EAOP within the microchannel reactor

Although the Ti interlayer does not improve the corrosion of DLC thin films electrode, using the Ti-contained thin films electrode, small red-brown particles were found suspending in the outlet solution. However, using the DLC thin films electrode without the Ti interlayer no small red-brown particles was found in outlet solution. These suspended particles in solution were investigated and characterized by ICP as shown in **Figure 4.16**. The DLC thin films electrode without the Ti interlayer contain no Cr and Ni elements from the corrosion and little Fe element from the substrate corrosion because when the DLC thin film is corroded to the surface of the substrate, the anode and cathode have the same stainless steel.

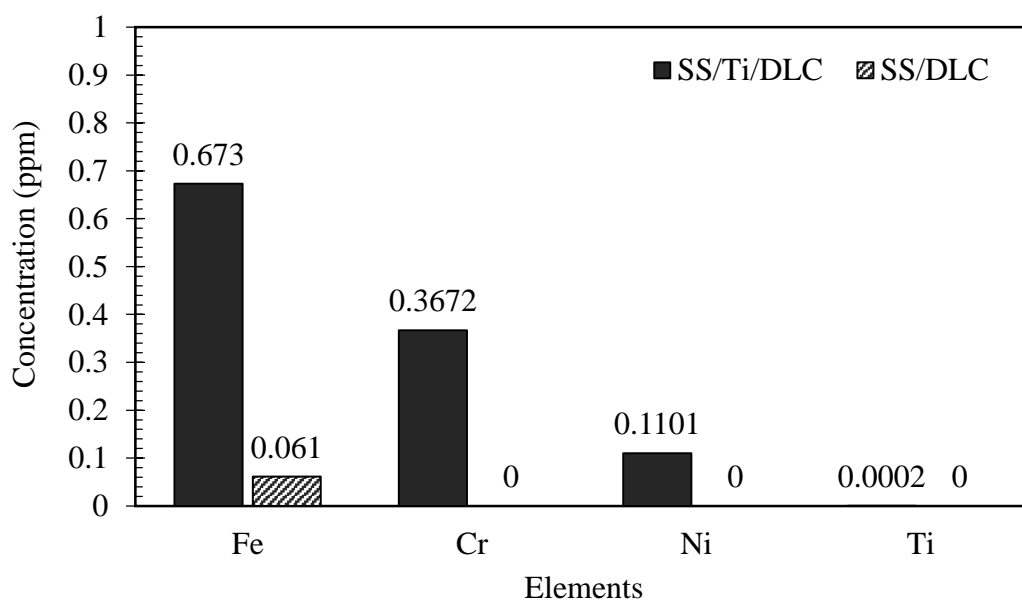
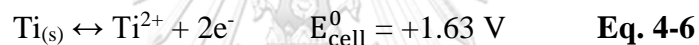
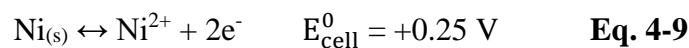
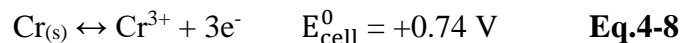
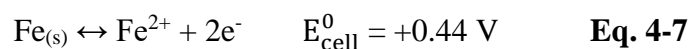


Figure 4.16 The concentration of contaminated elements detected in the outlet solution via the EAOP within a microchannel reactor

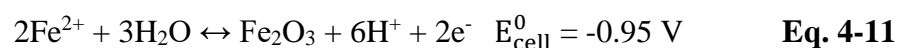
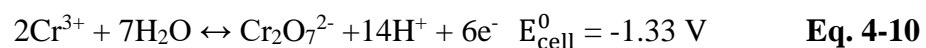
The Ti interlayer does not significantly decrease the corrosion of DLC thin films, so the DLC thin films are corroded to Ti surface. This makes the metal corrosion of electrode. Consequently, The DLC thin films electrode with the Ti interlayer have the corrosion of Fe, Cr, and Ni because when the DLC thin film is corroded to the surface of the substrate, the anode and cathode are not the same stainless steel material. The difference of the standard electrode potential causes the stainless steel in cathode and Ti interlayer in anode to corrode, so using Ti interlayer electrode leads to more corrosion than SS/DLC electrode. Therefore, the outlet solution of using the Ti interlayer includes the Fe, Cr, Ni, and Ti. At the anode, the corrosion of Ti element occurs from the oxidation reaction of Ti according to **Eq. 4-6**.



At the cathode, the 304 stainless steel consists of the Fe 68.6%, Cr 19%, Ni 9%, and others 3.4%. Thus, the standard potential is difference compared to Ti when DLC thin film was cored. The corrosion of these metal occurs from the oxidation reaction of the electrode according to **Eq. 4-7 to 4-9**.

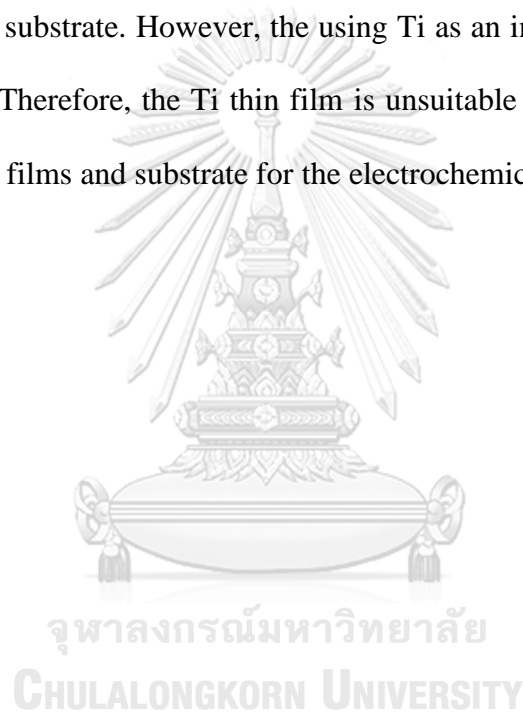


The Fe^{2+} and Cr^{3+} can be easily formed their oxide with water molecules according to the **Eq. 4-10 to 4-11**.



Hence, the outlet solution from the electrode with the Ti interlayer contains Fe, Cr, Ni, and Ti. The Fe_2O_3 and $\text{Cr}_2\text{O}_7^{2-}$ have the red-brown color, so the particles in the outlet solution are the Fe_2O_3 (iron oxide) and $\text{Cr}_2\text{O}_7^{2-}$ (chromium oxide) particles suspended in the solution during the EAOP within a microchannel reactor.

The corrosion of the DLC thin films electrodes is insignificantly decreased with using the Ti as an interlayer between the DLC thin films and the surface of the 304 stainless steel substrate. However, the using Ti as an interlayer lead to occurs the mantel corrosion. Therefore, the Ti thin film is unsuitable to be used as an interlayer between DLC thin films and substrate for the electrochemical electrode.



4.4 Effects of DLC thin films electrodes properties on behaviors of diuron degradation

Properties of the DLC thin films electrode synthesized via dc magnetron sputtering can be divided from XPS into three main properties; structures of carbon (sp^2 -to- sp^3), carbon to hydrogen bond (C-H), and carbon to oxygen bond (C=O). The properties of the electrodes were used to study the behaviors of the performance of diuron degradation, the electrode corrosion, and production of intermediates via the EAOP within the microchannel reactor.

4.4.1 Effects of carbon structures of DLC thin films electrodes

Properties of the DLC thin films electrodes were used to investigate effect of the carbon structure as shown in **Table 4.2**. Structure of two electrodes consist of different the ratio of sp^2 -to- sp^3 , but the fraction of C-O and C=O is not a significant difference. This indicates that these two electrodes have similar amount of C-O and C=O bonds. Moreover, These electrodes have negligible the amount of C-H bond, so these electrodes are suitable to study the effect of the carbon structure on diuron degradation.

Table 4.2 Properties of the DLC thin films electrodes with different carbon structure

Electrodes	sp^2 -to- sp^3	C-H fraction	C=O fraction	C-O fraction	O-C=O fraction
No.1 (●)	0.52	0	0.16	0.10	0.018
No.2 (▲)	0.70	0	0.16	0.22	0.021

The most important property of the electrochemical electrode is the ability of an electron transferred or electrical conductivity because the generation of hydroxyl radicals normally depending on electron transferred according to **Eq. 4-1**. In this research, electrical resistance has been investigated by two-wire method because it could representability of electrode to provide electron transfer through the electrodes. The electrical resistance of the carbon electrodes with different ratio of sp^2 -to- sp^3 is shown in **Figure 4.17**. The synthesized DLC thin films are Ohmic conductor material because the relationship of applied current and measured voltage is linear. The resistance of DLC thin films is not different when measured in different directions because the ohmic material can transfer electron as the same every direction. The high sp^2 content of the DLC thin film has the electrical resistance lower than the high sp^3 content electrode because the sp^2 (C=C) carbon structure of the carbon has a grain region smaller than the sp^3 (C-C) structure. The grain size has an effect on electron transferred because electron can easily transfer in a small grain region [53]. Furthermore, the sp^2 carbon structure also has a residual valence electron which can be transferred, but the sp^3 carbon structure does not have a residual valent electron. Thus, sp^2 carbon structure has the electrical resistance lower than the sp^3 carbon structure.

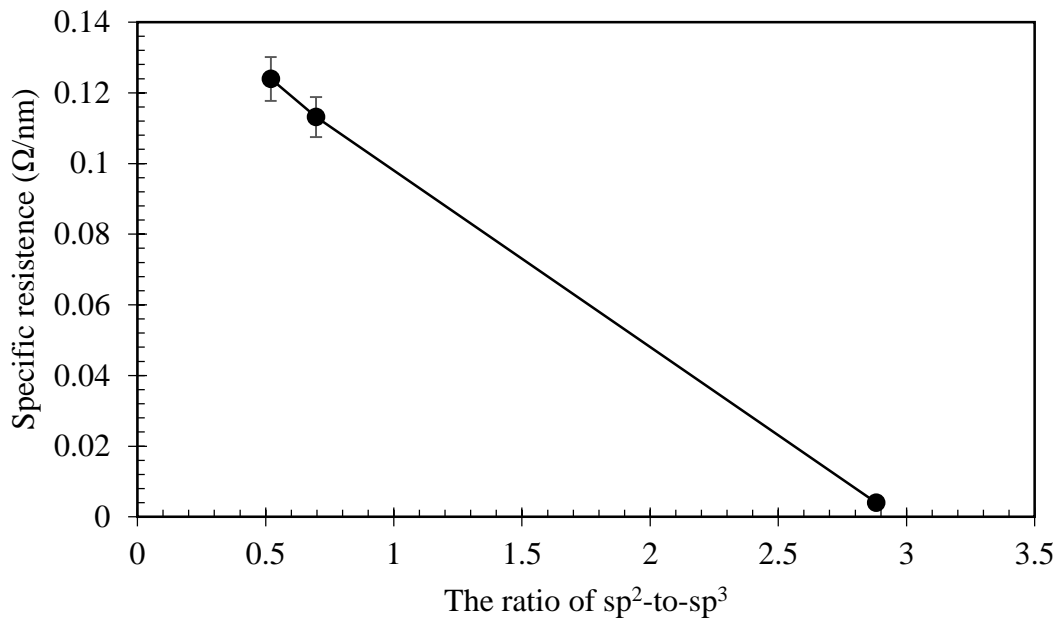


Figure 4.17 Correlation of electrical resistance and ratio of sp^2 -to- sp^3 structure in DLC thin films electrodes

The EAOP performance of the electrodes with various carbon structure was investigated by measuring amount of hydrogen peroxide generated is shown in **Figure 4.18**. The generation of hydrogen peroxide depends on the sp^2 -to- sp^3 ratio in structure of the carbon electrode. The amount of hydrogen peroxide is high with the high sp^2 -to- sp^3 ratio because sp^2 structure has a residual valence electron and small grain size. This property has an effect on the electrical conductivity so sp^2 carbon structure can provide electron transfer more effectively than the sp^3 structure. Therefore, the DLC thin films electrode with high sp^2 content can generate higher amount of highly active radicals than that of the sp^3 content. Moreover, the amount of hydrogen peroxide in pure DI water is higher than in diuron solution. This indicates that the hydroxyl radicals is used to decompose the diuron molecules.

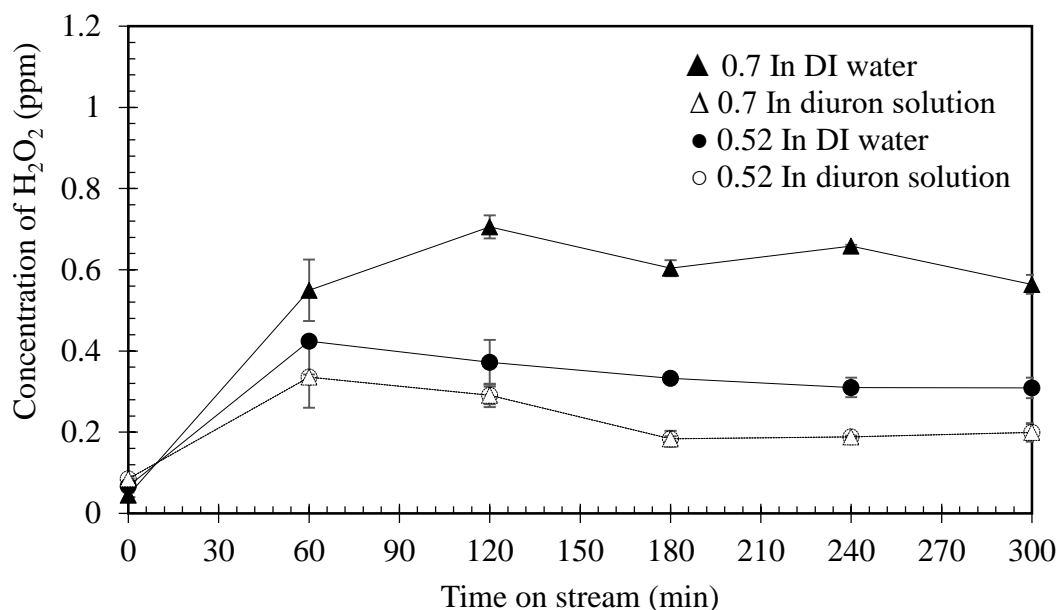


Figure 4.18 Correlation of concentration of hydrogen peroxide generated and time on stream at various the ratio of sp^2 -to- sp^3 of the DLC thin films electrode

Although the generation of hydrogen peroxide is steady, the performance of diuron degradation is unsteady because the generation of hydrogen peroxide has been a significant effect from dissolved oxygen in solution this confirms with removing the dissolved oxygen in the solution. The performance of diuron degradation with various the sp^2 -to- sp^3 ratio is shown in **Figure 4.19**. The DLC thin films electrode with the highest sp^2 -to- sp^3 ratio (0.70) possess the highest degradation performance, up to 65 percent by 100 seconds of residence time within a microchannel reactor because the electrode produced the hydroxyl radicals in large quantities. However, it could be observed that the performance of diuron degradation was unsteady. This behavior indicates that the corrosion of carbon has occurred at the surface of electrode during the degradation process because performance of the electrode depends on the surface properties.

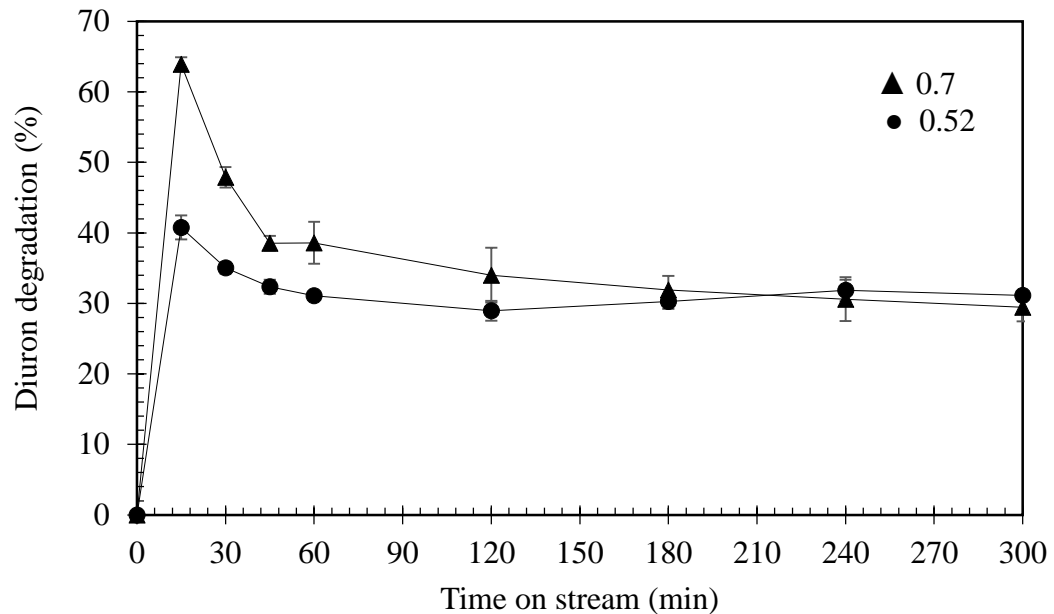


Figure 4.19 Correlation between performance of diuron degradation and time on stream various the ratio of sp^2 -to- sp^3 of DLC thin films

However, the performance of diuron degradation decreases during the EAOP at initial time, but the performance approach to steady at a long time with the EAOP. This behavior occurs from the transition of properties at the surface of electrodes. The surface property at the surface of DLC thin films electrode is not a significant difference after 300 minutes as shown in **Figure 4.20**. Performance of the highest initial ratio of sp^2 -to- sp^3 decreases more than the lowest ratio because its property is a significant difference after using for EAOP. The transition of this property is affected by the corrosion. The DLC thin films electrode has the ratio of sp^2 -to- sp^3 this represents the residual carbon at the surface of the electrodes.

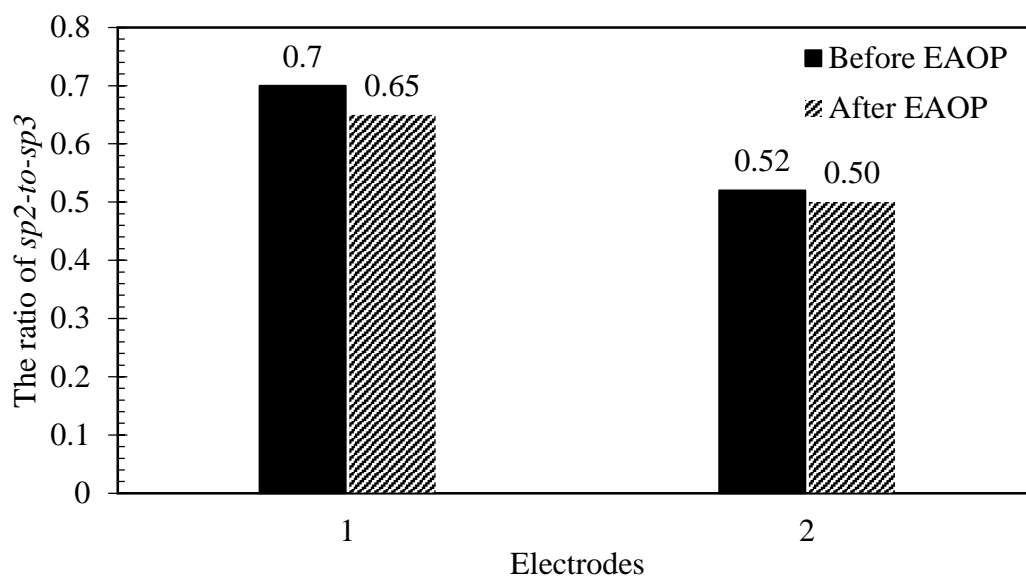


Figure 4.20 The ratio of sp^2 -to- sp^3 of DLC thin films electrodes after using for EAOP within the microchannel reactor

The corrosion of DLC thin films electrodes was investigated by measuring total organic carbon contaminated in the solution as shown in **Figure 4.21**. Corrosion of the DLC thin films electrodes depends on carbon structures. Results show that, electrode with higher sp^3 (C-C) content is less corrosive than the others because sp^3 structure enhances hardness and stability in carbon material. Diamond is one of materials that consist of the sp^3 structure. Corrosion of DLC thin films electrodes is unsteady because the corrosion depends on the amount of carbon at the surface of electrode. Corrosion of the DLC thin films electrodes normally occurs owing to oxidation reaction of carbon structure at the electrochemical electrode.

The corrosion rate of DLC thin films electrodes depends on the amount of carbon and properties at the electrode surface. The DLC thin films electrode with the highest sp^2 -to- sp^3 ratio has the highest corrosion at the initial time because it has high

sp^2 content. The corrosion rate is not a significant difference after a long time reaction because the properties of DLC thin films are indifferent. Because of the decreasing the amount of carbon at the surface of electrode, the corrosion rate is unsteady during the EAOP.

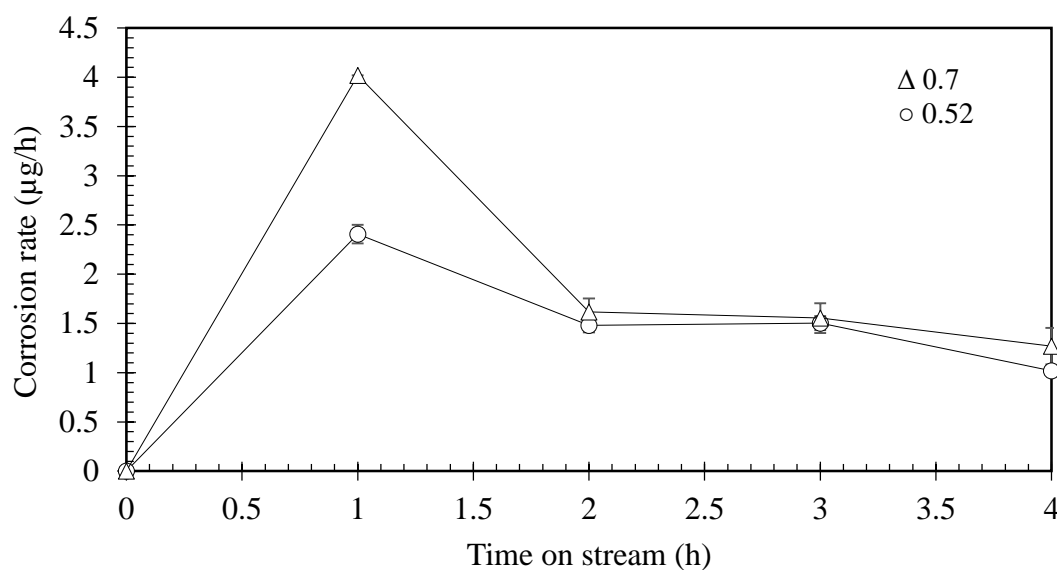


Figure 4.21 The correlation between corrosion rate and time on stream of DLC thin films electrode various ratio of sp^2 -to- sp^3

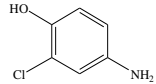
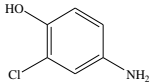
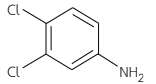
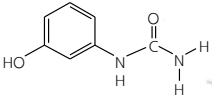
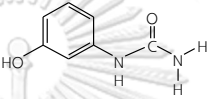
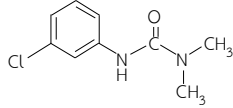
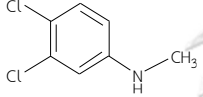
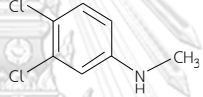
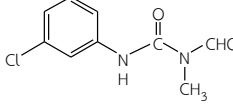
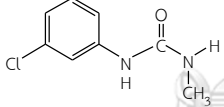
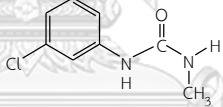
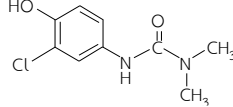
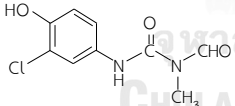
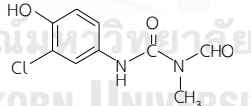
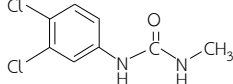
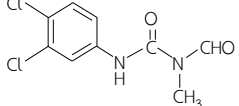
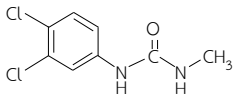
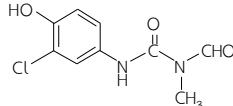
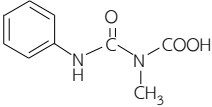
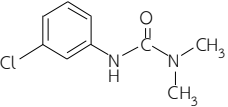
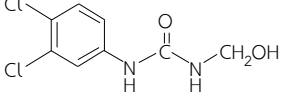
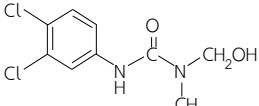
The corrosion mechanism of DLC thin films occurs because the molecules of water forming OH groups with carbon defect site. C-OH groups can be oxidized with water molecules at high potential [54]. Moreover, the corrosion did not only occurs from oxidation of C-OH bond but also it occurs from attacking of hydroxyl radicals. The hydroxyl radicals are a strong oxidizer when carbon surface attacked with hydroxyl radicals. These highly active radicals were generated from dissociation of water molecules at the surface of an anode according to the **Eq. 4-1**. Therefore, the

hydroxyl radicals can be adsorbed on the carbon surface. These highly active radicals can be attacked on another form of corroded carbon and carbon dioxide. The attacking of hydroxyl radicals on the surface carbon depends on stability of the carbon structure since the sp^3 structure is stronger than sp^2 structure. Consequently, corrosion of DLC thin films electrode depends on the ratio of sp^2 -to- sp^3 .

Moreover, the ratio of sp^2 -to- sp^3 has an effect on intermediates produced from the decomposition of diuron during EAOP within a microchannel reactor as shown in **Table 4.3**. The possible intermediates were investigated using LC-MS/MS. Consider it should be noted that intermediates no. 6 and no. 7 have a different position of hydroxyl radicals attacking. In comparison, the intermediates are significantly different from graphite electrode because the graphite electrode can generate more hydroxyl radicals. Therefore, a difference of sp^2 -to- sp^3 ratio had produced some different intermediates owing to the number of hydroxyl radicals generated and the position of oxidizing.

In summary, the sp^2 -to- sp^3 ratio of the DLC thin film electrode affects the behaviors of diuron degradation, i.e., degradation performance, corrosion, and intermediates via EAOP within the microchannel reactor.

Table 4.3 Intermediates produced during diuron degradation using DLC thin films electrodes with various ratio of sp^2 -to- sp^3 via EAOP within the microchannel reactor.

No.	The ratio of sp^2 -to- sp^3		
	0.52	0.70	2.88 (graphite)
1			
2			
3			
4			
5			
6			
7			
8			

4.4.2 Effects of C-H bond in DLC thin films electrodes

Not only the carbon structure affects diuron degradation but also the C-H bond in DLC thin films affects diuron degradation. The properties of DLC thin films electrodes were used to investigate the effects of the C-H bond as shown in **Table 4.4**. Each DLC thin film electrode has different fraction of C-H bond, but the ratio of sp^2 -to- sp^3 is not a significant difference. It could imply that the three DLC thin films electrodes have similarity composition of sp^2 and sp^3 carbon structure. Moreover, the electrodes have different fraction of C-O bond, but this property has insignificantly effect on degradation of diuron. The different C-O bond in DLC thin film does not effect on generation of hydrogen peroxide and diuron degradation. Therefore, the electrodes are suitable for studies the effect of the C-H bond in DLC thin film electrode on diuron degradation.

Table 4.4 Properties of DLC thin films electrodes with different amount of C-H bond

Electrodes	sp^2 -to- sp^3	C-H fraction	C=O fraction	C-O fraction	O-C=O fraction
No. 1 (●)	0.87	0	0.25	0.18	0.071
No. 2 (▲)	0.85	0.025	0.15	0.26	0.051
No. 3 (■)	0.84	0.25	0.12	0.30	0.242

The ability of electron transferred of the electrochemical electrode has a significant effect on performance of electrode. The electrical resistance of carbon electrodes with various fraction of C-H bond is shown in **Figure 4.22**. The electrical resistance represents mobility of electron transferred. The highest amount of C-H bond in DLC thin films electrode has the lowest electrical resistance because DLC

thin film with C-H bond (a-C:H) has a small grain region [31, 53]. The grain region has an effect on electron transferred because the electron can easily transfer in a small grain region. Consequently, the highest fraction of C-H bond possesses the best electrical conductivity.

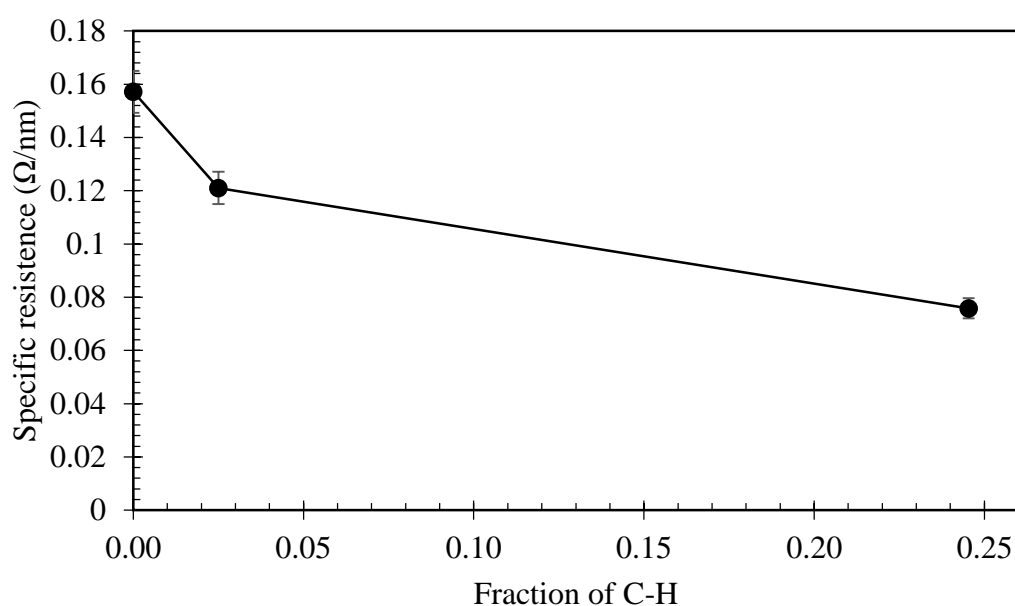


Figure 4.22 Correlation between electrical resistance and the fraction of C-H bond in DLC thin film electrode

The amount of hydrogen peroxide is used to investigate the performance of EAOP of DLC thin films electrode with various C-H fraction. The generation of hydrogen peroxide depends on fraction of C-H bond in DLC thin film electrode as shown in **Figure 4.23**. The highest fraction of C-H bond of the electrode can generate the highest amount of hydrogen peroxide because of the lowest electrical resistance. The generation of hydroxyl radicals usually depending on electron transferred

according to **Eq. 4-1**. Moreover, the amount of hydrogen peroxide in diuron solution is less than the amount of hydrogen peroxide in pure DI water because hydroxyl radicals are used to decompose the diuron molecules.

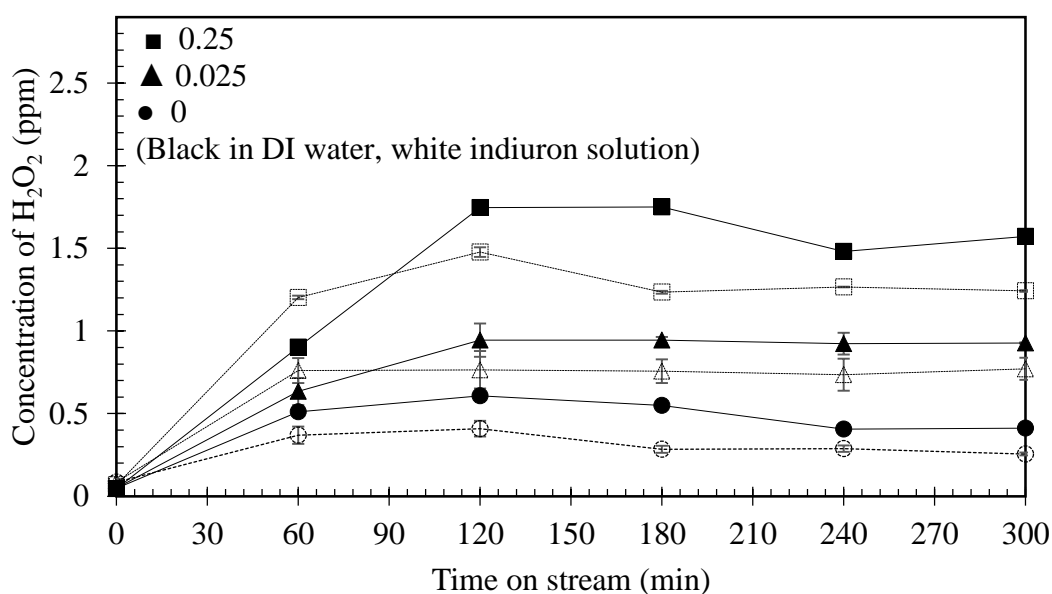


Figure 4.23 Correlation of hydrogen peroxide generated and time on stream various fraction of C-H bond in the DLC thin films electrode

The performance of diuron degradation depends on generation of hydroxyl radical. However, the generation of hydrogen peroxide is steady, but the performance of diuron degradation is unsteady because the generation of hydrogen peroxide of the DLC thin films electrode does not only occurs from the recombination of hydroxyl radicals. It has a significant effect owing to the dissolved oxygen in solution. Performance of degradation with various C-H fraction is shown in **Figure 4.24**. The DLC thin films electrode with the highest fraction of C-H bond (0.25) possess the

highest performance, up to 70 percent within 100 seconds of residence time in the microchannel reactor. However, the performance of diuron degradation had been decreased during the EAOP. This behavior indicates corrosion occurred on the surface of electrode.

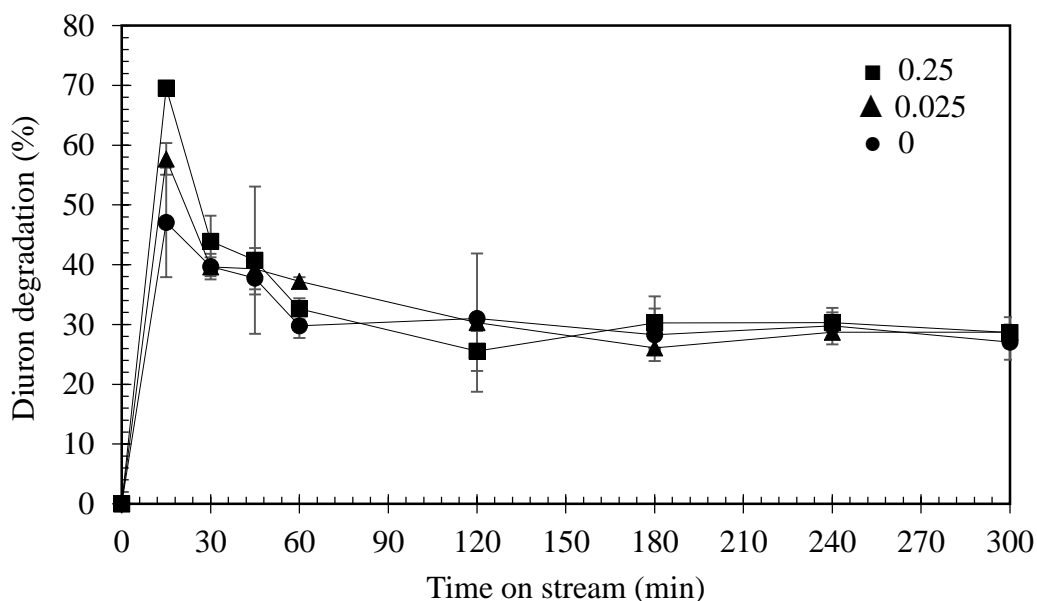


Figure 4.24 Correlation between performance of diuron degradation and time on stream at various fraction of C-H bond in the DLC thin films electrode

The performance of diuron degradation has been decreased during the EAOP at the initial time because the change of properties at the surface of electrodes. Moreover, the performance at a long time with the EAOP is steady. This behavior occurs from the surface property at the surface of DLC thin films electrode is not a significant difference. The transition of this property is affected by the corrosion.

The corrosion of DLC thin films electrode was investigated by the total organic carbon in the solution as shown in **Figure 4.25**. Corrosion of the DLC thin

films electrode does not only depend on carbon structure but also depends on C-H bond. The highest amount of C-H bond possesses the highest corrosion at electrode surface because C-H bond is unstable compared to structure of carbon. The amount of carbon at the surface of the electrode is decreased during the EAOP. Therefore, corrosion of the DLC thin films electrode is unsteady because the corrosion depends on amount of carbon of on surface electrode. The corrosion of DLC thin films occurs from oxidation reaction of the carbon structure and C-H bond with hydroxyl radicals. Due to its strong oxidizer, hydroxyl radical can attack carbon at the surface of the electrode.

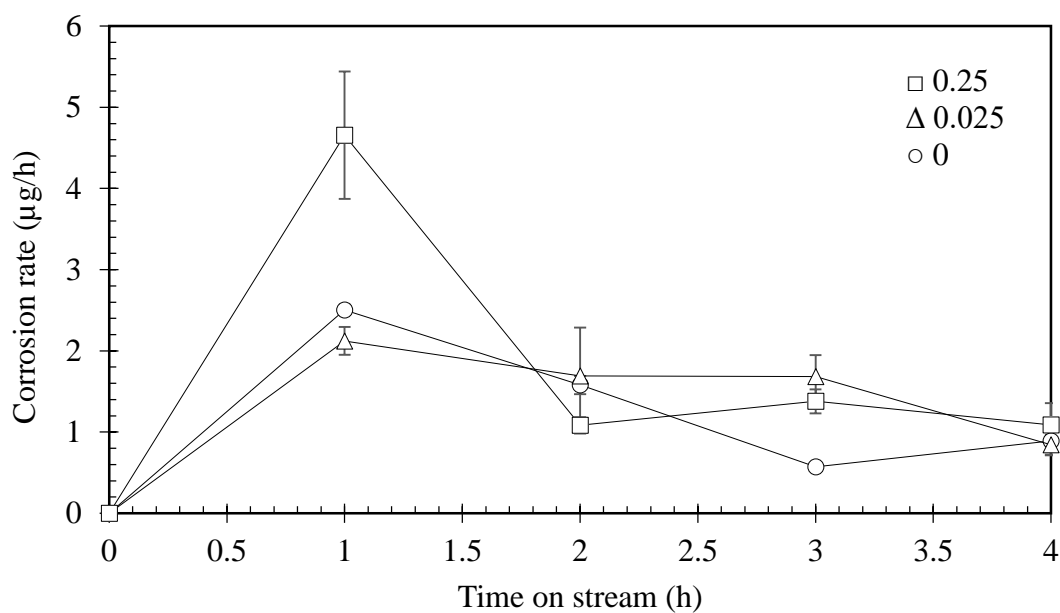


Figure 4.25 Correlation between corrosion rate and time on stream at various fraction of C-H bond in the DLC thin films electrode

The corrosion rate of DLC thin films electrodes depends on the amount of carbon and amount of C-H bond at the electrode surface. The DLC thin films electrode with the highest C-H bond has the highest corrosion at the initial time. The corrosion rate is not a significant difference after a long time reaction because the sp^2 -to- sp^3 ratio of DLC thin films is insignificantly different as shown in **Table 4.3**. The corrosion rate is decreased during the EAOP due to the decreasing the amount of carbon at the surface of electrode. The corrosion mechanism of DLC thin films with the C-H bond occurs from carbon defect site forming OH group with molecules of water. C-OH group can be oxidized with water molecules at a high potential [54]. Corrosion does not only occurs from the oxidation of carbon structure but also it occurs from the hydroxyl radicals. These hydroxyl radicals can produce corroded carbon atom and carbon dioxide. This behavior occurs similarly to the DLC thin film electrode various the sp^2 -to- sp^3 ratio.

Moreover, The hydroxyl radicals can adsorb on C-H bond. Adsorption of these highly active radicals can attack other hydroxyl radicals which were adsorbed on carbon forming the corrosion carbon and carbon dioxide. The amount of C-H bond is decreased after the EAOP as shown in **Table 4.5**. This result confirms that the C-H bond is corroded. Therefore, the property of DLC thin films is the same compared to the degradation performance of DLC thin films without C-H bond. The attacking of hydroxyl radicals with C-H bond on the surface depends on stability. This bond is not stable compared to C-C and C=C bond. Consequently, corrosion of DLC thin films electrode depends on fraction of C-H bond.

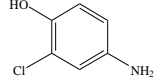
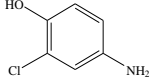
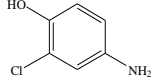
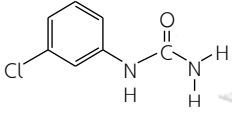
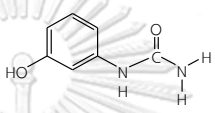
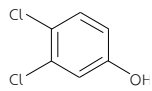
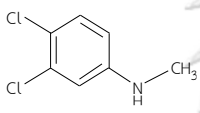
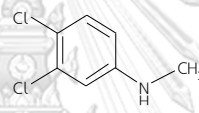
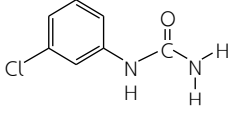
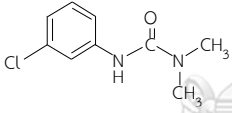
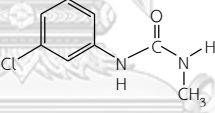
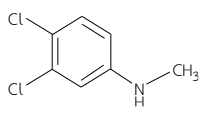
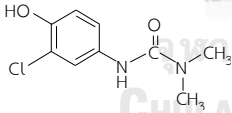
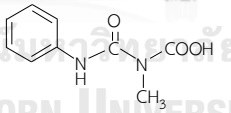
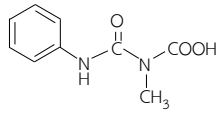
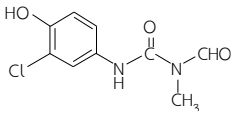
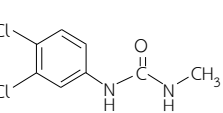
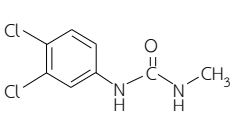
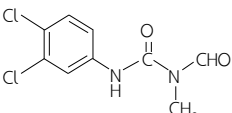
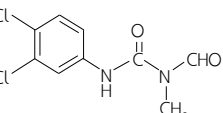
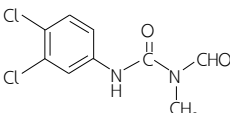
Table 4.5 Properties of DLC thin films electrodes before and after using via EAOP of high C-H bond

Electrodes No. 3 (■)	sp^2 -to- sp^3	C-H fraction	C=O fraction	C-O fraction
Before	0.84	0.025	0.117	0.301
After	0.66	0	0.149	0.191

Moreover, fraction of C-H bond affects intermediates produced from degradation of diuron during the EAOP as shown in **Table 4.6**. To compare with amount of C-H bond, the possible intermediates produced are very different the position of hydroxyl radicals attacking because difference of C-H fraction produces different number of hydroxyl radicals generated. Many hydroxyl radicals increase an opportunity of different attacking position on diuron molecules.

In summary, the fraction of C-H bond in the DLC thin film electrode affects the behaviors of diuron degradation, i.e., degradation performance, corrosion, and intermediates via EAOP within the microchannel reactor.

Table 4.6 Intermediates produced during diuron degradation using DLC thin films electrodes with various C-H contents via EAOP within the microchannel reactor.

No.	The fraction of C-H bond		
	0	0.025	0.25
1			
2			
3			
4			
5			
6			
7			

4.4.3 Effects of the C=O bond in DLC thin films electrodes

Not only the carbon structure and C-H bond affect diuron degradation but also the C=O bond in DLC thin films affects diuron degradation. The properties of DLC thin films electrodes were used to studies effects of C=O bond as shown in **Table 4.7**. These three DLC thin films electrodes have different fraction of C=O bond, but the ratio of sp^2 -to- sp^3 is not a significant difference. The fraction of C=O was varied with various operating pressure and fixed base pressure. Moreover, These electrodes do not have a C-H bond. Therefore, these electrodes are suitable to study the effects of the amount of C-H bond of DLC thin films electrodes on diuron degradation.

Table 4.7 Properties of DLC thin films electrodes with different amount of C=O bond

Electrodes	sp^2 -to- sp^3	C-H fraction	C=O fraction	C-O fraction	O-C=O fraction
No. 1 (●)	0.70	0	0.16	0.22	0.021
No. 2 (▲)	0.75	0	0.33	0.27	0.059
No. 3 (■)	0.60	0	0.36	0.19	0.242

The performance of the electrochemical electrode depends on the electrical resistance because the electrical resistance represents the ability of an electron transferred. The electrical resistance of the DLC thin films electrodes with different the amount of C=O bond is shown in **Figure 4.26**. The highest the amount of C=O bond of the DLC thin films electrode has the highest electrical resistance because the C=O bond has two lone pairs electron, so the lots of C=O bond increase the density of π -bond. Thus, the C=O bond in the DLC thin film improves the electrical resistance because the density of π -bond enhances the mobility of the electron.

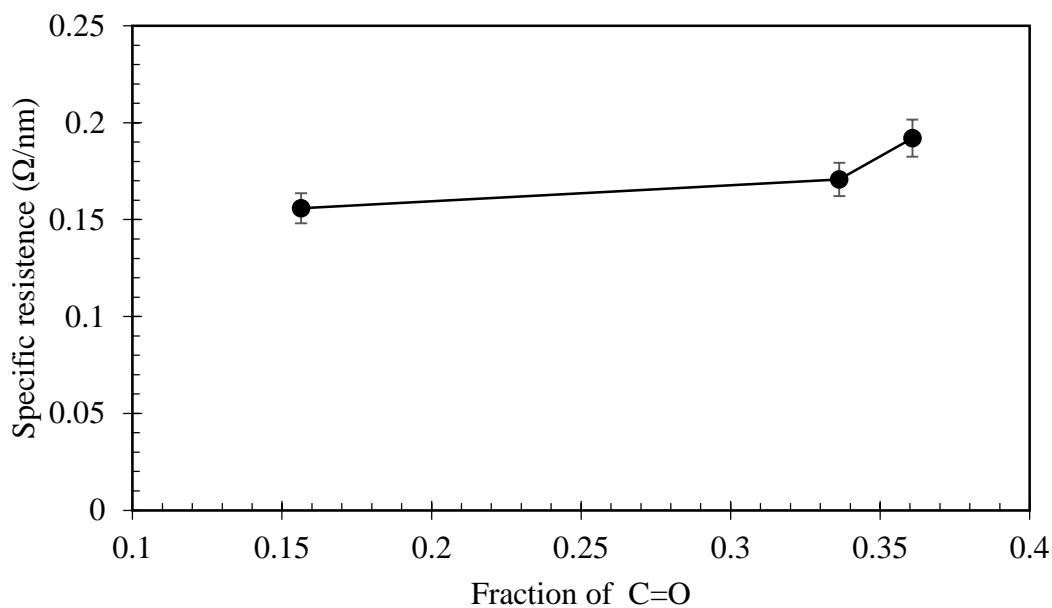


Figure 4.26 Correlation between electrical resistance and fraction of C=O bond

The performance of electrode with various amount of C=O bond was investigated by measuring amount of hydrogen peroxide generated during EAOP as shown in **Figure 4.27**. The generation of hydrogen peroxide depends on fraction of C=O bond in DLC thin films electrode. Not only the highest the amount of C=O bond has the lowest the electrical resistance but also the highest amount C=O bond of the electrode can generate the highest the amount of hydrogen peroxide because the C=O bond can make the electron transferred easily. Moreover, the amount of hydrogen peroxide generated in pure DI water is higher than in the diuron solution because hydroxyl radicals are used to decompose diuron molecules.

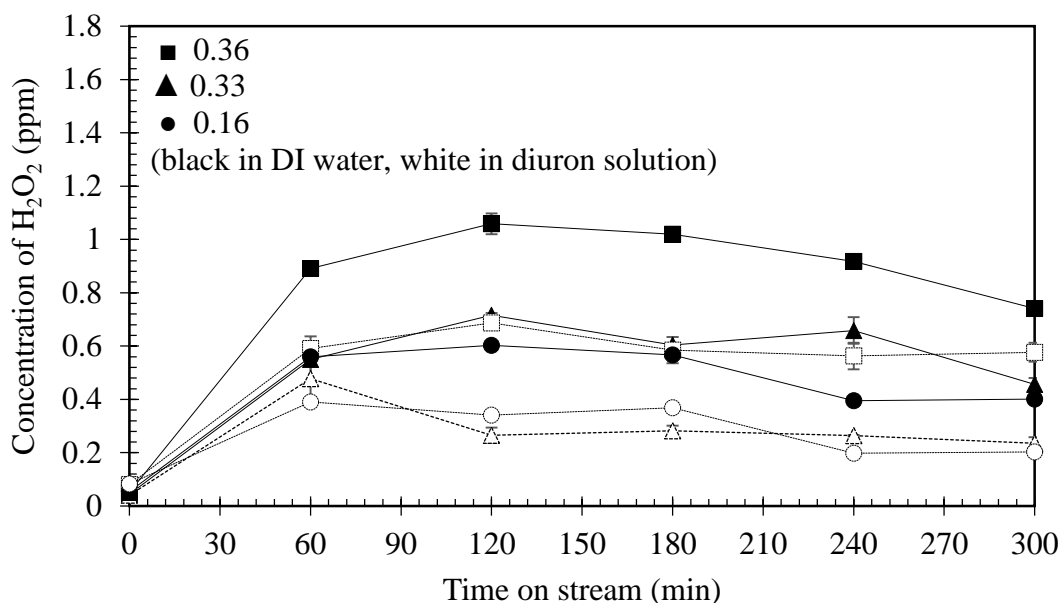


Figure 4.27 Correlation between concentration of hydrogen peroxide generated and time on stream at various fraction of C=O bond in the DLC thin films electrode

In the EAOP, performance of diuron degradation depends on the number of hydroxyl radicals generated. However, generation of hydrogen peroxide is steady, but degradation performance is unsteady because generation of hydrogen peroxide of DLC thin films electrode does not only occurs from the recombination of hydroxyl radicals. It has a significant effect from the dissolved oxygen in solution as same as the other properties of the DLC thin film electrode. Performance of diuron degradation with various fraction of C=O bond is shown in **Figure 4.28**. The DLC thin films electrode with the highest fraction of C=O bond (0.36) has the highest performance, up to 70 percent in 100 seconds of residence time within the microchannel reactor. However, performance of diuron degradation is decreased during degradation process. This behavior indicates that corrosion occurs on the

surface of electrodes because the performance of the electrode depends on the surface property.

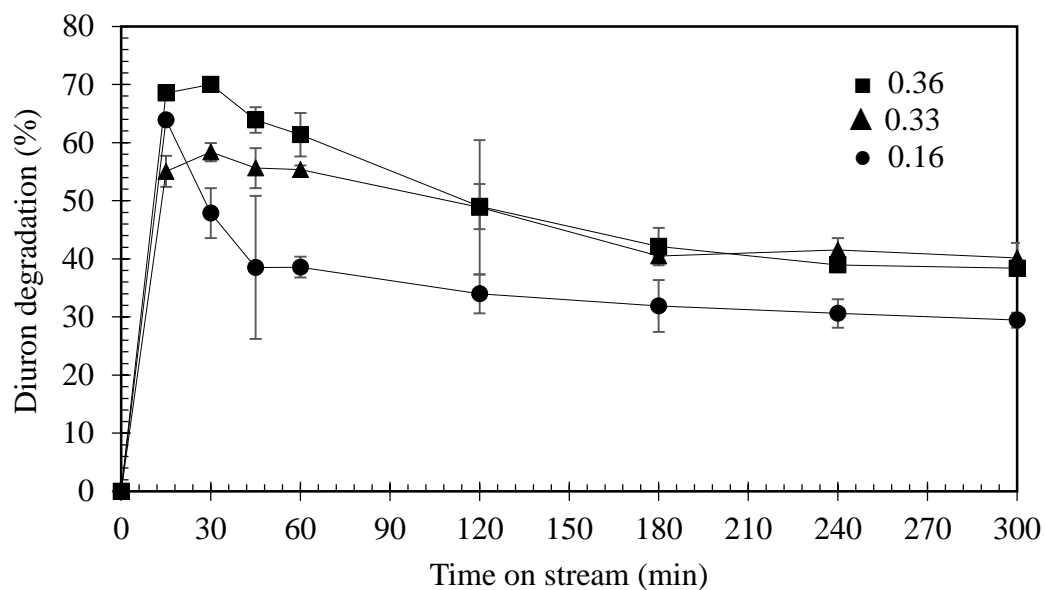


Figure 4.28 Correlation between performance of diuron degradation and time on stream at various fraction of C=O bond in the DLC thin films electrode

The performance of diuron degradation has been decreased during the EAOP at initial time because the change of properties at the surface of electrodes. Moreover, the performance at a long time with the EAOP is steady. This behavior occurs from the surface property at the surface of DLC thin films electrode is not a significant difference. The transition of this property is affected by the corrosion.

The corrosion of DLC thin films electrode was investigated by measuring total organic carbon in the solution as shown in **Figure 4.29**. Corrosion of the DLC thin films electrode not only depends on carbon structure and C-H bond but also the

corrosion depends on C=O bond in DLC thin films. The corrosion of the electrode with the highest amount of C=O bond occurs the highest because C=O bond is unstable compared to the carbon structures. Due to the thickness of DLC thin films electrodes is very thin, corrosion of DLC thin films electrode is unsteady because the corrosion depends on amount of carbon of the surface electrode. This corrosion of DLC thin films occurs from the oxidation reaction of C=O bond. Due to its strong oxidizer, the hydroxyl radical can attack the C=O bond.

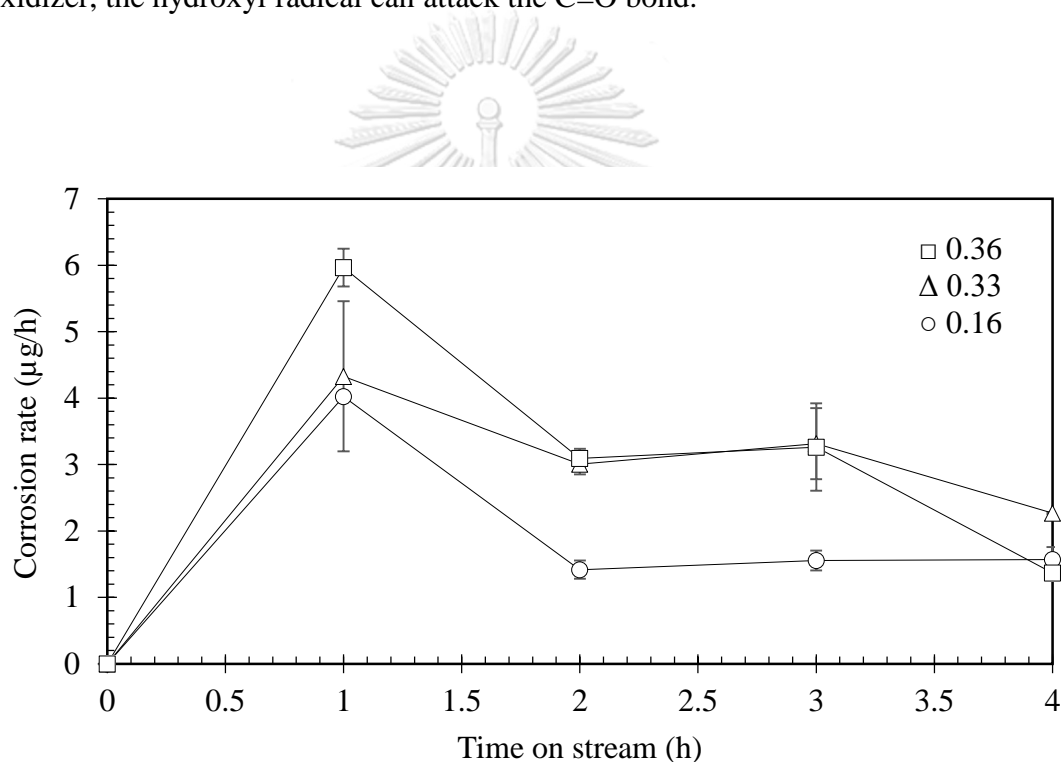


Figure 4.29 Correlation between corrosion rate and time on stream with various fraction of C=O bond in DLC thin films electrode

The corrosion mechanism of DLC thin films with C=O bond occurs from the carbon at the surface of electrode which was oxidized with water molecules at high potential [54]. Not only the corrosion occurs from the oxidation with water but also the corrosion occurs from the hydroxyl radicals with the structure of carbon. These highly active hydroxyl radicals can produce corrosion carbon and carbon dioxide. This behavior occurs similarly to the other properties (i.e., the structure of carbon and the C-H bond) in the DLC thin film electrode. Moreover, hydroxyl radicals can adsorb on C=O bond. The adsorption of these hydroxyl radicals can attack with the others which were adsorbed on the carbon forming the corrosion carbon and carbon dioxide. The C=O fraction of DLC thin film after using in EAOP is less than before using as shown in **Table 4.8**. This result confirms that the C=O bond is corroded. The attacking of hydroxyl radicals with C=O bond at the surface depends on the stability. Moreover, the performance of diuron degradation of DLC thin films is slowly decreased because the ratio of sp^2 -to- sp^3 is increased. This C=O bond is not stable comparing to the carbon structure. Consequently, corrosion of DLC thin films electrode depends on fraction of C=O bond.

Table 4.8 Properties of DLC thin films electrodes before and after using via EAOP of high C=O bond

Electrodes No. 3 (■)	sp^2 -to- sp^3	C-H fraction	C=O fraction	C-O fraction
Before	0.59	0	0.361	0.193
After	0.73	0	0.235	0.314

Furthermore, fraction of C=O bond has an effect on intermediates produced from degradation of diuron during the EAOP as shown in **Table 4.9**. To compare with various the amount of C=O bond, the possible intermediates are very different the position of hydroxyl radicals attacking because the difference of C=O fraction produces different number of hydroxyl radicals generated. These many hydroxyl radicals increase the opportunity for attacking different position on diuron molecules. Also, C=O bond of the DLC thin film can generate free ketyl radicals, this radical can oxidize diuron molecules, so the intermediates are a difference.

In summary, the fraction of C=O bond in the DLC thin film electrode affects the behaviors of diuron degradation, i.e., degradation performance, corrosion, and intermediates via EAOP within the microchannel reactor.

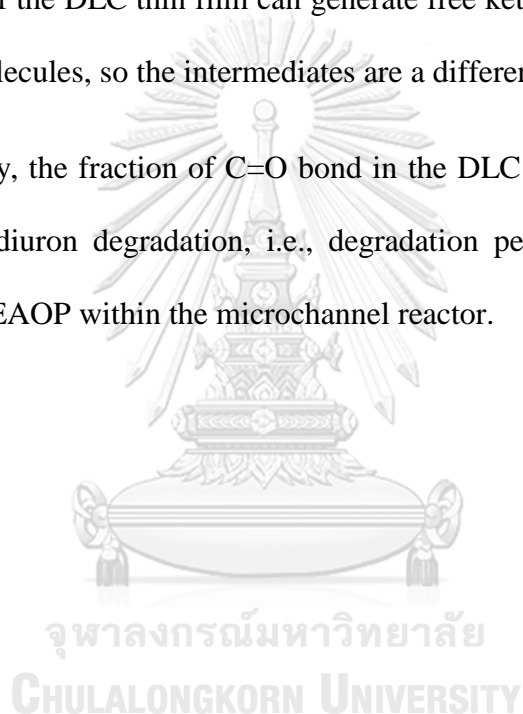
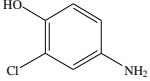
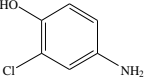
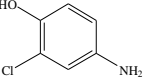
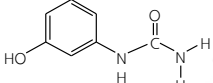
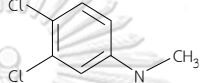
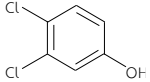
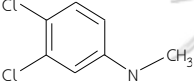
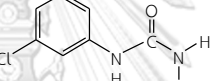
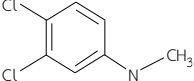
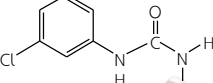
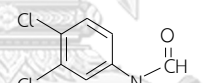
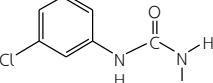
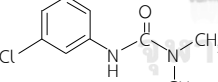
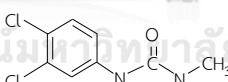
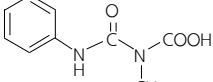
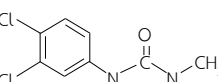
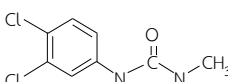
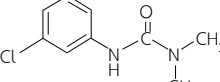
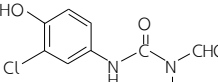
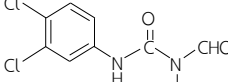
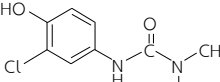
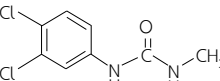


Table 4.9 Intermediates produced during diuron degradation using DLC thin films electrodes with various C=O contents via EAOP within a microchannel reactor.

No.	The fraction of C=O bond		
	0.16	0.33	0.36
1			
2			
3			
4			
5			
6			
7			
8			

4.5 Comparison of properties of DLC thin films electrodes on behaviors of diuron degradation

Each property of DLC thin films (carbon structure, C-H bond, and C=O bond) has the difference of degradation behaviors. The most important property of electrochemical electrode is mobility of electron. The electrical resistance was used to characterize DLC thin film electrodes because this property represented the ability of electron transferred. Electrical resistance of DLC thin films electrode with the highest the number of sp^2 (C=C) structure, C-H bond, and C=O bond is shown in **Figure 4.30**. Comparison between DLC thin film with the highest sp^2 structure and C=O bond, the electrical resistance of the highest sp^2 structure is lower than the highest C=O bond because sp^2 structure has a residual valence electron. This free electron can move easily. However, C=O bond increase density of π -bond enhanced the ability of electron transferred, but this property is insignificant effect on the ability of electron transferred when compared to residual valence electron and small grain region properties. The comparison between DLC thin film with the highest sp^2 structure and C-H bond, the electrical resistance of the highest sp^2 structure is higher than the highest C-H bond. Although DLC thin films with the C-H bond have the sp^2 -to sp^3 ratio lower than DLC thin film with the highest sp^2 -to- sp^3 ratio, the a-C:H have grain region smaller than ta-C. Therefore, the synthesized DLC thin films which the highest the amount of C-H has the lowest the electrical resistance.

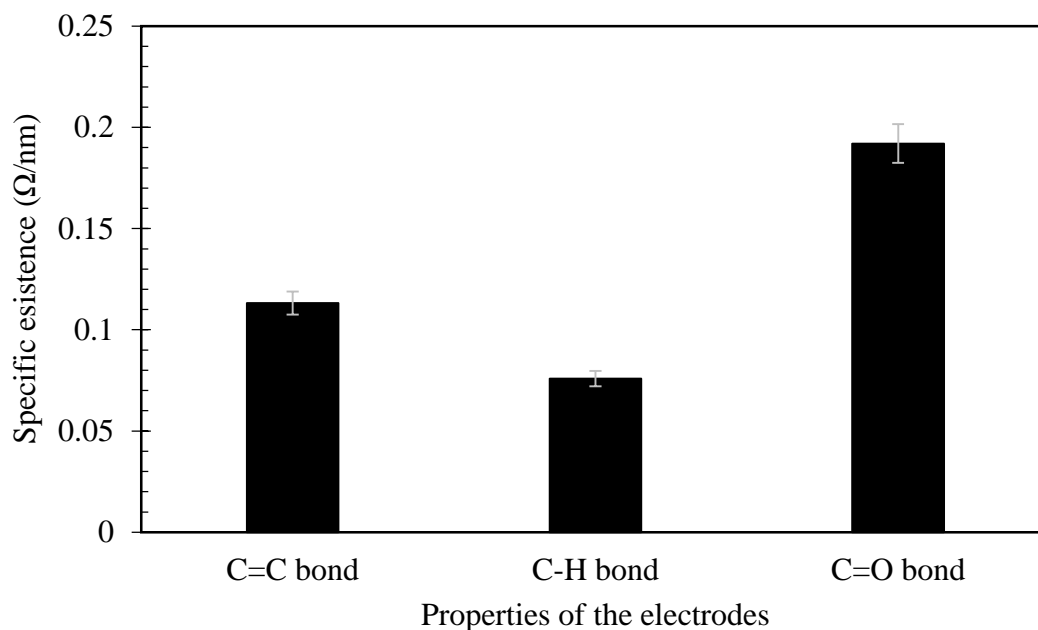


Figure 4.30 Correlation between electrical resistances and the highest of each property of DLC thin films electrodes

The comparison of performance with the highest each of properties of DLC thin films electrodes was investigated by measuring amount of hydrogen peroxide generated during the EAOP as shown in **Figure 4.31**. DLC thin films electrode with the lowest electrical resistance can generate the highest amount of hydrogen peroxide. This result confirms that the electrochemical performance depends on the ability of electron transferred. However, the relationship between electrical resistance and the amount of hydrogen peroxide is not linear relationship. Therefore, not only the electrical resistance but also other properties (i.e., surface area) of electrode effect on the generation of hydroxyl radicals.

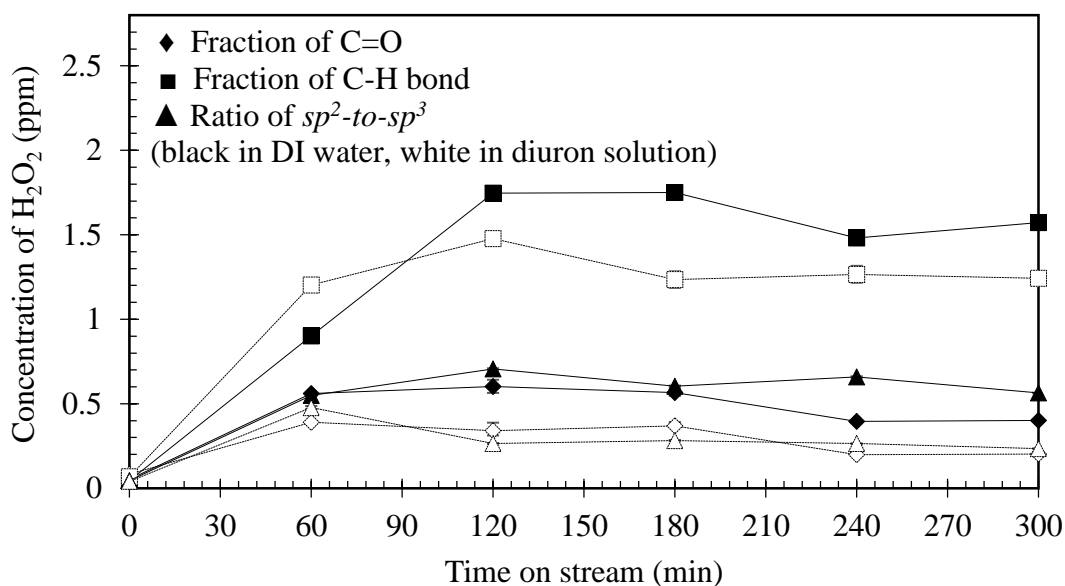


Figure 4.31 Correlation between concentrations of hydrogen peroxide generated and time on stream with various properties of the DLC thin films electrode

The performance of diuron degradation of synthesized DLC thin films electrode depends on the number of hydroxyl radicals generated. However, the generation of hydrogen peroxide of the highest each property (i.e., the *sp*²-to-*sp*³ ratio, fraction of C-H bond, and fraction of C=O bond) is steady, but the performance of diuron degradation is unsteady because the generation of hydrogen peroxide does not only occurs from the recombination of hydroxyl radicals. Therefore, The generation of hydroxyl radicals has a significant effect from the dissolved oxygen in solution. The performance of diuron degradation is shown in **Figure 4.32**. All of DLC thin films electrodes with the highest each of properties have the highest performance, up to 70 percent in 100 seconds of residence time within a microchannel reactor at initial time. However, the performance of diuron degradation of these electrodes is decreased during the degradation process this behavior indicates that carbon at the

surface of electrodes occurs the corrosion because the performance of the electrode depends on the surface property. Although the highest the amount of C=O bond has the degradation behavior difference the highest the sp^2 carbon structure and C-H bond. The performance of DLC thin film with the highest amount of C=O bond is slowly decreased.

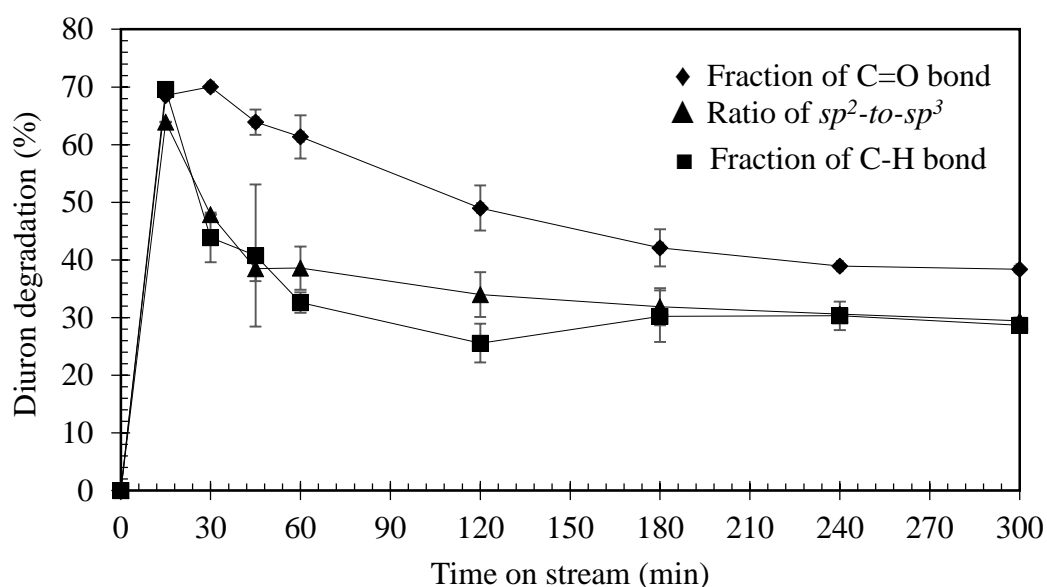


Figure 4.32 Correlation between performance of diuron degradation and time on stream with various properties of the DLC thin films electrode

The corrosion of DLC thin films electrode with the highest each property was investigated by the total organic carbon in the solution as shown in **Figure 4.33**. In the results, the corrosion of the DLC thin films electrodes depends on the carbon structure, the amount of C-H bond, and the amount of C=O bond. The corrosion of the electrode with the highest amount of the C-H bond and C=O bond occurs higher than the sp^2 and sp^3 carbon structure because the C-H bond and C=O bond are unstable.

Moreover, the sp^3 has the hardness and stability similar to the diamond. The comparison the corrosion of the C-H bond and C=O bond, the C=O bond has the corrosion higher than the C-H bond because the C-H bond is more stable than the C=O bond. Considered the corrosion all of the DLC thin film electrodes, the corrosion rate is unsteady because the amount of carbon at the surface of the electrode is decreased during the EAOP.

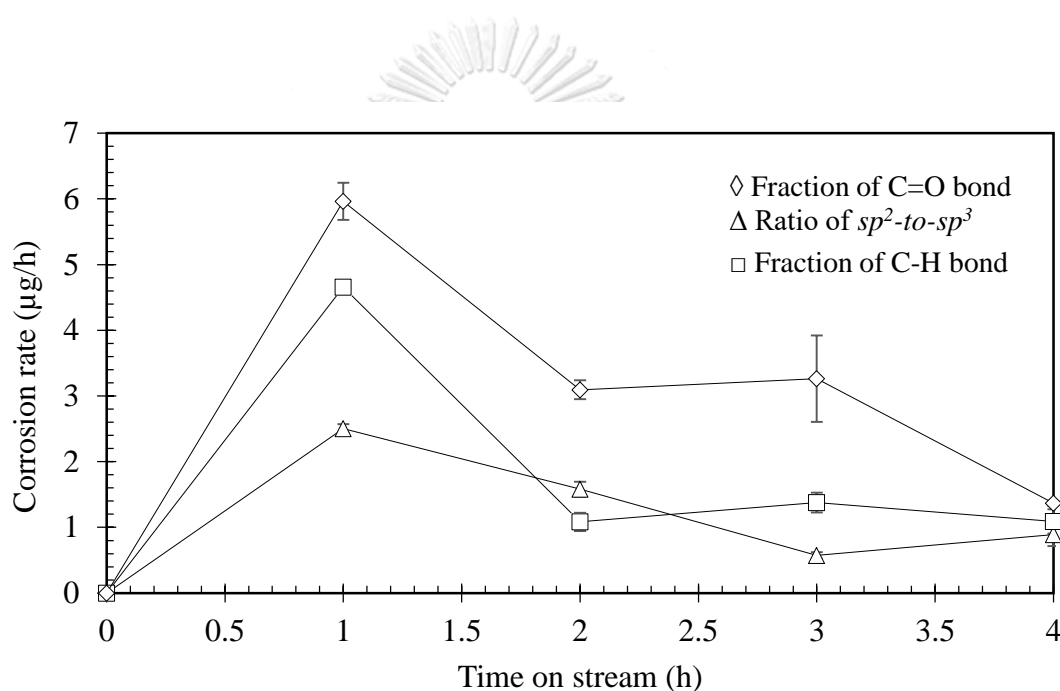


Figure 4.33 The correlation between the corrosion rate and time on stream various the properties of the DLC thin films electrode

Not only the three properties of the DLC thin films electrodes affect the performance of diuron degradation and the corrosion but also these properties affect the intermediates produced from the degradation of diuron during the EAOP within a microchannel reactor as shown in **Table 4.10**. The intermediates produced from each of properties of the DLC thin film electrodes are very different because the position of hydroxyl radicals attacking is the difference. The position of attacking depends on the amount of highly active radicals and the side of diuron molecules adsorb on the surface of the DLC thin film electrode. Considering the highest the amount of C-H bond, this bonding demonstrates the positive electricity ($\delta^-C-H\delta^+$) because carbon attracts electrons more strongly than hydrogen. Therefore, the diuron molecules prefer to adsorb the ketone group (C=O) on the surface with the C-H bond because this ketone group demonstrates the negative electricity ($\delta^+C=O\delta^-$) because oxygen attracts electrons more strongly than carbon [55]. Moreover, the highest the amount of C=O bond, this bonding demonstrate the negative electricity ($\delta^+C=O\delta^-$), so the diuron molecules prefer to adsorb the C-H bond on the surface with the C=O bond because this bond demonstrates the positive electricity ($\delta^-C-H\delta^+$). Therefore, these behaviors increase the opportunity of attacking at the different position on diuron molecules.

In summary, the highest of C-H fraction in the DLC thin films electrode has the lowest the electrical resistance. Moreover, this the highest property makes the highest of the degradation performance, up to 70% in 100 seconds of residence time within a microchannel reactor. Moreover, the highest of fraction C=O bond in the DLC thin films electrode has the highest the corrosion, but it has the smallest decrease in the degradation performance

Table 4.10 Intermediates produced during diuron degradation using DLC thin films electrodes different properties via EAOP within a microchannel reactor.

No.	The properties of DLC thin films electrodes		
	sp^2 -to- sp^3	C-H	C=O
1			
2			
3			
4			
5			
6			
7			
8			

CHAPTER 5 CONCLUSIONS AND RECOMMENDATIONS

This chapter has the three main sections including a summary of the results, conclusions, and recommendation for future work.

5.1 Summary of results

The summary of the results of this research is the following:

1. In EAOP within a microchannel, the DLC thin films electrode has corrosion less than when using the graphite electrode.
2. The Ti as an interlayer is not significantly improved the corrosion of DLC thin films electrodes.
3. The using Ti as an interlayer is unsuitable for electrochemical electrode because this interlayer leads to occurs corrosion of cathode.
4. The highest of C-H fraction in the DLC thin films electrode has the lowest electrical resistance. Moreover, this C-H fraction makes the highest of the degradation performance, up to 70% in 100 seconds of residence time within a microchannel reactor.
5. The highest of fraction C=O bond in the DLC thin films electrode has the highest corrosion, but it has the smallest decrease in the degradation performance.
6. The intermediates produced during the EAOP within a microchannel reactor depend on the properties of the DLC thin film electrode, i.e., the sp^2 -to- sp^3 ratio, fraction of C-H bond, and fraction of C=O bond.

5.2 Conclusions

The DLC thin film electrode has the potential used for the anode in the EAOP within a microchannel. The DLC thin films electrode improve the corrosion compared to the graphite electrode. Moreover, the properties of the DLC thin film electrode (i.e., the sp^2 -to- sp^3 ratio, fraction of C-H bond, and fraction of C=O bond) effect on the degradation performance, the electrical resistance, the corrosion, and the intermediates produced. Furthermore, the C-H bonds in the DLC thin films enhance the electrical conductivity. Although the C=O bonds in the DLC thin films enhance the degradation performance, the C=O bonds have the highest the corrosion. The highest each of properties make the highest the degradation performance, up to 70% in 100 seconds of residence time within a microchannel reactor. However, the performance is decreased during the reaction time that affected by the corrosion of the DLC thin films electrode.

5.3 Recommendations

1. Increasing the fraction of C-H in DLC thin films for improving the electrical conductivity.
2. Investigating the pathway of the intermediates produced during the EAOP within a microchannel reactor.
3. Studying the toxicity of the intermediates in outlet solution from the EAOP within a microchannel reactor.



REFERENCES

1. Giacomazzi, S. and N. Cochet, *Environmental impact of diuron transformation: a review*. Chemosphere, 2004. **56**(11): p. 1021-1032.
2. Bouquet-Somrani, C., et al., *Photocatalytic degradative oxidation of Diuron in organic and semi-aqueous systems over titanium dioxide catalyst*. New Journal of Chemistry, 2000. **24**(12): p. 999-1002.
3. Maldonado Rubio, M.I., et al., *Photo-Fenton degradation of alachlor, atrazine, chlorfenvinphos, diuron, isoproturon and pentachlorophenol at solar pilot plant*. International Journal of Environment and Pollution, 2006. **27**(1-3): p. 135-146.
4. Villaverde, J., et al., *Bioremediation of diuron contaminated soils by a novel degrading microbial consortium*. Journal of Environmental Management, 2017. **188**(Supplement C): p. 379-386.
5. Chen, G.-C., et al., *Adsorption of diuron and dichlobenil on multiwalled carbon nanotubes as affected by lead*. Journal of Hazardous Materials, 2011. **188**(1): p. 156-163.
6. Polcaro, A.M., et al., *Electrochemical degradation of diuron and dichloroaniline at BDD electrode*. Electrochimica Acta, 2004. **49**(4): p. 649-656.
7. Komtchou, S., et al., *Removal of atrazine and its by-products from water using electrochemical advanced oxidation processes*. Water Research, 2017. **125**(Supplement C): p. 91-103.
8. Lin, H., et al., *Removal of artificial sweetener aspartame from aqueous media by electrochemical advanced oxidation processes*. Chemosphere, 2017. **167**(Supplement C): p. 220-227.
9. Enache, T.A., et al., *Hydroxyl radicals electrochemically generated in situ on a boron-doped diamond electrode*. Electrochemistry Communications, 2009. **11**(7): p. 1342-1345.
10. Khongthon, W., et al., *Degradation of diuron via an electrochemical advanced oxidation process in a microscale-based reactor*. Chemical Engineering Journal, 2016. **292**(Supplement C): p. 298-307.
11. Guenfoud, F., M. Mokhtari, and H. Akrou, *Electrochemical degradation of malachite green with BDD electrodes: Effect of electrochemical parameters*. Diamond and Related Materials, 2014. **46**(Supplement C): p. 8-14.
12. Zhang, Z., et al., *Degradation of creatinine using boron-doped diamond electrode: Statistical modeling and degradation mechanism*. Chemosphere, 2017. **182**(Supplement C): p. 441-449.
13. Bai, L., et al., *Wear and friction between smooth or rough diamond-like carbon films and diamond tips*. Wear, 2017. **372-373**(Supplement C): p. 12-20.
14. Wu, H., et al., *Effects of diamond-like carbon film on the corrosion behavior of NdFeB permanent magnet*. Surface and Coatings Technology, 2017. **312**(Supplement C): p. 66-74.
15. Coşkun, Ö.D. and T. Zerrin, *Optical, structural and bonding properties of diamond-like amorphous carbon films deposited by DC magnetron sputtering*. Diamond and Related Materials, 2015. **56**(Supplement C): p. 29-35.
16. Kosukegawa, H., et al., *Structure and electrical properties of molybdenum-containing diamond-like carbon coatings for use as fatigue sensors*. Diamond and Related Materials, 2017. **80**(Supplement C): p. 38-44.

17. Son, M.J., et al., *Enhanced electrochemical properties of the DLC films with an arc interlayer, nitrogen doping and annealing*. Surface and Coatings Technology, 2017. **329**(Supplement C): p. 77-85.
18. Swann, S., *Magnetron sputtering*. Physica in Technol, 1988. **19**.
19. Ribeiro, A.R., et al., *An overview on the advanced oxidation processes applied for the treatment of water pollutants defined in the recently launched Directive 2013/39/EU*. Environment International, 2015. **75**(Supplement C): p. 33-51.
20. Ehrfeld, W., V. Hessel, and H. Löwe, *State of the Art of Microreaction Technology*, in *Microreactors*. 2000, Wiley-VCH Verlag GmbH & Co. KGaA. p. 1-14.
21. Yao, X., et al., *Review of the applications of microreactors*. Renewable and Sustainable Energy Reviews, 2015. **47**(Supplement C): p. 519-539.
22. Robertson, J., *Diamond-like amorphous carbon*. Materials Science and Engineering: R: Reports, 2002. **37**(4): p. 129-281.
23. Hideki MORIGUCHI, H.O.a.M.T., *History and Applications of Diamond-Like Carbon Manufacturing Process*. sei technical review, 2016.
24. Kelly, P.J. and R.D. Arnell, *Magnetron sputtering: a review of recent developments and applications*. Vacuum, 2000. **56**(3): p. 159-172.
25. Zhang, S., X. Lam Bui, and Y. Fu, *Magnetron sputtered hard a-C coatings of very high toughness*. Surface and Coatings Technology, 2003. **167**(2): p. 137-142.
26. Zeng, A., et al., *MICROSTRUCTURE AND ELECTROCHEMICAL BEHAVIOR OF SPUTTERED DIAMOND-LIKE CARBON FILMS*. International Journal of Modern Physics B, 2002. **16**(06n07): p. 1024-1030.
27. Sonoda, T., S. Nakao, and M. Ikeyama, *Surface Modification of Stainless Steel by Coating with DLC/Ti Bi-Layered Film Using Sputter-Deposition*. Transactions of the Materials Research Society of Japan, 2011. **36**(3): p. 337-340.
28. Laurila, T., et al., *Diamond-like carbon (DLC) thin film bioelectrodes: Effect of thermal post-treatments and the use of Ti adhesion layer*. Materials Science and Engineering: C, 2014. **34**(Supplement C): p. 446-454.
29. Yan, X., et al., *Characterization of hydrogenated diamond-like carbon films electrochemically deposited on a silicon substrate*. Vol. 37. 2004. 2416.
30. Nesov, S.N., et al., *Effect of carbon nanotubes irradiation by argon ions on the formation of SnO₂-x/MWCNTs composite*. Nuclear Instruments and Methods in Physics Research Section B: Beam Interactions with Materials and Atoms, 2017. **410**: p. 222-229.
31. Al Mahmud, K.A.H., et al., *Tribological characteristics of amorphous hydrogenated (a-C:H) and tetrahedral (ta-C) diamond-like carbon coating at different test temperatures in the presence of commercial lubricating oil*. Surface and Coatings Technology, 2014. **245**: p. 133-147.
32. Katsumata, H., et al., *Photocatalytic degradation of diuron in aqueous solution by platinumized TiO₂*. Journal of Hazardous Materials, 2009. **171**(1-3): p. 1081-1087.
33. Oturan, M.A., et al., *Kinetics of oxidative degradation/mineralization pathways of the phenylurea herbicides diuron, monuron and fenuron in water during application of the electro-Fenton process*. Applied Catalysis B: Environmental.

- 97(1-2): p. 82-89.
34. Farre, M.J., et al., *Evaluation of the intermediates generated during the degradation of Diuron and Linuron herbicides by the photo-Fenton reaction*. Journal of Photochemistry and Photobiology A: Chemistry, 2007. **189**(2-3): p. 364-373.
 35. Carrier, M., et al., *Removal of herbicide diuron and thermal degradation products under Catalytic Wet Air Oxidation conditions*. Applied Catalysis B: Environmental, 2009. **91**(1-2): p. 275-283.
 36. Canle López, M., et al., *Mechanisms of Direct and TiO₂-Photocatalysed UV Degradation of Phenylurea Herbicides*. ChemPhysChem, 2005. **6**(10): p. 2064-2074.
 37. Salvestrini, S., P. Di Cerbo, and S. Capasso, *Kinetics of the chemical degradation of diuron*. Chemosphere, 2002. **48**(1): p. 69-73.
 38. F. I. Eissa, N. A. Zidan, and H. Sakugawa. *Remediation of pesticide-contaminated water by advanced oxidation processes*. in *The 11th International Conference on Environmental Science and Technology*. 2009. Chania, Crete, Greece.
 39. Chen, W.-H. and T.M. Young, *Influence of nitrogen source on NDMA formation during chlorination of diuron*. Water Research, 2009. **43**(12): p. 3047-3056.
 40. Mazellier, P., J. Jirkovsky, and M. Bolte, *Degradation of Diuron Photoinduced by Iron(III) in Aqueous Solution*. Pesticide Science, 1997. **49**(3): p. 259-267.
 41. Malato, S., et al., *Photocatalytic Treatment of Diuron by Solar Photocatalysis: Evaluation of Main Intermediates and Toxicity*. Environmental Science & Technology, 2003. **37**(11): p. 2516-2524.
 42. Oturan, M.A., et al., *Kinetics of oxidative degradation/mineralization pathways of the phenylurea herbicides diuron, monuron and fenuron in water during application of the electro-Fenton process*. Applied Catalysis B: Environmental, 2010. **97**(1-2): p. 82-89.
 43. Oturan, N., et al., *Study of the toxicity of diuron and its metabolites formed in aqueous medium during application of the electrochemical advanced oxidation process "electro-Fenton"*. Chemosphere, 2008. **73**(9): p. 1550-1556.
 44. Macounová, K., et al., *Kinetics of photocatalytic degradation of diuron in aqueous colloidal solutions of Q-TiO₂ particles*. Journal of Photochemistry and Photobiology A: Chemistry, 2003. **156**(1-3): p. 273-282.
 45. Feng, J., et al., *Degradation of diuron in aqueous solution by ozonation*. Journal of Environmental Science and Health, Part B: Pesticides, Food Contaminants, and Agricultural Wastes, 2008. **43**(7): p. 576 - 587.
 46. Carrier, M., et al., *Photocatalytic Degradation of Diuron: Experimental Analyses and Simulation of HO₂ Radical Attacks by Density Functional Theory Calculations*. The Journal of Physical Chemistry A, 2009. **113**(22): p. 6365-6374.
 47. Wu, T. and J.D. Englehardt, *A New Method for Removal of Hydrogen Peroxide Interference in the Analysis of Chemical Oxygen Demand*. Environmental Science & Technology, 2012. **46**(4): p. 2291-2298.
 48. Butler, I.B., M.A.A. Schoonen, and D.T. Rickard, *Removal of dissolved oxygen from water: A comparison of four common techniques*. Talanta, 1994. **41**(2): p. 211-215.

49. Wu, L. and D.W. Shoesmith, *An Electrochemical Study of H₂O₂ Oxidation and Decomposition on Simulated Nuclear Fuel (SIMFUEL)*. *Electrochimica Acta*, 2014. **137**: p. 83-90.
50. Yamanaka, I., *Direct and Safe Synthesis of O₂ and H₂ Using Fuel Cell Reactors*. *Journal of the Japan Petroleum Institute*, 2014. **57**(6): p. 237-250.
51. Sikora, A., et al., *Electrical properties of boron-doped diamond-like carbon thin films deposited by femtosecond pulsed laser ablation*. *Applied Physics A*, 2009. **94**(1): p. 105-109.
52. Prapakornrattana, P., *DEGRADATION OF DIURON VIA ELECTROCHEMICAL ADVANCED OXIDATION PROCESS*, in *Department of Chemical Engineering*. 2016, Chulalongkorn University: Thailand.
53. Massi, M., et al., *Electrical and structural characterization of DLC films deposited by magnetron sputtering*. *Journal of Materials Science: Materials in Electronics*, 2001. **12**(4): p. 343-346.
54. Arun Pandey, Z.Y., Mallika Gummalla, Vadim V. Atrazhev, Nikolay Yu Kuzminykh, Vadim I. Sultanov, and Sergei Burlatsky, *A Carbon Corrosion Model to Evaluate the Effect of Steady State and Transient Operation of a Polymer Electrolyte Membrane Fuel Cell Fuel Cells, Electrolyzers, and Energy Conversion*. *J. Electrochem. Soc*, 2013. **160**(9): p. F972-F979.
55. Ouellette, R.J. and J.D. Rawn, *1 - Structure of Organic Compounds*, in *Principles of Organic Chemistry*, R.J. Ouellette and J.D. Rawn, Editors. 2015, Elsevier: Boston. p. 1-32.



APPENDIX

จุฬาลงกรณ์มหาวิทยาลัย
CHULALONGKORN UNIVERSITY

Appendix A

Calibration Data Analysis

Concentration of hydrogen peroxide in outlet solution can determine as following;

1. Preparation of reagent A

First, ammonium molybdate (0.01 g), sodium hydroxide (0.1 g), and potassium chloride (3.3 g) were mixed with deionized water. Then, solution was added into the volumetric flask. Finally, the deionized water was added until the total volume is 50 ml.

2. Preparation of reagent B

First, potassium hydrogen phthalate (1 g) was mixed with deionized water and added into the volumetric flask. Finally, the solution was added deionized water until the total volume is 50 ml.

3. Determination of hydrogen peroxide using UV-vis spectroscopy

The sample solution (1 ml) was mixed with 1 ml of reagent A and 1 ml of reagent B. The deionized water (3 ml) was used as blank solution. The hydrogen peroxide was detected in wavelength at 350 nm. The standards of hydrogen peroxide were prepared different concentration (0, 2, 4, 6, 8, and 10 ppm) for making calibration curve of hydrogen peroxide.

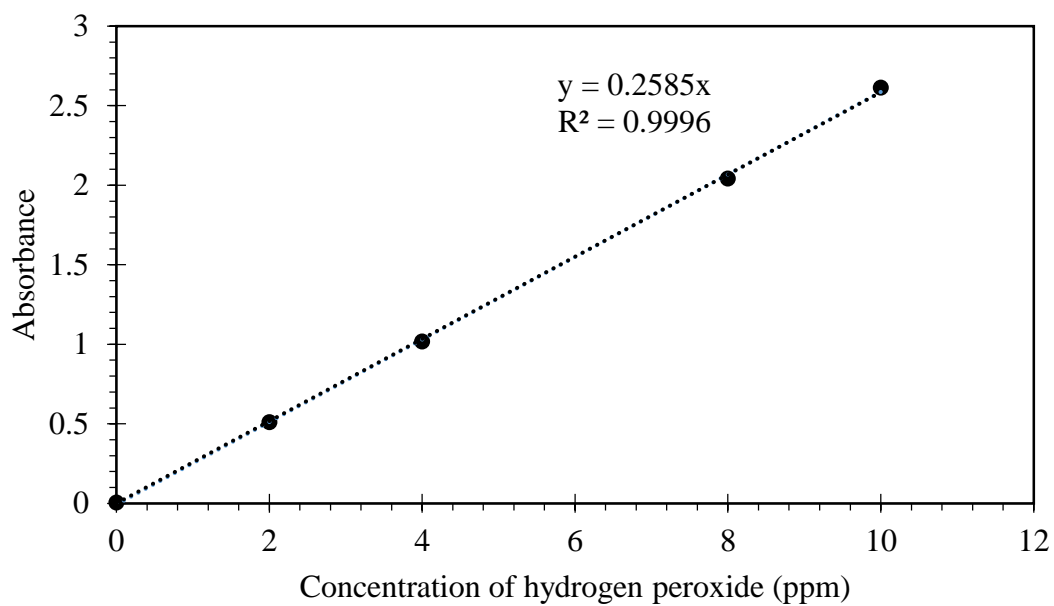


Figure A- 1 Calibration curve of hydrogen peroxide

Concentration of diuron can determine using HPLC. The standards of diuron solution were prepared different concentration (0, 2, 5, 10, 20, and 30 ppm) with deionized water for making calibration curve of diuron.

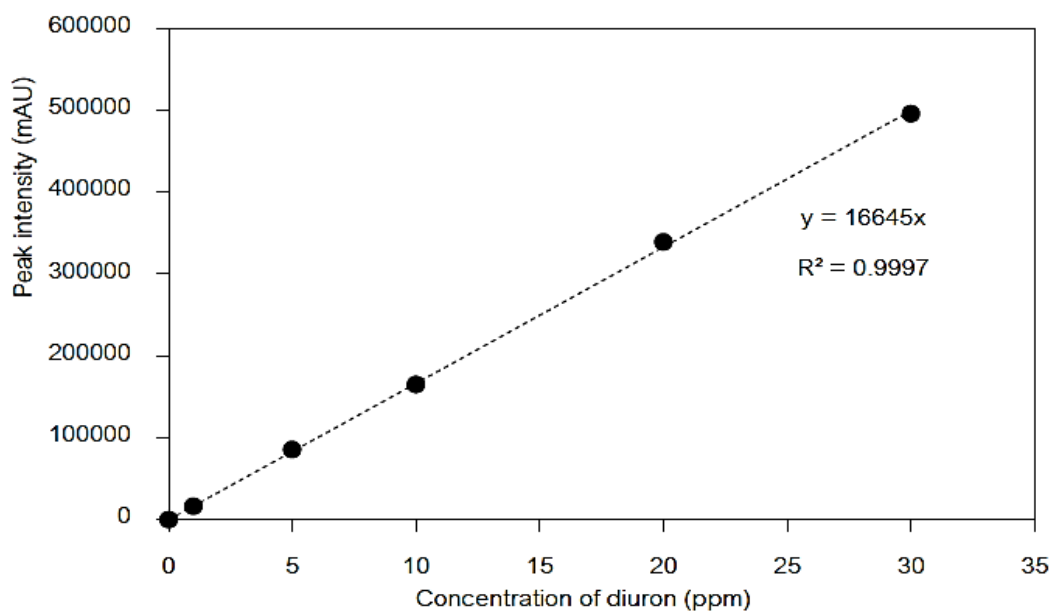


Figure A- 2 Calibration curve of diuron

Appendix B

Deconvolution of XPS Data

The convoluted peaks of XPS data were used OriginPro 8.5 program. The convoluted peak was fitted with the Gaussian model. The position and FWHM of convoluted peaks were defined following the literature reviews.

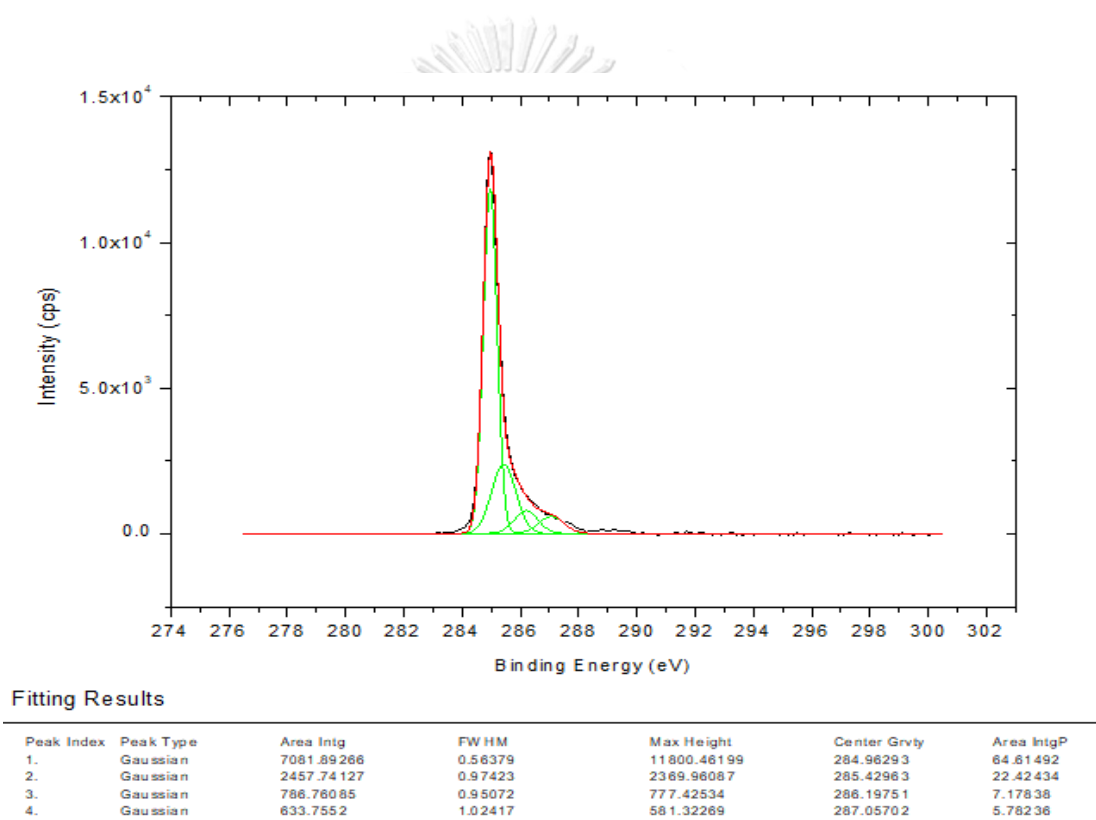


Figure B- 1 Deconvolution of C 1s peak of the graphite sheet

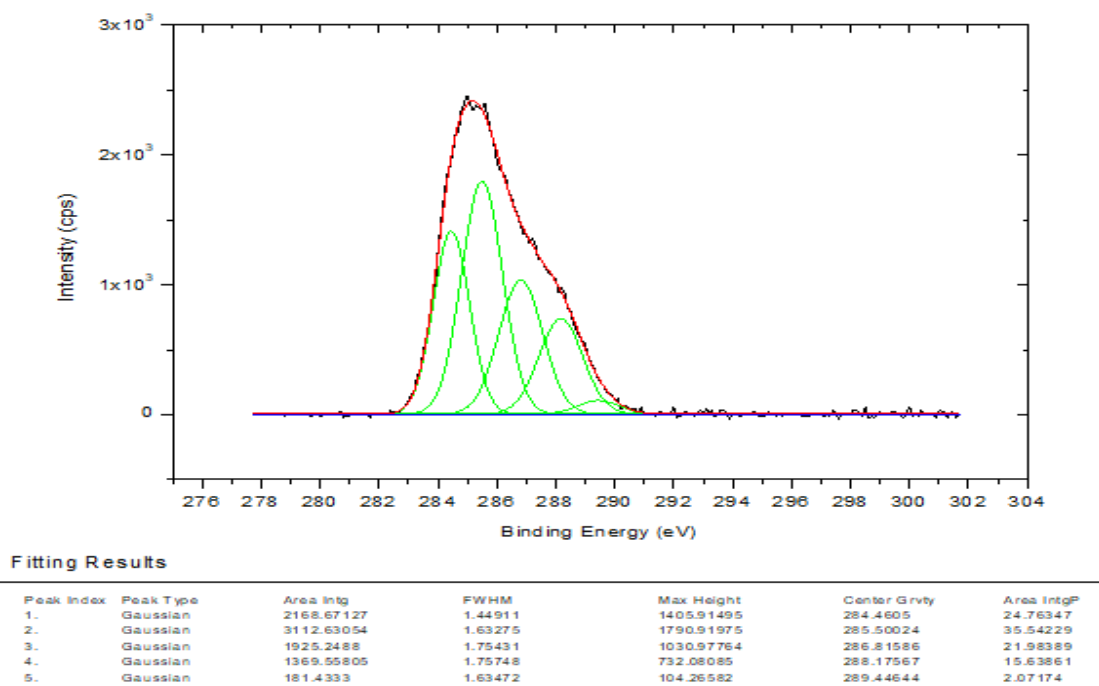


Figure B- 2 Deconvolution of C 1s peak of DLC thin films synthesized under operating pressure at 5 mtorr

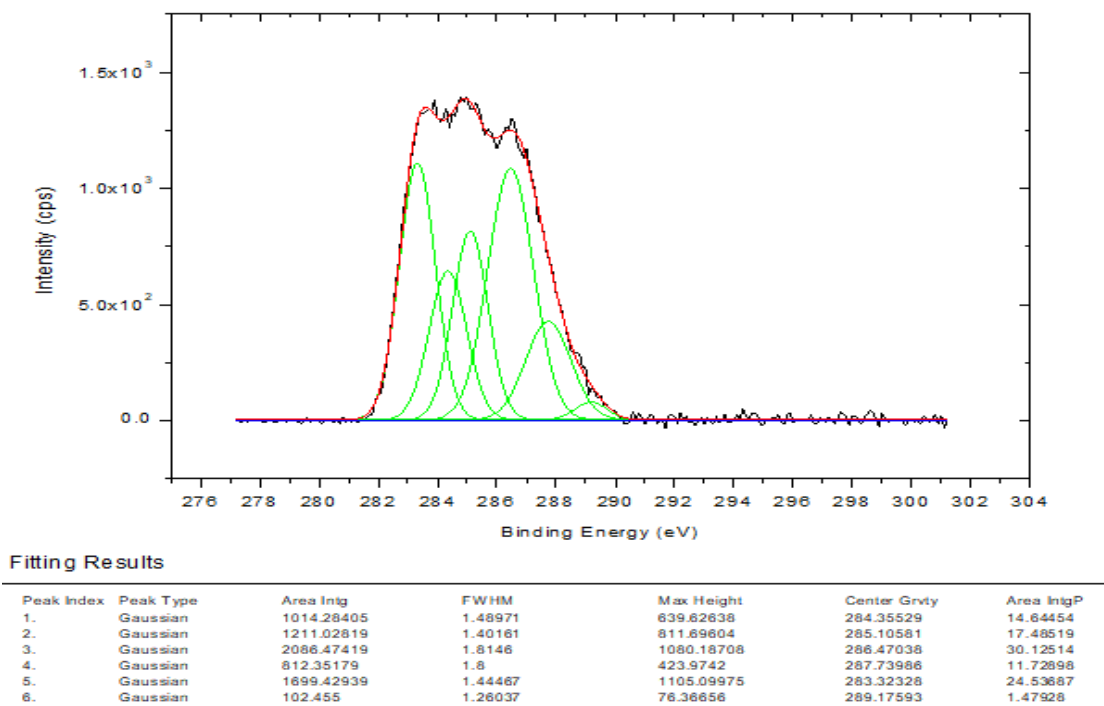


Figure B- 3 Deconvolution of C 1s peak of DLC thin films synthesized under operating pressure at 10 mtorr

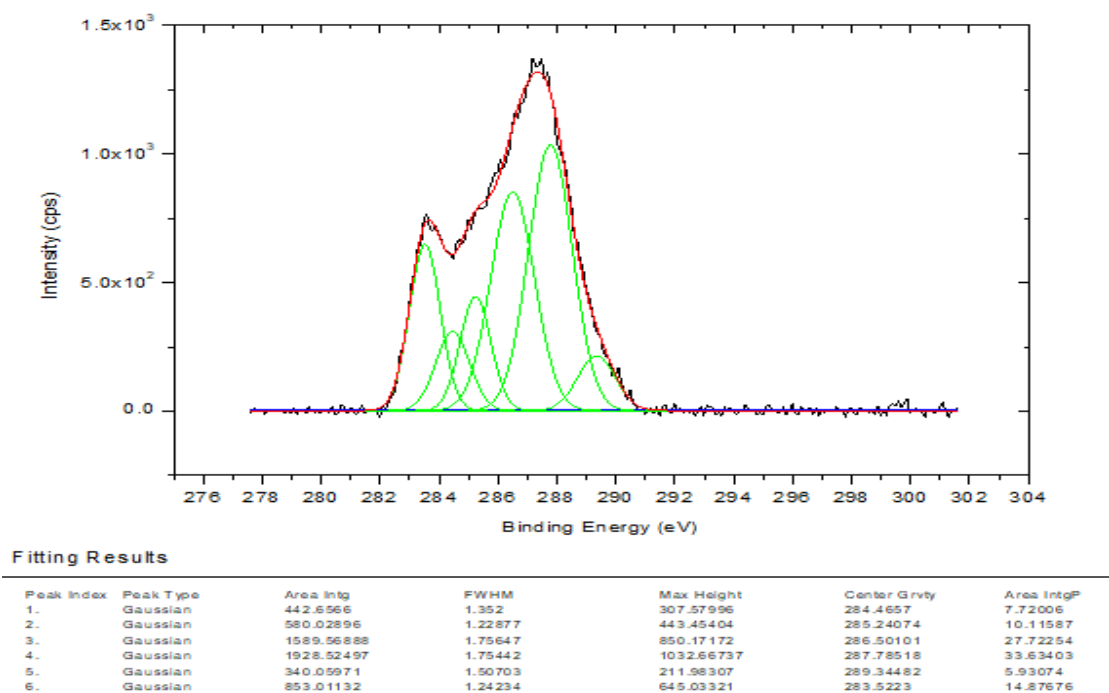


Figure B- 4 Deconvolution of C 1s peak of DLC thin films synthesized under operating pressure at 20 mtorr

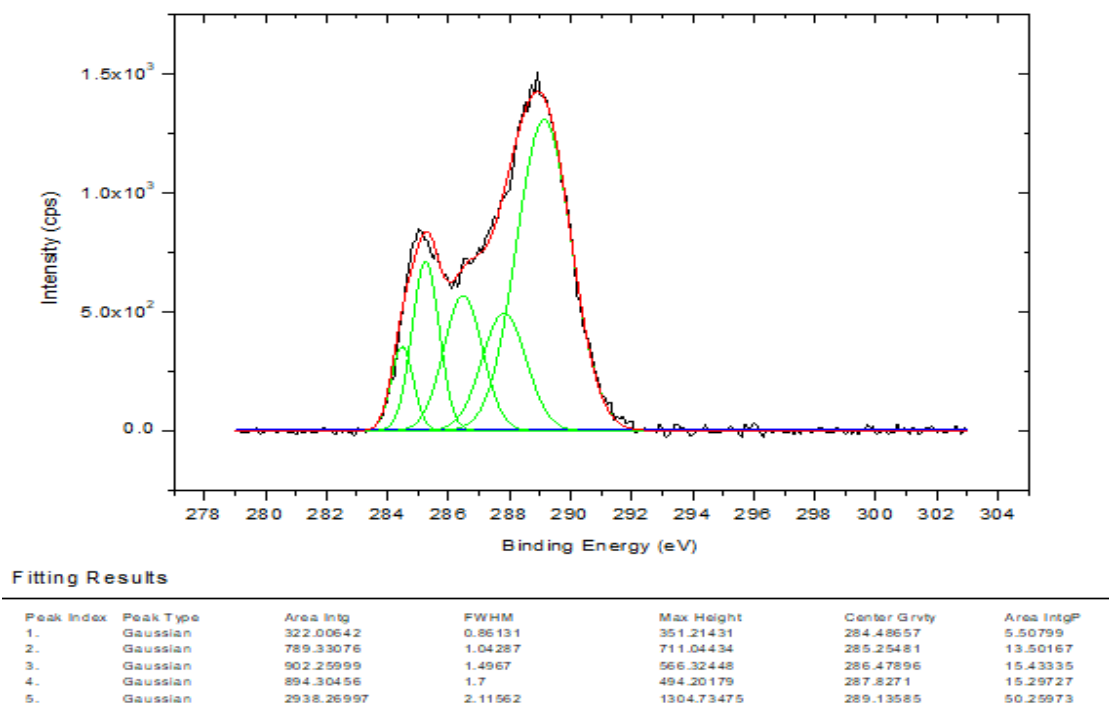
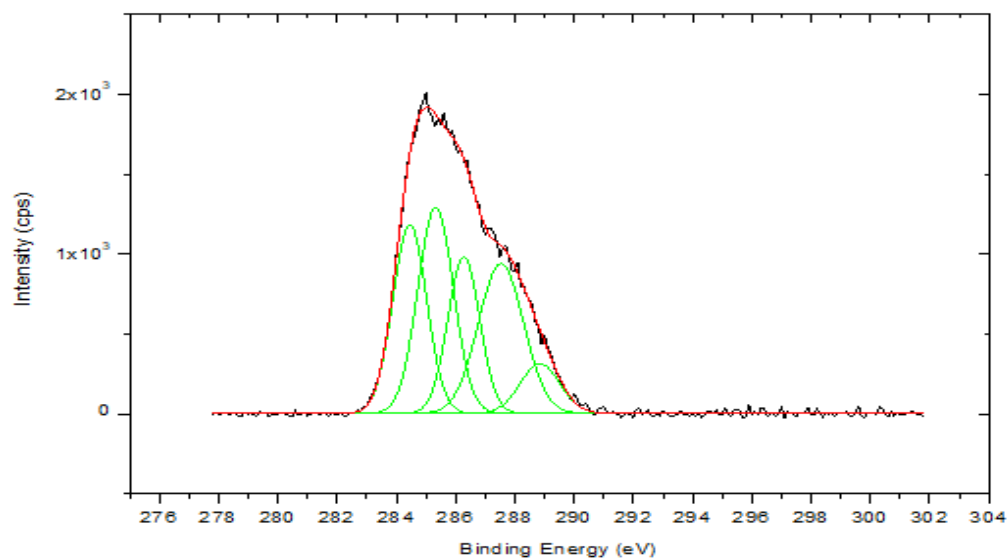


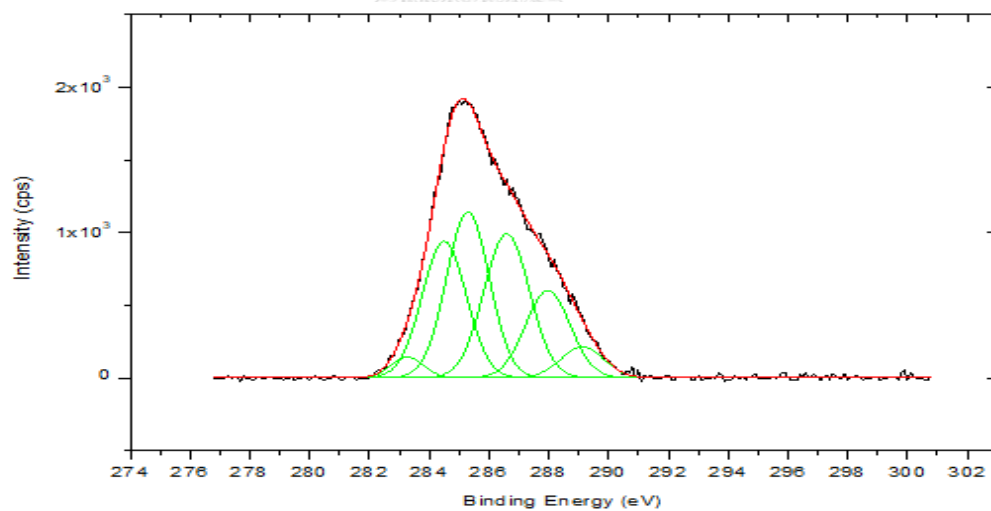
Figure B- 5 Deconvolution of C 1s peak of DLC thin films synthesized under operating pressure at 25 mtorr



Fitting Results

Peak Index	Peak Type	Area Intg	FWHM	Max Height	Center Grvty	Area IntgP
1.	Gaussian	1685.38671	1.34198	1179.83426	284.45593	23.25156
2.	Gaussian	1935.40066	1.41134	1288.27039	285.3321	26.70075
3.	Gaussian	1318.35913	1.26539	978.76455	286.27979	18.18806
4.	Gaussian	1791.71421	1.7964	936.98682	287.53567	24.71846
5.	Gaussian	517.62674	1.57073	309.58662	288.85097	7.14117

Figure B- 6 Deconvolution of C 1s peak of DLC thin films synthesized under base pressure at 5×10^{-5} mbar



Fitting Results

Peak Index	Peak Type	Area Intg	FWHM	Max Height	Center Grvty	Area IntgP
1.	Gaussian	1727.28312	1.73096	937.44307	284.5077	23.54319
2.	Gaussian	2039.40083	1.68173	1139.23857	285.29663	27.79742
3.	Gaussian	1889.05327	1.79673	987.71039	286.59697	25.74815
4.	Gaussian	1116.64811	1.75424	597.98994	287.97374	15.22012
5.	Gaussian	186.98692	1.24015	141.64654	283.27592	2.54867
6.	Gaussian	377.28408	1.66749	212.55608	289.12267	5.14245

Figure B- 7 Deconvolution of C 1s peak of DLC thin films synthesized under base pressure at 6×10^{-5} mbar

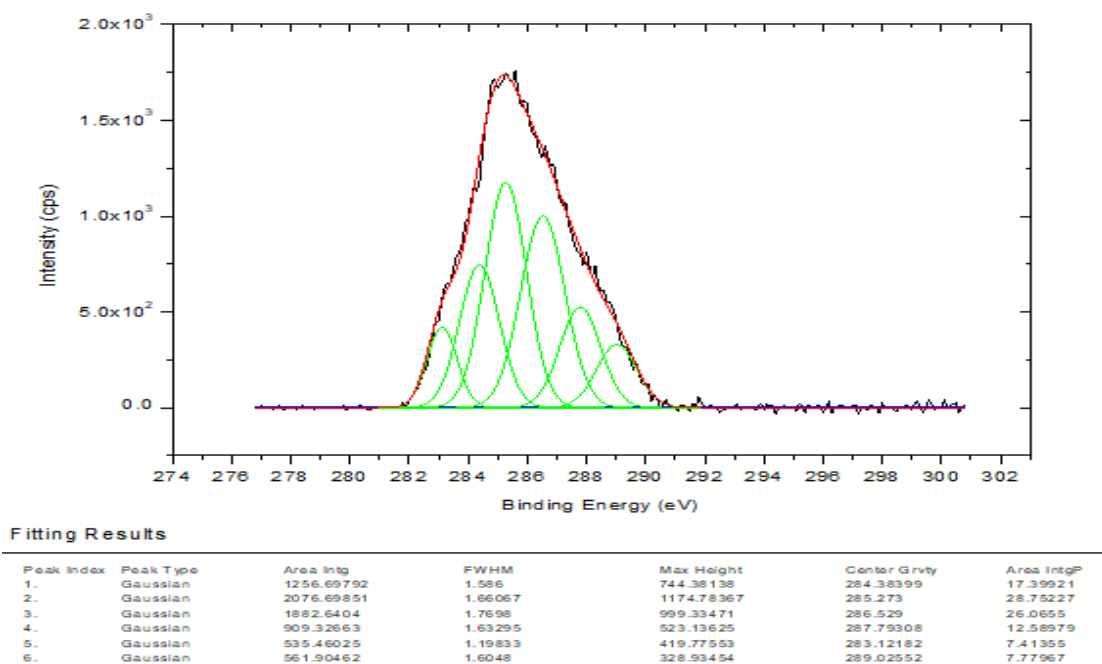


Figure B- 8 Deconvolution of C 1s peak of DLC thin films synthesized under base pressure at 7×10^{-5} mbar

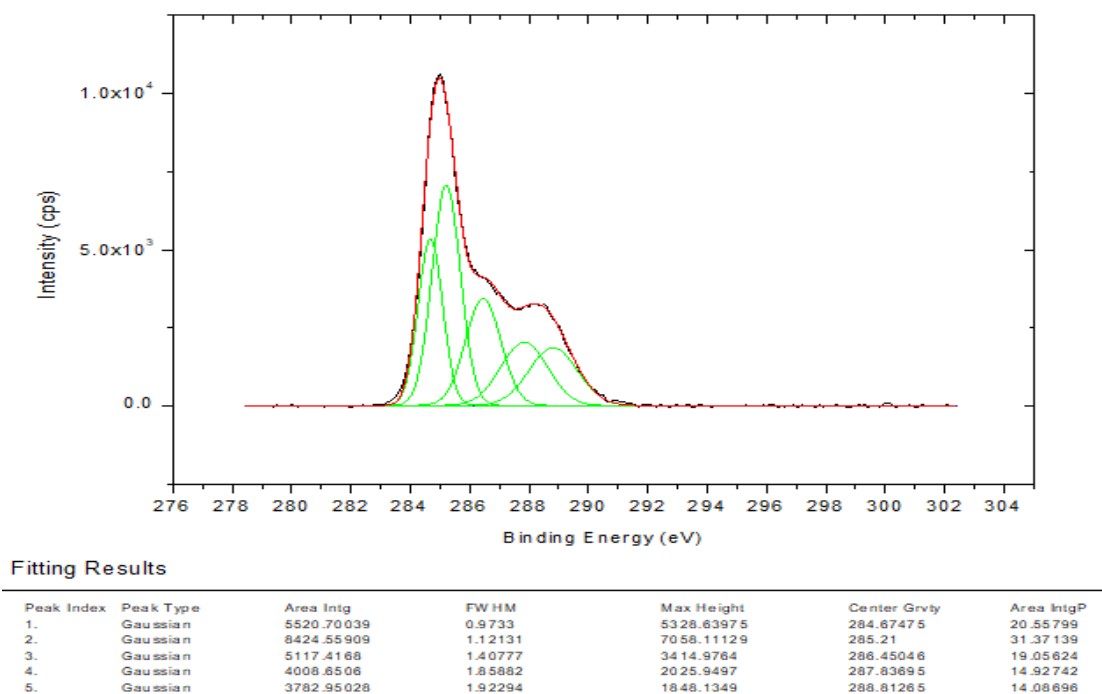


Figure B- 9 Deconvolution of C 1s peak of DLC thin films synthesized under operating pressure at 5 mtorr after used in EAOP

Appendix C

Liquid Chromatography-Mass/Mass Spectrum Data

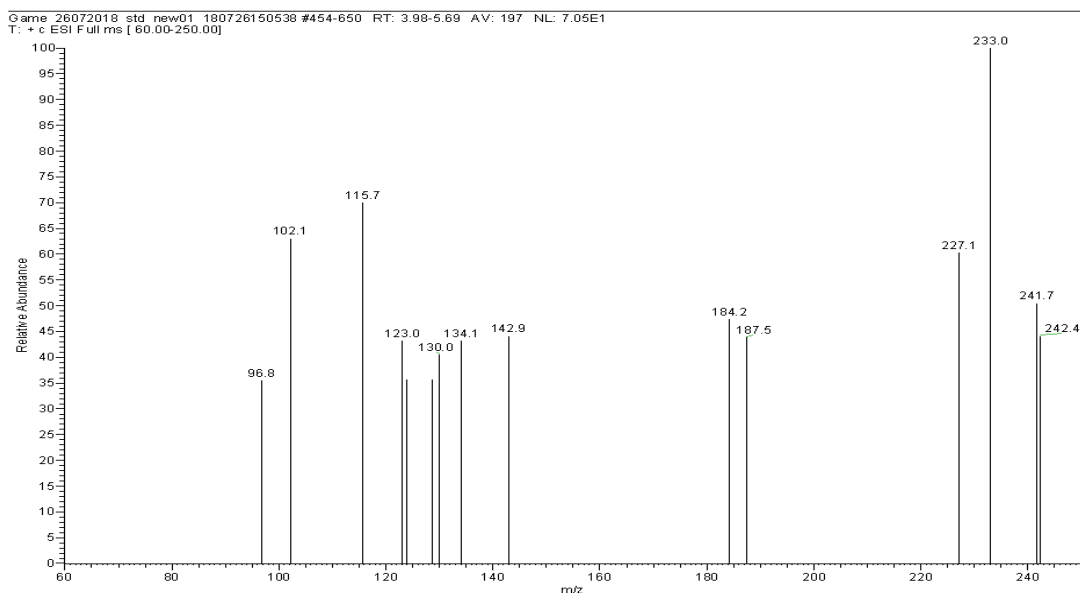


Figure C- 1 Full scan spectrum of diuron

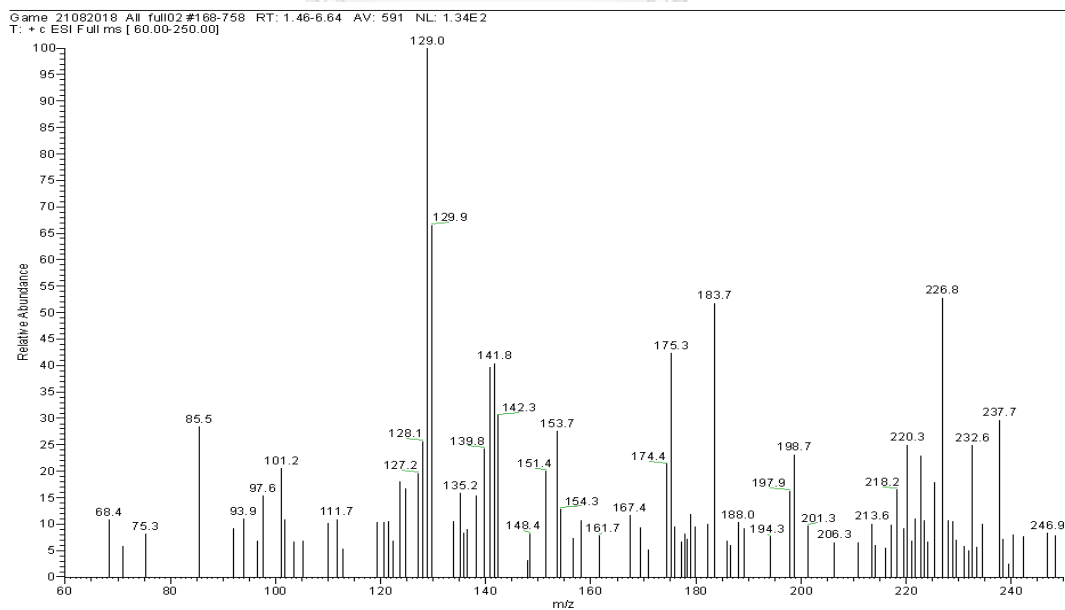


Figure C- 2 Full scan spectrum of outlet solution using DLC thin films electrode with 0.7 of sp²-sp³ ratio

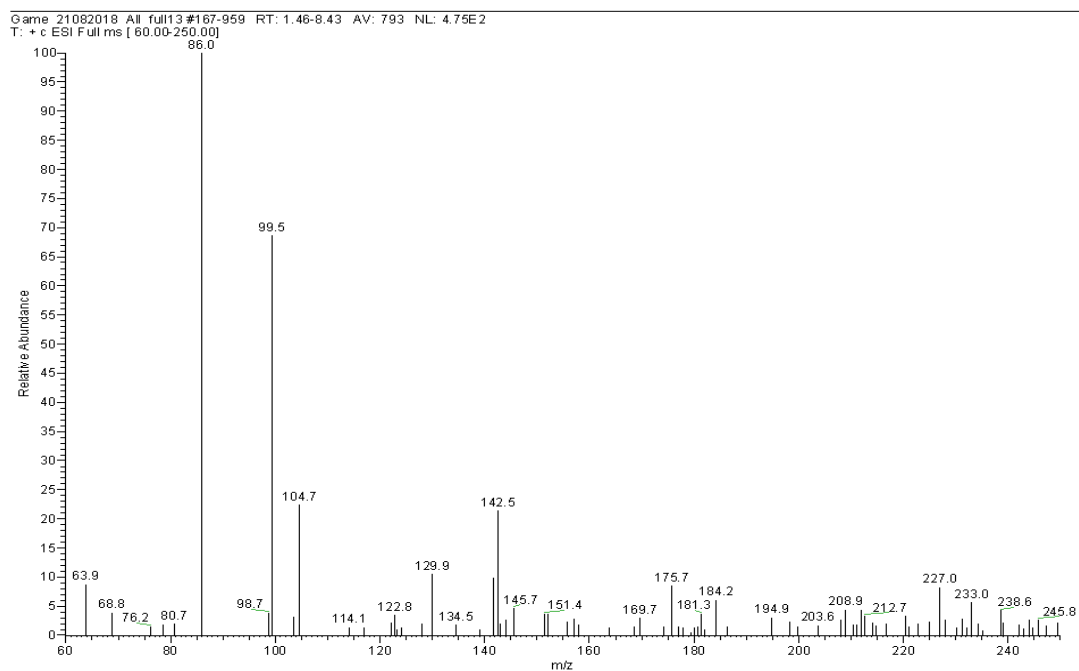


Figure C- 3 Full scan spectrum of outlet solution using DLC thin films electrode with 0.52 of sp²-sp³ ratio

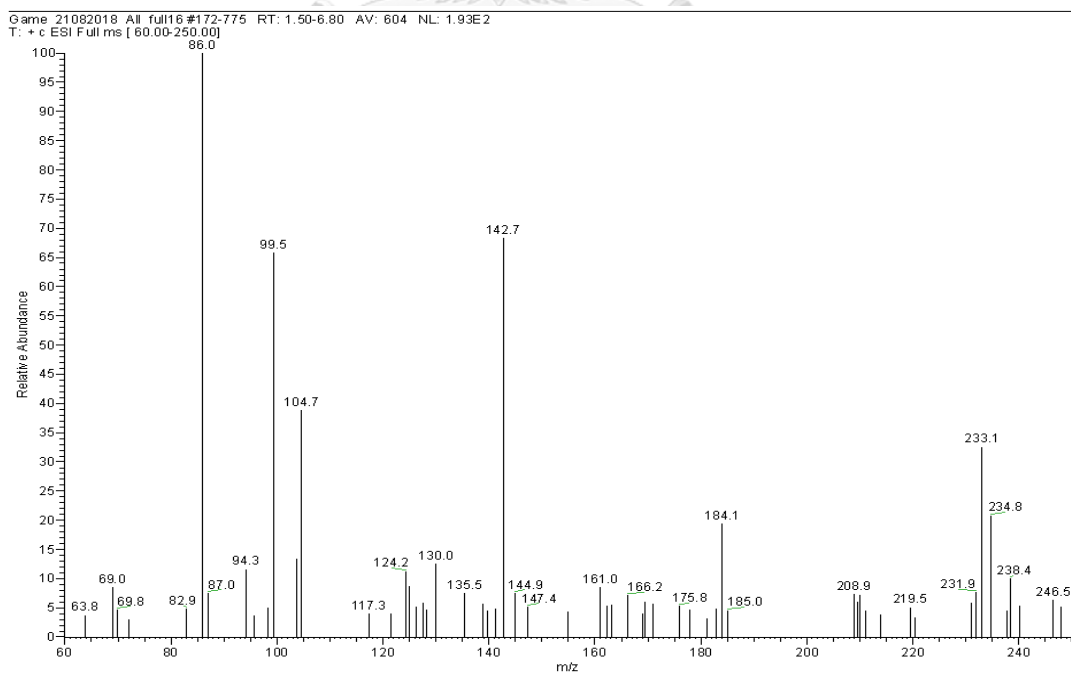


Figure C- 4 Full scan spectrum of outlet solution using DLC thin films electrode with 2.88 of sp²-sp³ ratio

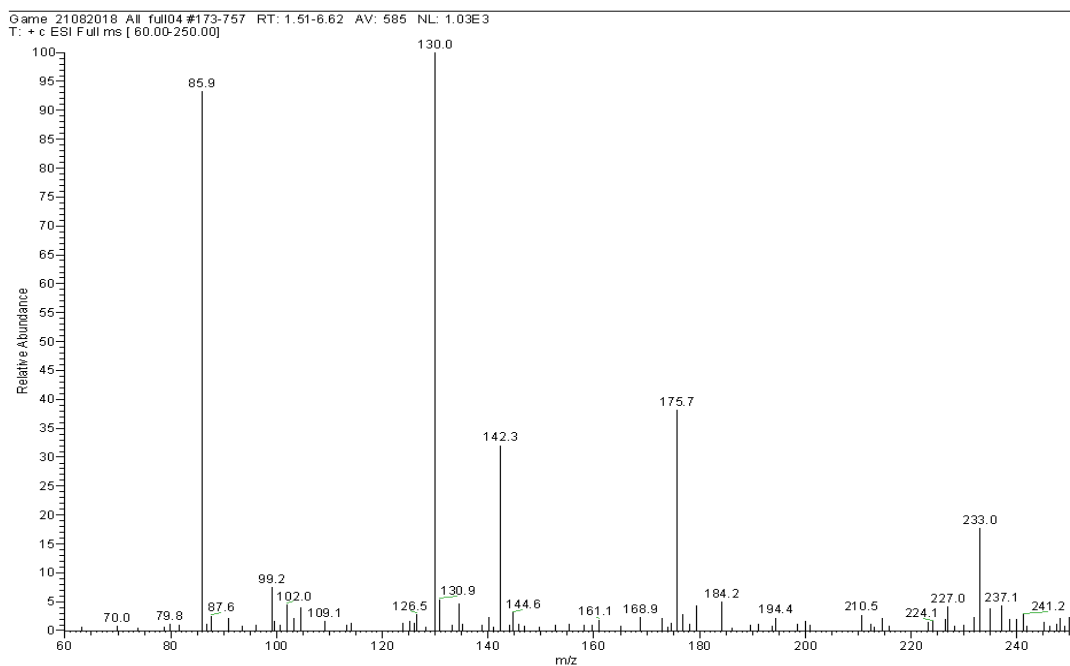


Figure C- 5 Full scan spectrum of outlet solution using DLC thin films electrode with 0.25 of fraction of C-H bond

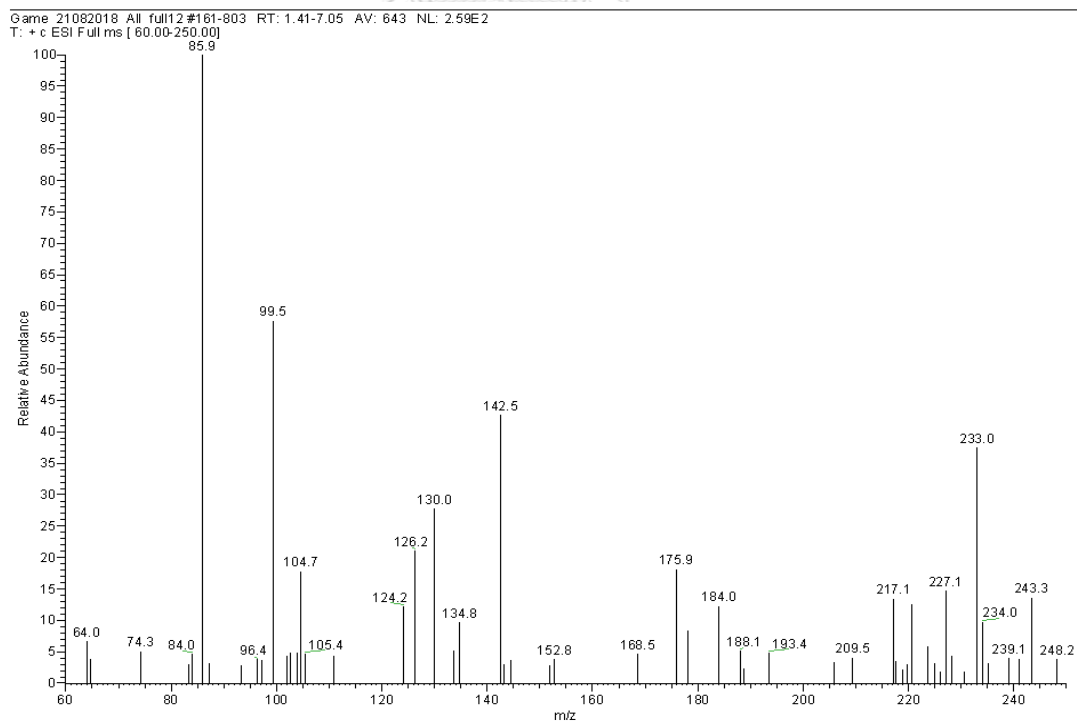


Figure C- 6 Full scan spectrum of outlet solution using DLC thin films electrode with 0.025 of fraction of C-H bond

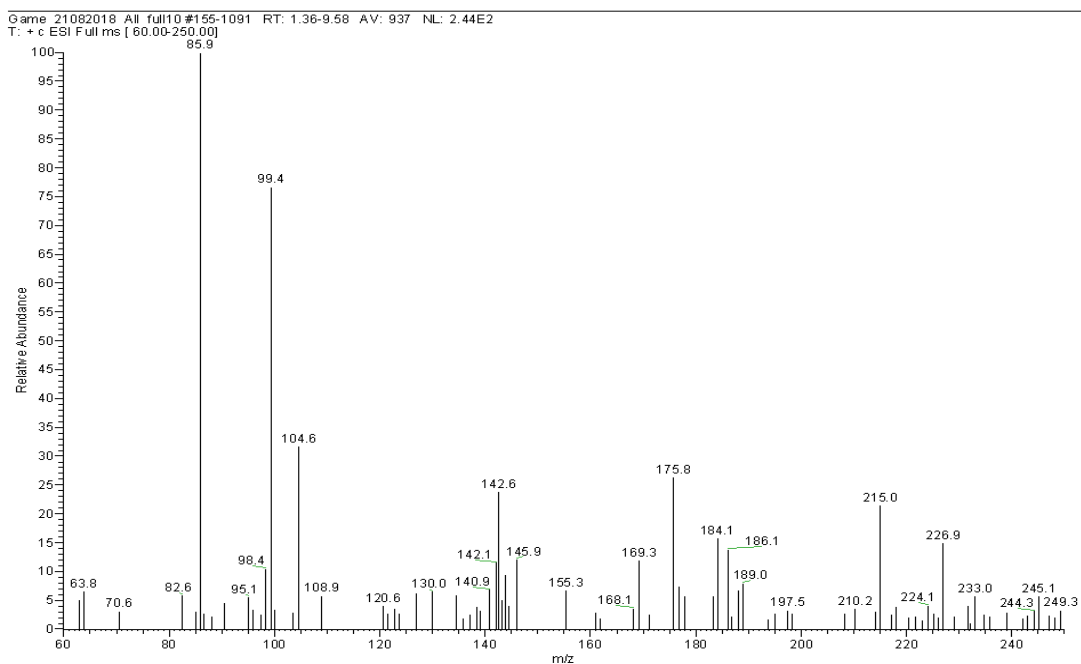


Figure C- 7 Full scan spectrum of outlet solution using DLC thin films electrode with 0.00 of fraction of C-H bond

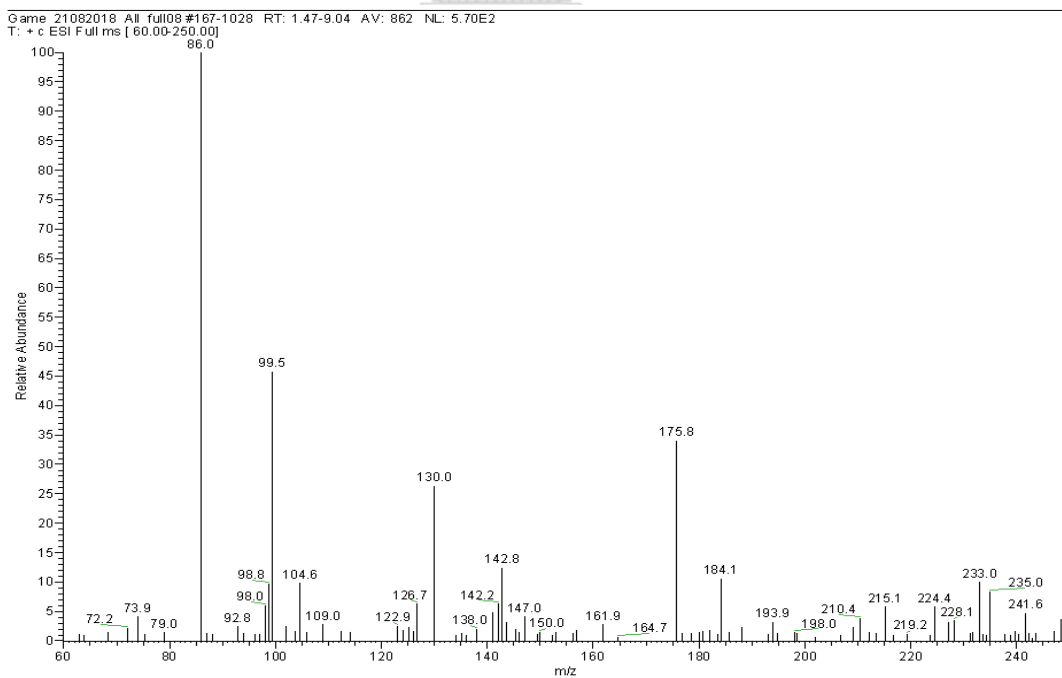


Figure C- 8 Full scan spectrum of outlet solution using DLC thin films electrode with 0.36 of fraction of C=O bond

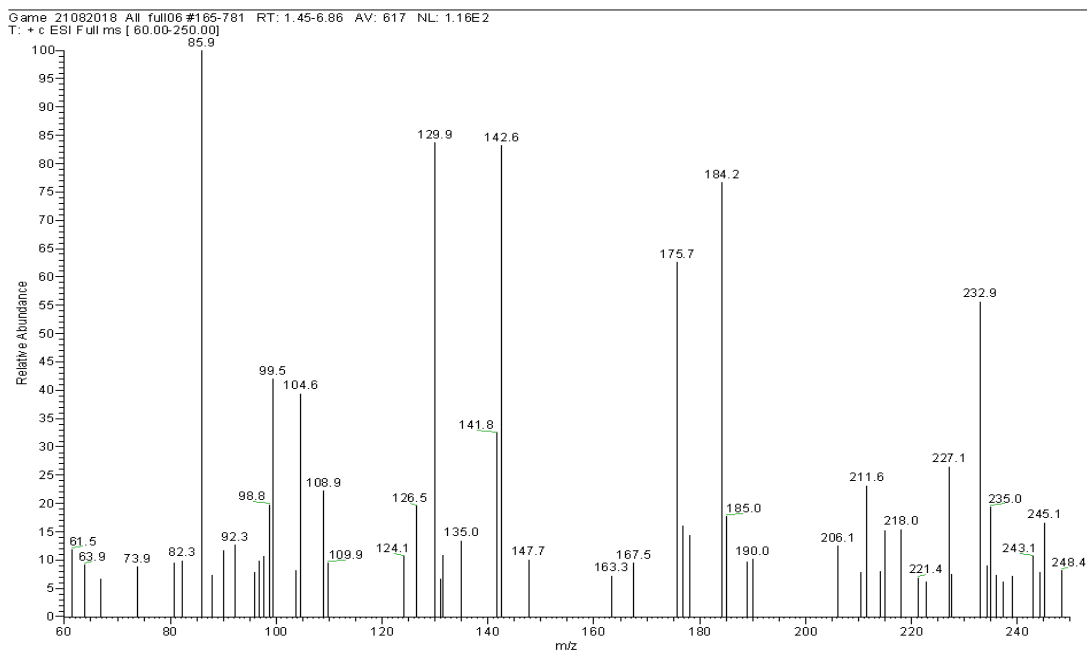


Figure C- 9 Full scan spectrum of outlet solution using DLC thin films electrode with 0.33 of fraction of C=O bond

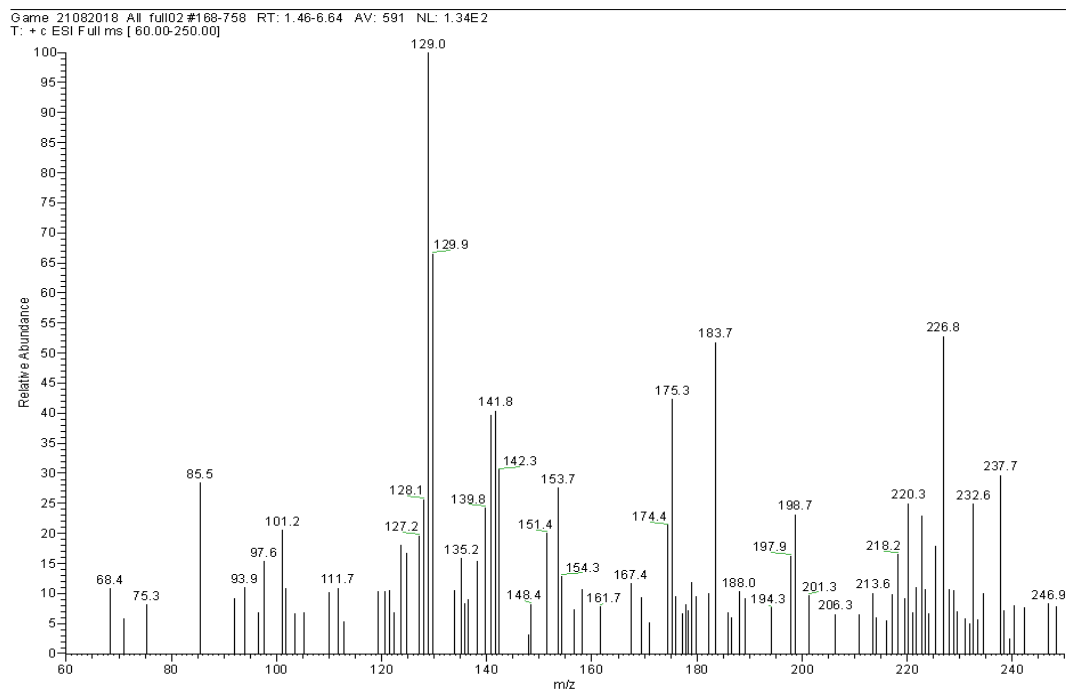


Figure C- 10 Full scan spectrum of outlet solution using DLC thin films electrode with 0.16 of fraction of C=O bond

Appendix D
Additional Data

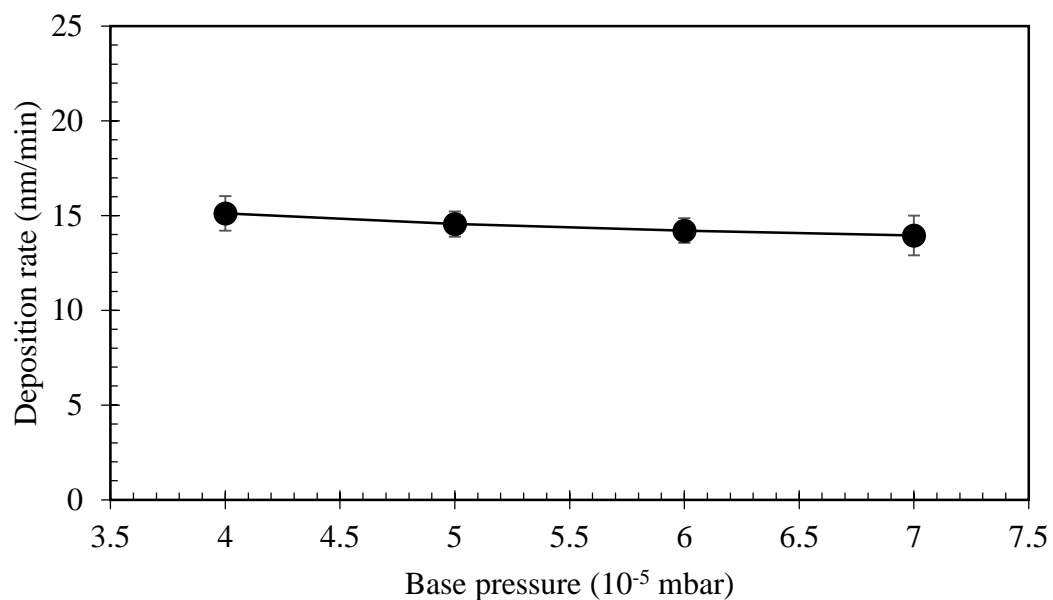


Figure D- 1 The deposition rate of DLC thin films under various base pressure in the range of 4×10^{-5} mbar to 7×10^{-5} mbar

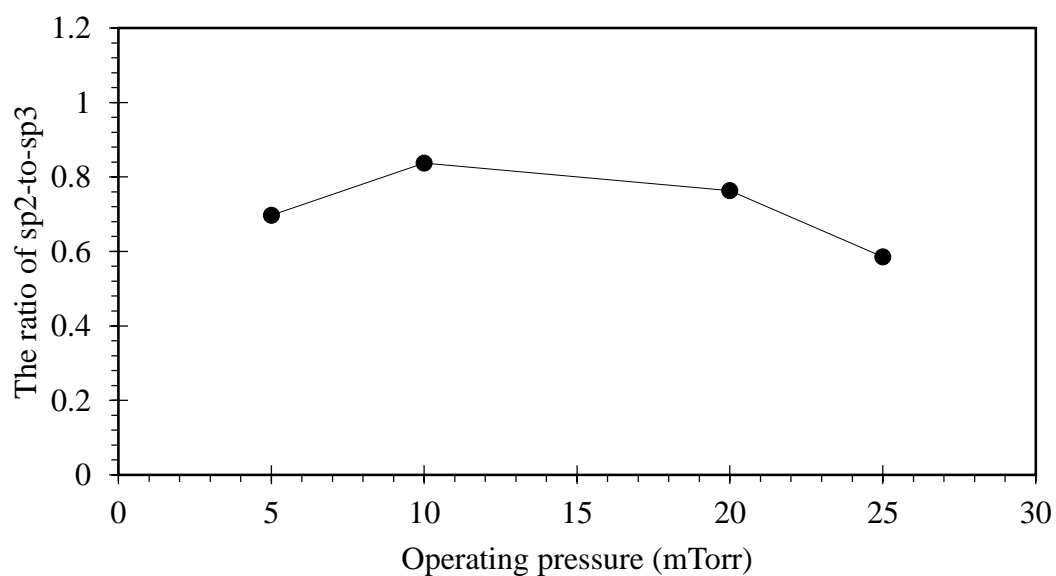


Figure D- 2 The ratio of sp^2 -to- sp^3 of the DLC thin films electrodes deposited under various the operating pressure

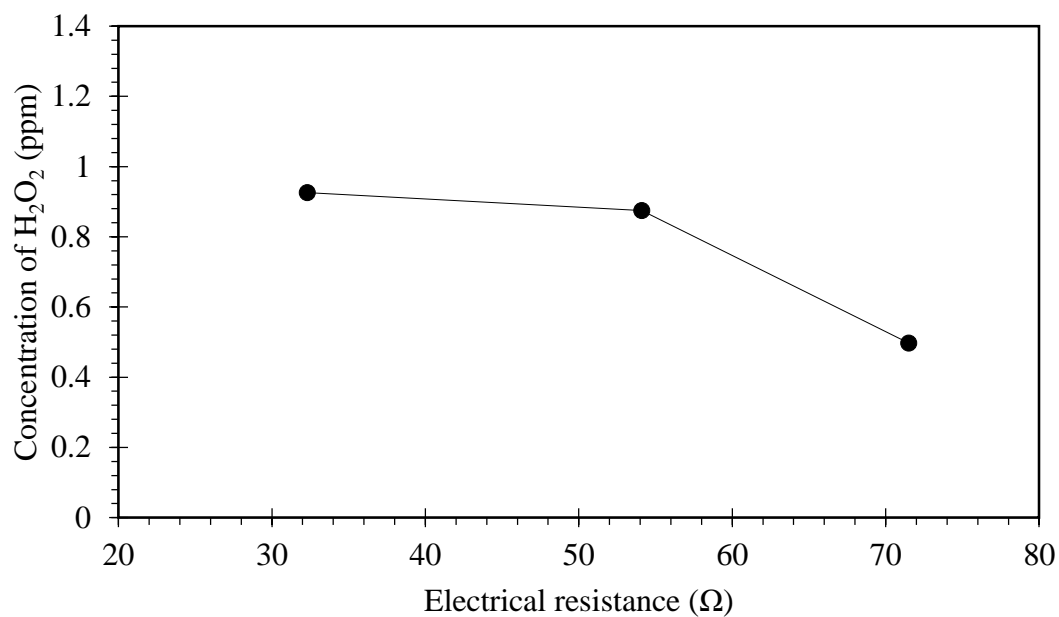


Figure D- 3 Relationship of electrical resistance and concentration of H_2O_2 generated

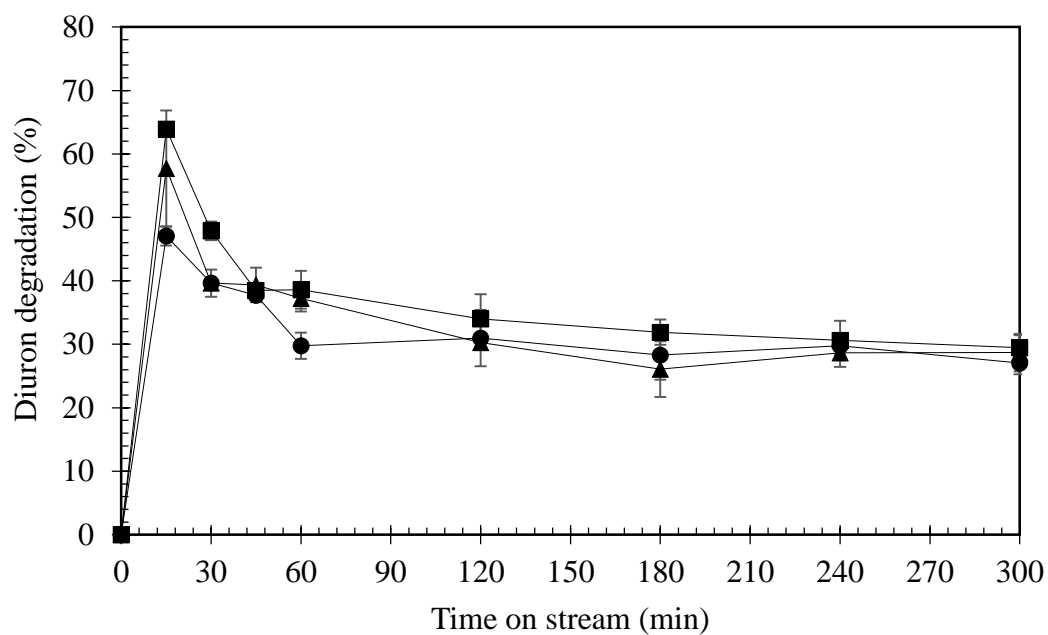


Figure D- 4 Correlation between performance of diuron degradation and time on stream at various fraction of C-O bond in the DLC thin films electrode

VITA

NAME Nimit Kantiyawong

DATE OF BIRTH 24 March 1993

PLACE OF BIRTH Kamphaeng Phet, Thailand

INSTITUTIONS ATTENDED Chemical Engineering, Naresuan University in Bachelor of Engineering

HOME ADDRESS 32 Moo.5 Tambon Thakhunram, Amphoe Mueang Kamphaeng Phet, Kamphaeng Phet, Thailand 62000

PUBLICATION Nimit Kantiyawong, Boonchoat Paosawatyanong, Varong Pavarajarn, "MODIFICATION OF ELECTRODE BY DIAMOND-LIKE CARBON FOR ELECTROCHEMICAL ADVANCED OXIDATION OF DIURON". Proceedings of The Pure and Applied Chemistry International Conference 2018 (PACCON 2018), Thailand.